**Andreia Teixeira Ferreira**
Licenciada em Bioquímica

# Phage Display as a Tool for Generation of Bio-therapeutic Agents for Breast Cancer

Dissertação para a obtenção do grau de Mestre em
Genética Molecular e Biomedicina

Orientador: Doutora Ana Barbas
Co-orientador: Doutor Tiago Bandeiras

Júri:

Presidente: Doutora Ilda Sanches
Arguente: Doutor Colin E. McVey

FACULDADE DE CIÊNCIAS E TECNOLOGIA
UNIVERSIDADE NOVA DE LISBOA

**Setembro de 2015**

**Andreia Teixeira Ferreira**
Licenciada em Bioquímica

# Phage Display as a Tool for Generation of Bio-therapeutic Agents for Breast Cancer

Dissertação para a obtenção do grau de Mestre em
Genética Molecular e Biomedicina

Orientador: Doutora Ana Barbas
Co-orientador: Doutor Tiago Bandeiras

Júri:

Presidente: Doutora Ilda Sanches
Arguente: Doutor Colin E. McVey

FACULDADE DE CIÊNCIAS E TECNOLOGIA
UNIVERSIDADE NOVA DE LISBOA

**Setembro de 2015**

Phage Display as a tool for generation of bio-therapeutic agents for Breast Cancer

## Agradecimentos

Em primeiro lugar quero deixar um agradecimento muito especial aos meus orientadores, Doutora Ana Barbas e Doutor Tiago Bandeiras. Agradeço por me terem aceitado e por todo o apoio, amizade e pela confiança que depositaram em mim durante todo o percurso.

Também quero agradecer à Márcia por ter sido a minha parceira nesta caminhada, pela simpatia e por toda a ajuda e disponibilidade na realização deste projeto. Fomos equipa nos bons e nos maus momentos e conseguimos sempre ultrapassar todos os obstáculos.

O meu muito obrigado a todos os meus colegas de ambos os laboratórios. Às super mulheres do laboratório 4.15, Joana, Inês, Fernanda, Liliana, Khrystyna, Gabriela, Sandra e também ao António, por me terem apoiado, por me ensinarem a ser sempre melhor e a desenvolver o meu sentido crítico, e principalmente pelos bons momentos que partilhamos. Aos colegas do SBDD, Cristiana, Paulo, Micael, Joana, Ana Teresa, Elisa, Pedro e Sara pelo companheirismo, aprendizagem e especialmente pela boa disposição e pelas gargalhadas, que tanto me animaram e fizeram com que me sentisse sempre mais feliz.

Agradeço a toda a Unidade de Cristalografia do ITQB, pelo auxílio e por tudo aquilo que me ensinaram. À Unidade de Tecnologia de Células Animais do IBET por me ajudarem sempre que precisei e ao ITQB/IBET que tornou possível a realização desta tese.

Queria também agradecer aos meus amigos por me terem apoiado e por acreditarem em mim. Ao meu namorado, que embora longe, me deu força para continuar e sempre me incentivou a trabalhar mais e melhor.

Finalmente, quero agradecer à minha família, em especial aos meus pais que estiveram sempre do meu lado, ajudando-me a ultrapassar as dificuldades e apoiando todas as minhas decisões.

## Resumo

A via Notch é uma via de sinalização conservada, que desempenha um papel fundamental em vários processos celulares tais como renovação de células estaminais, divisão e diferenciação celular e apoptose. Em mamíferos, encontram-se descritos quatro recetores e cinco ligandos da via Notch, cuja interação se dá através dos seus domínios extracelulares, causando uma ativação da transcrição de diferentes genes alvo. A elevada expressão dos ligandos da via Notch tem sido detetada em vários tipos de cancro, incluindo o cancro da mama, o que sugere que estas proteínas representam possíveis alvos terapêuticos.

O principal objetivo deste trabalho foi gerar proteínas alvo de boa qualidade e, recorrendo à tecnologia de *phage display*, selecionar anticorpos inibidores de função específicos para os ligandos da via Notch. O *Phage Display* é uma poderosa técnica que permite gerar anticorpos altamente específicos para fins terapêuticos, e já mostrou ser um método muito fiável para a identificação e validação de novos alvos relacionados com o cancro. Adicionalmente, pretendíamos resolver a estrutura tridimensional dos ligandos Notch isolados e em complexo com os anticorpos selecionados.

Neste trabalho, foi primeiramente otimizada a expressão e purificação de um mutante do ligando Delta-like 1 de humano (hDLL1-DE3) através do *refolding* de corpos de inclusão de *E.coli*. Para confirmar a atividade biológica da proteína produzida foram realizados estudos funcionais que revelaram que o tratamento com a proteína hDLL1-DE3 levou a uma modelação da transcrição de genes alvo da via Notch. Numa segunda fase deste estudo, por *phage display*, foram gerados fragmentos de anticorpo (*Fabs*) específicos para a hDLL1-DE3 utilizando a proteína produzida como alvo, dos quais o melhor *Fab* foi selecionado para determinar as melhores condições de expressão. Paralelamente, múltiplas condições de cristalização foram testadas para a proteína hDLL1-DE3 purificada, mas até à data nenhuma gerou um resultado positivo.



**Palavras-chave:** Sinalização Notch, Cancro da mama, Expressão de proteína, Phage Display, Fragmentos de anticorpo, Cristalização.

## Abstract

Notch is a conserved signalling pathway, which plays a crucial role in a multiple cellular processes such as stem cell self-renewal, cell division, proliferation and apoptosis. In mammalian, four Notch receptors and five ligands are described, where interaction is achieved through their extracellular domains, leading to a transcription activation of different target genes. Increased expression of Notch ligands has been detected in several types of cancer, including breast cancer suggesting that these proteins represent possible therapeutic targets.

The goal of this work was to generate quality protein targets and, by phage display technology, select function-blocking antibodies specific for Notch ligands. Phage display is a powerful technique that allows the generation of highly specific antibodies to be used for therapeutics, and it has also proved to be a reliable approach in identifying and validating new cancer-related targets. Also, we aimed at solving the tri-dimensional structure of the Notch ligands alone and in complex with selected antibodies.

In this work, the initial phase focused on the optimization of the expression and purification of a human Delta-like 1 ligand mutant construct (hDLL1-DE3), by refolding from *E. coli* inclusion bodies. To confirm the biological activity of the produced recombinant protein cellular functional studies were performed, revealing that treatment with hDLL1-DE3 protein led to a modulation of Notch target genes. In a second stage of this study, Antibody fragments (Fabs) specific for hDLL1-DE3 were generated by phage display, using the produced protein as target, in which one good Fab candidate was selected to determine the best expression conditions. In parallel, multiple crystallization conditions were tested with hDLL1-DE3, but so far none led to positive results.

**Keywords:** Notch signalling, Breast cancer, Protein expression, Phage Display, Antibody fragments, Crystallisation.

## Contents

1. Introduction ........ 1
1.1 Notch signalling ........ 1
1.1.1 Notch discovery- a story about a fly's wing ........ 1
1.1.2 Notch signalling pathway ........ 1
1.1.3 Structural features of Notch and its canonical ligands ........ 3
1.1.3.1 Structural insights ........ 5
1.1.4 Post-translational modifications ........ 6
1.1.4.1 Ubiquitination ........ 6
1.1.4.2 Glycosylation ........ 6
1.1.5 Notch signalling and disease ........ 6
1.1.5.1 Notch as an oncogene ........ 6
1.1.5.2 Angiogenesis ........ 7
1.1.5.3 Cancer stem cells ........ 7
1.1.5.4 Breast cancer ........ 8
1.1.5.5 Notch inhibition as a treatment for cancer ........ 8
1.2 Phage display: antibodies development ........ 9
1.2.1 The antibody molecule ........ 9
1.2.2 Generation of an antibody library ........ 11
1.2.3 Filamentous bacteriophages and phagemid vectors ........ 12
1.2.4 Pannings ........ 13
1.3 Goals ........ 14
2- Materials and methods ........ 15
2.1 Molecular Biology ........ 15
2.1.1 Notch ligands cloning ........ 15
2.1.1.1 pET-47b (+) (*E.coli*) and pHL-sec (mammalian – HEK293T) ........ 15
2.1.1.2 pETfh8 ........ 15
2.2 Protein expression in *E.coli* ........ 17
2.2.1 Expression tests ........ 17
2.2.2 Expression and purification of hDll1-DE3 – *E.coli* ........ 18
2.2.2.1 Solubilisation with Guanidine-HCl and L-arginine refolding ........ 18
2.2.2.2 Solubilisation with urea and refolding ........ 18
2.3 Protein expression in mammalian cells HEK293T ........ 19
2.3.1 Cell culture ........ 19
2.3.2 Expression tests in HEK293T ........ 19
2.3.3 Expression and purification of hDLL1-DE3 in HEK293T ........ 20
2.3.2.1 First strategy ........ 20
2.3.2.2 Second strategy ........ 20
2.4 Phage display ........ 21
2.4.1 Fab Library – IBET λ immune library ........ 21
2.4.2 Pannings on microplates ........ 21

2.4.3 Glycerol stock ........ 22
2.4.4 Input and Output titration ........ 22
2.4.5 Phage Amplification ........ 22
2.4.6 Phage pools analysis by Fab-on phage ELISA ........ 23
2.4.7 Individual clones analysis ........ 23
2.4.7.1 Clones rescue (5mL amplification) ........ 23
2.4.7.2 Fab-on-Phage ELISA........ 23
2.4.8 Pannings on immunotubes ........ 24
2.4.9 Individual clones analysis ........ 24
2.4.9.1 Fab-on-phage expression plates and glycerol stocks ........ 24
2.4.10 Characterization of the positive clones ........ 24
2.4.11 Soluble Fab (sFab) expression in pCOMB3XSS ........ 25
2.4.12 sFab Cloning and expression tests in pT7 ........ 25
2.4.13 Protein titration ........ 25
2.5 SDS-PAGE electrophoresis and Western Blot ........ 26
2.6 Protein quantification ........ 26
2.7 Thermal shift assay (TSA) ........ 27
2.8 Protein Crystallization ........ 27
2.9 Functional assay for hDLL1-DE3 ........ 28
2.9.1 Cell culture and treatments ........ 28
2.9.2 RNA purification, cDNA synthesis and gene expression analysis by real-time quantitative polymerase chain reaction (qRT-PCR) ........ 28
3 - Results and Discussion ........ 31
3.1 Notch ligands Expression in *E.coli* ........ 31
3.1.1 Expression screening in pET47 (b) + ........ 31
3.1.2 Cloning and expression tests with a solubility-inducing fusion protein ........ 34
3.2 Expression in mammalian cells (HEK293T) ........ 36
3.2.1 Expression tests in pHL-sec ........ 36
3.2.2 hDLL1-DE3 expression and purification ........ 38
3.2.2.1 First strategy ........ 38
3.2.2.2 Second strategy ........ 40
3.2.4 Selection of specific Fabs for hLL1-DE3 - Panning ........ 43
3.2.5 Assessment of Phage Pools Reactivity ........ 45
3.2.6. Assessment of selected individual clones reactivity ........ 45
3.3 Protein refolding from inclusion bodies in *E.coli* – hDLL1-DE3 (pET47(b)+) ........ 47
3.3.1 Solubilisation with Guanidine-HCl and L-arginine refolding ........ 47
3.3.2 Solubilisation of the Inclusion Bodies with urea ........ 51
3.3.2.1 Protein thermal stability - Thermal shift assay ........ 56
3.3.2.2 - Biologic activity or functional characterization of recombinant protein ........ 57
3.3.2.2.1 Cell line evaluation ........ 57
3.3.2.2.2 Modulation of Notch1-dependent genes by hDLL1-DE3 ........ 58
3.3.2.3 Crystallization experiments to obtain hDLL1-DE3 3D structure ........ 61
3.3.3 Assessment of target quality for phage display - hDLL1-DE3 titration ........ 63

3.3.4 Panning for hLL1-DE3 obtained from inclusion bodies ........ 63
3.3.5 Assessment of Phage Pools Reactivity ........ 64
3.3.6 Assessment of selected individual clones reactivity ........ 64
3.3.7 sFab characterization ........ 66
3.3.8 sFab expression in pCOMB3xss – clone 20 ........ 66
3.3.9 sFab expression in pT7 – clone 20 ........ 67
3.3.9.1 Expression tests ........ 67
3.4 Conclusions and future perspectives ........ 68
4 References ........ 71
5 Appendix ........ i
5.1 Reagent List ........ i
5.2 Strains genotype ........ iii
5.3 Buffers and Solutions ........ iv
5.3.1 hDLL1-DE3 purification from *E.coli* (inclusion bodies) ........ iv
5.3.1.1 Solubilisation with Guanidine-HCl and refolding with L-arginine ........ iv
5.3.1.2 Solubilisation with urea and refolding ........ iv
5.3.2 hDLL1-DE3 purification from HEK293T ........ v
5.3.2.1 First srategy ........ v
5.3.2.2 Second strategy ........ v
5.4 Mass spectrometry report (provided by Mass Spectometry Unit (UniMS), ITQB/Ibet, Oeiras, Portugal ........ vi
5.5 Supplementary figures ........ vii

## List of Figures

Figure 1.1 - Notch signalling pathway. ........................................................................................ 2
Figure 1.2 - Illustration of Notch receptors and ligands domains ........................................................ 4
Figure 1.3 - Structures obtained for Notch receptor and Notch ligands. ............................................... 5
Figure 1.4 - Antibody structure. ..................................................................................................... 10
Figure 1.5 - The V(D)J recombination. ........................................................................................... 11
Figure 1.6 - Representation of antibody structure and fragments.. ..................................................... 11
Figure 1.7 - M13 use in phage display. essential for phage replication. .............................................. 12
Figure 1.8 - Phage display cycle for selection of Ab fragments. .......................................................... 13

Figure 3.1 - SDS-PAGE of expression tests in hJag1-ME3. ................................................................ 31
Figure 3.2 - SDS-PAGE of expression tests in hDLL1-DE3. ................................................................ 34
Figure 3.3 - Anti-His Western blot results for hDLL1-DE3 soluble fractions. ....................................... 34
Figure 3.4 - Illustration of the constructs cloned in pETfh8. ............................................................... 35
Figure 3.5 - Anti-His Western Blot of expression tests in pETfh8 with hDLL1_DSL.. ........................... 35
Figure 3.6 - Anti-His Western Blot of expression tests in pETfh8 with hDLL1_EGF3.. ........................ 35
Figure 3.7 - Anti-His Western Blot of expression tests for hDLL1-DE6 and hDLL1-DE3 in 6-well plates.. ............................................................................................................................................. 36
Figure 3.8 - pAAVPURO control for expression tests in hDLL1-DE3. ................................................. 38
Figure 3.9 - Chromatogram of elution of hDLL1-DE3 from the HisTtrap column –first strategy.. ......... 38
Figure 3.10 - SDS-PAGE of hDLL1-DE3 elution from the Histrap column – first strategy.. .................. 39
Figure 3.11 - SEC chromatogram for hDLL1-DE3 – first strategy. ........................................................ 39
Figure 3.12 - SDS-PAGE of elution of hDLL1-DE3 from SEC – first strategy. .................................... 40
Figure 3.13 - SDS-PAGE hDLL1-DE3 final pool – first strategy. ......................................................... 40
Figure 3.14 - Chromatogram of elution of hDLL1-DE3 from the Histrap column – second strategy. ... 41
Figure 3.15 - SDS-PAGE of elution of hDLL1-DE3 from the Histrap column – second strategy. ......... 41
Figure 3.16 - SEC chromatogram for hDLL1-DE3 – second strategy. ................................................. 42
Figure 3.17 - SDS-PAGE of hDLL1-DE3 elution from SEC – second strategy. ................................... 42
Figure 3.18 - SDS-PAGE hDLL1-DE3 final pools – second strategy. .................................................. 42
Figure 3.19 - Titration of hDLL1-DE3.. ........................................................................................... 43
Figure 3.20 - Titration of phages selected for hDLL1-DE3. ................................................................ 45
Figure 3.21 - Fab-on-phage ELISA of individual clones selected against hDLL1-DE3. ....................... 46
Figure 3.22 - Fab-on-phage ELISA of individual clones - Comparison of Anti-Fab with hDLL1-DE3... 46
Figure 3.23 - SDS-PAGE: washing and solubilisation of inclusion bodies. .......................................... 48
Figure 3.24 - Chromatogram of Desalting – purification of hDLL1-DE3.. ............................................ 48
Figure 3.25 - SDS-PAGE after desalting of hDLL1-DE3. .................................................................... 49
Figure 3.26 - Analytical SEC of hDLL1-DE3. ...................................................................................... 49
Figure 3.27 - TSA for hDLL1-DE3. 20µg of protein were used. A.U – Arbitrary Units. ......................... 50
Figure 3.28 - Anti-His Western Blot of hDLL1-DE3 large scale production. ........................................ 51

Figure 3.29 - Chromatogram of AIC – elution step. ........ 52
Figure 3.30 - SDS-PAGE of AIC.M – Marker; Inj – Inject; FT – Flow-through; F- Fractions. ........ 52
Figure 3.31 - Chromatogram of Histrap 1st injection – elution step. ........ 53
Figure 3.32 - SDS-PAGE Histrap – 1st injection. A.. ........ 54
Figure 3.33 - Chromatogram of Histrap 2nd injection – elution step.. ........ 54
Figure 3.34 - SDS-PAGE of Histrap – 2nd Injection. ........ 55
Figure 3.35 - SDS-PAGE of hDLL1-DE3 purified from inclusion bodies. ........ 55
Figure 3.36 - Analytical SEC hDLL1-DE3 pool 5. Blue line – UV; Pink line – Inject. ........ 56
Figure 3.37 - TSA for hDLL1-DE3 – pool 5... ........ 56
Figure 3.38 - mRNA levels of *hNotch1* and *hDLL1* in different cell lines.. ........ 57
Figure 3.39 - mRNA levels of *hNotch1* and *hDLL1* in iPSCs in response to hDLL1-DE3. The values were normalized against the HPRT1 (control gene) mRNA levels in the same sample. ........ 58
Figure 3.40 - mRNA levels of *Hes-1* in HCC1954 in response to hDLL1-DE3 treatment. ........ 59
Figure 3.41 - mRNA levels of *Hey-1* in HCC1954 in response to hDLL1-DE3 treatment. ........ 59
Figure 3.42 - mRNA levels of hNotch1 in HCC1954 in response to hDLL1-DE3 treatment.. ........ 60
Figure 3.43 - Titration of hDLL1-DE3 – results from 2.5 to 20µg/ml of target. ........ 63
Figure 3.44 - Titration of pools from round 2 and 3 - hDLL1-DE3. ........ 64
Figure 3 45 - Titration of pools from round 2 and 3 -Anti-Fab. ........ 64
Figure 3.46 - Individual clones selected with hDLL1-DE3 – round 2. ........ 65
Figure 3.47 - Individual clones selected with hDLL1-DE3 – round 3. ........ 65
Figure 3.48 - Anti-Fab Western blot of soluble Fab expression in Shuffle – clone 20.. ........ 68

Figure 5.1 - SDS-PAGE of expression tests in hDLL1-ME6. ........ vii
Figure 5.2 - Anti-His Western Blot of expression tests for hDLL1-DE6 and hDLL1-DE3 in T25cm$^2$. ........ vii
Figure 5.3 - Anti-His Western Blot of hDLL1-DE3 large scale production in HEK293T. ........ viii
Figure 5.4 - Transfection efficiency evaluation after 48 hours post-transfection in T225cm$^2$. ........ viii
Figure 5.5 - Illustration of pCOMB3XSS. Adapted from *Cabral, 2014.* ........ viii

## List of Tables

Table 2.1 - Primers used to amplify Notch ligands. R.E. – Restriction enzymes. ................................ 16
Table 2.2 - Primers used in qRT-PCR reactions ...................................................................... 29

Table 3.1 - Conditions tested for expression of Notch ligands cloned in pET47 (b) + ......................... 32
Table 3.2 - Conditions tested for expression of Notch ligands cloned in pHL-sec............................... 37
Table 3.3 - Summary of hDLL1-DE3 panning. ....................................................................... 44
Table 3.4 - Conditions tested for expression of sFab (clone 20)........................................................ 67
Table 3 5 - Summary of Notch ligands expression strategies.............................................................. 69
Table 3.6 - Summary of hDLL1 – DE3 purification strategies ............................................................. 69

Table 5.1 - List of reagents used. ................................................................................................i

## Abbreviations

| | |
|---|---|
| Ab | Antibody |
| ADAM | A Disintegrin and A Metalloprotease |
| AIC | Anionic Exchange Chromatography |
| ANK | Ankyrin |
| Bp | Basepair |
| BSA | Bovine Serum Albumin |
| BME | Beta- mercaptoethanol |
| C | Constant |
| CBF-1 | C-promoter binding factor 1 |
| CD | Circular Dichroism |
| cDNA | Complementary DNA |
| CDR | Complmentary Determining Region |
| CH | Constant  Heavy chain |
| CL | Constant Llight chain |
| CSC | Cancer stem cell |
| CV | Column Volume |
| DLL | Delta-like |
| DMEM | Dulbecco's modified Eagles's medium |
| DMSO | Dimethyl sulfoxide |
| DNA | Deoxyribonucleic Acid |
| dNTPs | Deoxynucleotides tri-phosphate |
| DOS | Delta and OSM-11 Motif |
| DPBS | Dulbecco's Phospahte Buffer Saline |
| DSL | Delta/Serrate/LAG-2 |
| DTT | Dithiothreitol |
| *E.coli* | *Escherichia coli* |
| EDTA | Ethylenediamine tetraacetic acid |
| EGF | Epidermal Growth Factor-like Repeat |
| ELISA | Enzyme-Linked Immunosorbent Assay |
| EMT | Epidermal-to- mesenchymal transition |
| ER | Endoplasmic reticulum |
| Fab | " antigen binding Fragment" |
| FBS | Fetal Bovine Serum |
| Fc | "crystallisable Fragment" |
| Fh8 | *Fasciola hepatica* antigen 8kDa |
| FR | Framework regions |
| g3p | Gene 3 protein |
| g8p | Gene 8 protein |
| GFP | Green fluorescence protein |
| GSH | Reduced Glutathione |
| GSI | Gamma-secretase inhibitors |
| GSSG | Oxidised Glutathione |
| HD | Heterodimerization Domain |
| HEK | Human Embryonic Kidney |
| HES | hairy/enhancer of split |
| HIF-1α | Hypoxia Inducible Factor-1 alpha |
| HRP | Horseradish peroxidase |
| ICD | Intracellular  Domains |
| Ig | Immunoglobulin |
| IPTG | Isopropyl β-D-1-thiogalactopyranoside |
| Jag | Jagged |
| kDa | Kilo Daltons |
| LC | Light Chain |
| LNR | Lin12-Notch Repeats |
| mAb | Monoclonal antibody |
| MAPK | Mitogen activated protein kinase |
| Mib | Mind bomb |
| MNNL | Module N-Terminal of Notch |
| MOI | multiplicity of infection |
| mRNA | Messenger RNA |
| Neur | Neuralized |
| NICD | Notch Intracellular Domain |
| NLS | Nuclear Localization Signal |
| NRR | Negative Regulatory Region |
| NT | N-terminal |
| o/n | overnight |
| OD | Optical Density |
| $OD_{600nm}$ | Optical density at 600nm |
| PAGE | Polyacrylamide Gel electrophoresis |
| PB | Power Broth |
| PBS | Phosphate  Buffer Saline |
| PBST | PBS-Tween 0.05% |
| PCR | Polymerase Chain Reaction |
| PDB | Protein Data Bank |
| PEG | Polyethylene Glycol |
| PEI | Polyethylenimine |
| PEST | Proline, Glutamate, Serine and Threonine rich Sequence |
| pI | Isoelectric Point |
| RAM | Rbp-associated Molecule |
| RNA | Ribonucleic acid |
| rpm | Rotation per minute |
| scFv | Single-chain variable fragments |
| SDS | Sodium Dodecyl Sulphate |
| SEC | Size Exclusion Chromatography |
| ssDNA | Single-stranded DNA |
| Su(H) | Supressor of hairless |
| TAD | Transactivation domain |
| T-ALL | T-Cell Acute Lymphoblastic Leukemia |
| TEA | trimethylamine |
| TGF-β | Transforming Growth Factor beta |
| Tm | Melting Temperature |
| TMAO | Trimethylamine N-oxide |
| TMB | 3,3′,5,5′-Tetramethylbenzidine |
| TMB | Transmembrane domain |
| TSA | Thermal Shift Assay |
| V | Variable |
| VEGF | Vascular Ensothelial Growth |
| WT | Wild type |
| γ-secretase | gamma-secretase |

# 1. Introduction

Over the past 30 years Notch signalling knowledge has grown in an exponential way. This pathway, discovered almost a century ago, is known for its crucial influence in metazoan development and effect on many cellular processes like differentiation, proliferation and apoptosis. Given the impact of the Notch in cell-fate it is normal to think that any mutation within this pathway will cause great disturbance. In fact, there are several diseases related with an abnormal function of Notch signalling.

## 1.1 Notch signalling

### 1.1.1 Notch discovery- a story about a fly's wing

In 1914, investigators of Thomas Morgan´s group described a mutation in *Drosophila* that originated several serrations on the fly's wing and they named the mutant *Notch* (Dexter *et al.,* 1914). This study contributed to the development of the genetic field and provided a link between development biology and genetics. Many years later, in the first Notch review Morgan Ted Wright emphasized its important role: "If one was asked to choose the single most important genetic variation concerned with the expression of the genome during embryogenesis in *Drosophila melanogaster*, the answer would have to be the Notch *locus*" (Wright, 1970). Studies concerning the Notch pathway have been growing over the years and nowadays there are many groups working to increase the knowledge in this interesting and vast field.

### 1.1.2 Notch signalling pathway

Notch pathway is crucial during embryonic development and it is also involved in stem-cell maintenance and regulation of homeostasis in adult's tissues (Artavanis-Tsakonas *et al.,1999*; Gridley, 1997, 2003). This canonical pathway has two main groups of players: Notch receptors and Notch ligands. The first are cell-surface proteins capable of transducing short-range signals when interacting with ligands present on neighbouring cells. There are four receptors in mammalian, namely Notch 1-4. On the other hand, five ligands are described for mammalian – Delta-like 1, 3 and 4 (DLL1-4), Jagged 1 and 2 (Jag1 and Jag2), all part of the DSL (Delta, Serrate, LAG-2) family (Kopan and Illagan, 2009).

Canonical signalling requires a direct communication between the Notch receptor and its ligand, and since the two are present in adjacent cells, physical cell contact is required to trigger signal transduction. So, in order to have a productive signalling the presence of two distinct cell-types is necessary, some expressing the Notch receptors – signal receiving cells, and others expressing DSL ligands - signal sending cells (Kopan and Illagan, 2009). However, frequently, two adjacent cells may express both the ligand and the receptor, and in this particular situation it is the ratio between the number of functional ligands and receptors in the cell that determines its fate. As such, cells expressing more ligands become a signal-sending cell, whereas the ones that express more receptor become the signal-receiving cells (Gibert and Simpson, 2003; Heitzler and Simpson, 1991). The mechanisms underlying this differentiation remain unclear, although some studies about cis-inhibitory interactions between the receptor and the ligand suggest that both may be related (Sprinzak *et al.,* 2010).

After its synthesis in the endoplasmic reticulum (ER), the Notch receptor is cleaved by protein convertases (Furin-processing) in site 1 (S1), originating a heterodimeric protein that is linked by non-covalent interactions (Logeat *et al.,* 1998). In the Golgi, the receptor can be glycosylated, by glycosyl–transferases (e.g. Fringe), and it is the glycosylation pattern acquired that will be responsible for determination of the subsequent response to different ligands (Kopan, 2012). The heterodimeric protein generated by Furin-processing interacts with DSL ligands and induces a conformational change in the Notch extracellular domain. This allows the proteolytic cleavage of the whole domain by protease ADAM10 (A Disintegrin and A Metalloprotease) at site 2 (S2) (Brou *et al.,* 2000). Then, gamma-secretase (γ-secretase) cleaves Notch in its transmembrane domain (S3), leading to the release of the Notch intracellular domain (NCID) and its migration to the nucleus where it will activate the transcription of several target genes (e.g. genes from hairy/enhancer of split (HES) family) (Iso and Hamamori, 2003; Lubman *et al.,* 2004; Borggrefe and Oswald., 2009). For that purpose, NCID promotes the release of the repressor (Co-R) and forms transcriptional complexes with Deoxyribonucleic Acid (DNA)-binding factor CSL (C-promoter binding factor 1 (CBF-1), suppressor of hairless (Su(H)), lin-12 and glp-1 (Lag-1)) and the coactivator Mastermind, therefore allowing gene transcription, which is dependent on the cellular context (Cave, 2011; Petcherski and Kimble, 2000; Wu *et al.,* 2000) (Figure 1.1).

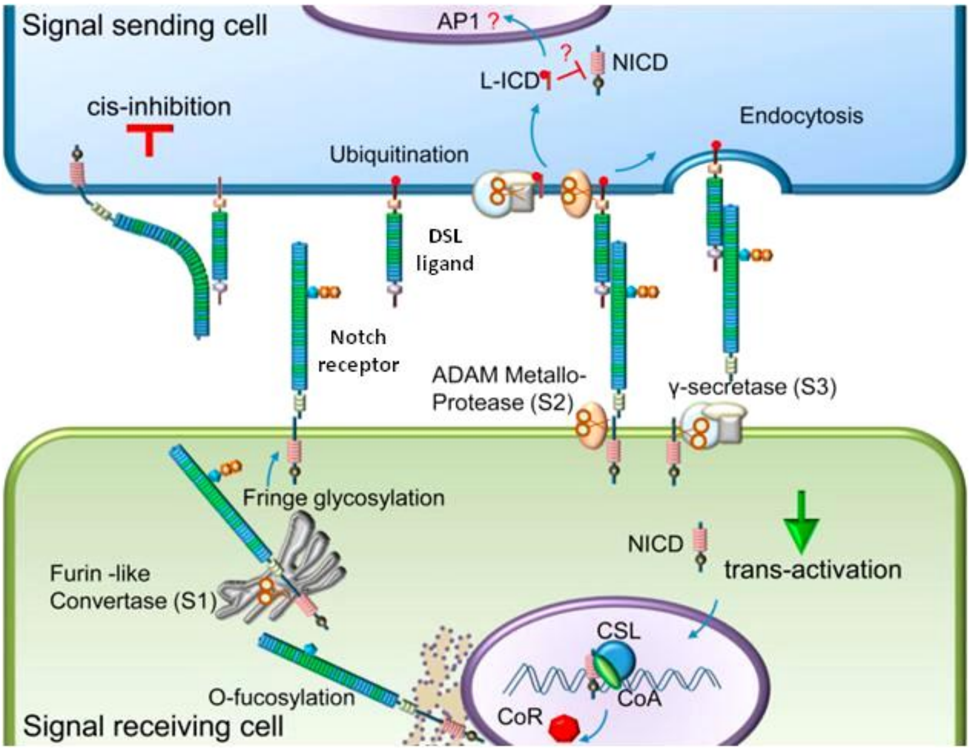


**Figure 1.1 - Notch signalling pathway.** The first step is the interaction between the ligand and the receptor present in adjacent cells. Next, three proteolytic events occur on Notch receptors, at S2 and S3, by the action of ADAM and γ-secretase enzymes, respectively. The last cleavage releases the NCID that is released and translocates into the nucleus to activate gene transcription. This activation occurs when the NCID promotes the release of the repressor (Co-R) and allows the formation of an activation complex constituted by Mam and DNA-binding factor CSL. Figure adapted from Chillakuri *et al.,* 2012.

NCID contains a Proline, Glutamate, Serine and Threonine rich Sequence (PEST) that marks the polypeptide to rapid degradation (Fryer *et al.,* 2004). For that reason, canonical Notch pathway activation does not result in large signal amplification because cleavage, dissociation and destruction of the receptor occurs during transduction. Thus, unlike other systems, in Notch signalling there is a linear response between the receptor activation and transcript activation (Wang *et al.,* 2011a).Recent studies emphasize the role of the signal-sending cell (expressing the DSL ligands), suggesting that processing of ligands and endocytosis (into the signal-sending cell) of the receptor/ligand complex are required for signalling activation (Ahimou *et al.,* 2004; Klueg and Muskavitch, 1999; Nichols *et al.,* 2007).

### 1.1.3 Structural features of Notch and its canonical ligands

Mammals have four Notch receptors (Notch 1-4) that are large single-pass type I transmembrane proteins (Figure 1.2). All Notch proteins present an extracellular domain with 29-36 tandem epidermal growth factor like repeats (EGFs) that can be calcium binding domains thus influencing signalling productivity (Raya *et al.,* 2004). Moreover, these repeats have been described as being very important for structure and affinity determination of Notch in ligand binding (Cordle *et al*., 2008b). The EGFs are followed by a negative regulatory region (NRR) composed by three cysteine-rich Lin12-Notch repeats (LNR) and a heterodimerization domain (HD). The NRR region plays a crucial role in inhibiting Notch activation in the absence of ligands. Next to the NRR region is the transmembrane domain (TMB) followed by the NICD. The last contains a Rbp-associated Molecule (RAM) domain that is linked to seven intercellular ankyrin (ANK) repeats by a long and unstructured linker containing a nuclear localization sequence (NLS). Right after the ANK domain is an extra nuclear localization sequence (NLS) and a transactivation domain (TAD). In the C-terminal, a PEST sequence is present and it is responsible for regulation of NCID stability (Figure 1.2) (Kopan and Illagan, 2009).

Notch ligands or DSL ligands are characterized by the presence of a domain called DSL (Delta, Serrate, and Lag2). Like mentioned above, there are five DSL ligands in mammalian classified based on Delta and Serrate of *Drosophila.* Therefore, for mammalian the ligands are nominated as Delta-like (DLL1, DLL3 and DLL4) and Serrate (Jagged) – like (Jag1 and Jag2) (Kopan and Illagan, 2009), and they are all type I transmembrane proteins (Figure 1.2). Although the intracellular domains (ICD) of the Notch ligands present a very low sequence homology (Pintar *et al*., 2007), all ligands share a common organization of their extracellular domains that includes an N-terminal (NT) domain followed by the DSL domain and tandem EGFs. These last domains (EGFs) can, in certain situations, be considered calcium binding domains (Figure 1.2) (D'Souza *et al.,* 2010). Several studies reported that mutations in some residues of the DSL domain lead to a loss in Notch signalling, proving that this domain is essential for ligand-receptor binding (Henderson *et al.,* 1994, 1997; Tax *et al.,* 1994). However, in 1999 Shimizu and his collaborators proved that the DSL domain is required, but not sufficient, for ligand interactions with the receptor. There is also a special motif that plays a key role in Notch binding, that is present in the first two EGFs and is named DOS (Delta and OSM- 11- like proteins) (Cordle *et al.,* 2008a). Canonical ligands have another conserved domain that seems important for function – NT domain. This domain is subdivided into two regions, N1 and N2, being N2 involved in ligand membrane association and endocytosis (Hamel *et al.,* 2010).

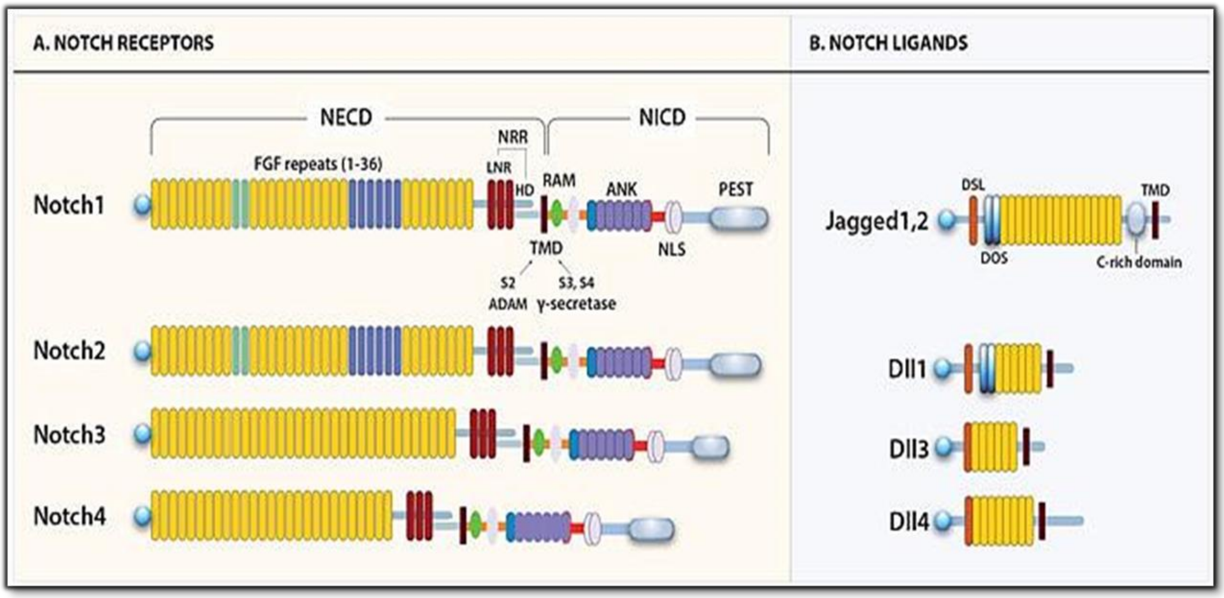


**Figure 1.2- Illustration of Notch receptors and ligands domains**. **A.** Notch receptors' domains. All receptors share the same domains that are included in NECD (Notch extracellular domain) and NICD (Notch intracellular domain).The EGF-like repeats vary from 29 to 36 and regarding the following domains, the receptors share the same structure → NRR (negative regulatory region) that includes three LNRs (cysteine-rich LNR repeats – in red) and an HD (heterodimerization domain); TMD (transmembrane domain) followed by the NCID that is composed by an RAM domain, an ANK : (ankyrin repeat domain - in purple), a NLS (nuclear localizing sequences) and finally a PEST domain (region rich in proline (P), glutamine (E), serine (S) and threonine (T) residues**). B.** Notch ligands' domains. Ligands are grouped into two categories, Serrate-like (Jagged1, Jagged2) and Delta-like (Dll1, Dll3, Dll4). Ligands share the N-terminal domain, the DSL (Delta/Serrate/LAG-2) domain and the EGF-like repeats. Jagged1 and Jagged2 contain a cysteine-rich domain and together with Delta-like 1 ligand they have two DOS (Delta and OSM-11-like proteins) domains. Figure from Yavropoulou *et al.,* 2015.

Experiments designed for the assessment of Notch-ligand interactions with Notch receptors and Jag1 have assigned the minimal binding regions necessary to activate signalization. Initially it was proved that EGFs 11 and 12 of the receptor are necessary and sufficient to bind the ligand (Rebay *et al.,* 1991). However, other studies revealed that EGFs 25-26 probably interact with EGFs 11-13 keeping Notch in its basal state in an inactive form (Sharma *et al.,* 2013). Regarding the DSL ligands minimal binding region it was shown that DSL to EGF2 regions of Jagged1 are critical for binding to Notch2, in a saturated and $Ca^{2+}$ dependent-manner, using two different techniques: a solid-phase binding assay, and a cell based binding assay, using both receptor and ligand mutated forms (Shimizu *et al.,* 1999).

### 1.1.3.1 Structural insights

In 2004, the first structure of a Notch1 receptor fragment was solved by NMR (Hambleton *et al.,* 2004) and four years later a crystal structure of the same region (EGF11-13) was determined (Cordle *et al.,* 2008a). Regarding the Notch ligands, Jag1 structure was the first one to be solved by Cordle and his collaborators, and the x-ray structure published comprised only the minimal binding region. The authors showed that this fragment with four domains adopts a rod-shaped conformation, like the one previously reported for the receptor Notch1 (Cordle *et al.,* 2008a). Recently, a second structure of the same ligand was solved with the receptor-binding region together with the Module N-terminal domain (MMNL) (Chillakuri *et al.,* 2013).This year, Kershaw and co-authors solved the DLL1 N-terminal section containing DSL and EGF1-6 domains, which can now be analysed in close comparison to Jag1 (Kershaw *et al.,* 2015).

In Figure 1.3 it is possible to visualize the similarities between the structures, which are characterized by poor secondary structure content and an extended conformation (except for EGF5-6 of Dll1). These proteins are composed mostly by β-sheets and loops and present a conserved disulphide-bond pattern. In the Notch receptor structure it is possible to observe multiple binding sites for $Ca^{2+}$ ion in the minimal binding region (EGF11-13) and, similarly Jag1 structure presents a $Ca^{2+}$ that binds to the N-terminal region. The N-terminal is a C2 phospholipid recognition domain that binds phospholipid bilayers in a calcium-dependent manor and mutations in this region can lead to a reduction in Notch activity (Chillakuri *et al.,* 2013). Also, the comparison between DLL1 and Jag1 structures reveals that the C2 domains are different, suggesting probable different lipid binding properties.

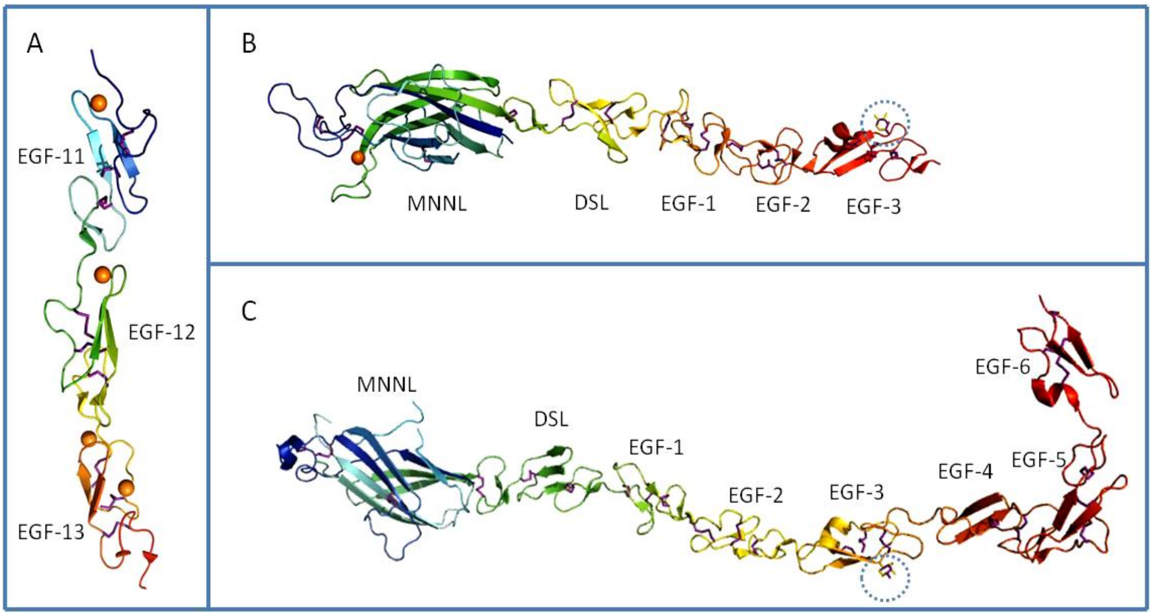


**Figure 1.3 - Structures obtained for Notch receptor and Notch ligands.** (images obtained using PyMol tool where the blue domains represent the N-terminus and the red domains represent the C-terminus). **A.** Notch EGF11-13 structure published by Cordle *et al* (PDB 2VJ3); **B.** Jagged 1 EGF1-3 structure, containing a N-terminal C2 domain published by Chillakuri *et al* (PDB 4CC0); **C.** Delta-like EGF1-6 structure, also containing the N-terminal C2 domains, published by Kershaw *et al* (PDB 4XBM). The dashed blue circle signalizes the fucose binding site and the orange sphere represents the $Ca^{2+}$ atom. The disulphide bonds are represented as purple sticks.

### 1.1.4 Post-translational modifications

#### 1.1.4.1 Ubiquitination

Notch ligands levels at cell surface are regulated by ubiquitination which is also crucial for signalling activity. Two E3 ligases - Neuralized (Neur) and Mind bomb (Mib), interact with ICDs of Notch ligands and influence Notch signalling by ubiquitination of these ligands in the lysine residues, leading to consequent endocytosis and degradation. Studies performed in *Drosophila* support the idea that Neur-induced endocytosis functions to stimulate ligand signalling activity (Deblandre *et al.,* 2001; Lai *et al.,* 2001; Pavlopoulos *et al.,* 2001; Yeh *et al.,* 2001). However, studies in mice did not show the same results, suggesting that the mammalian homolog of Neur is probably not essential for Notch signalling, and other reports proved that other E3 ligases play this role in mammalian. For example, it was proved that Mib ubiquitinates DLL1 and enhances its endocytosis. Nevertheless, this ligase is not capable of reversing the cis-inhibitory effects of the DLL1 ligand in receiving-cells (Koo *et al.,* 2005). Interestingly, Song and his collaborators found that in mammalian cells, Mib is the E3 ligase that triggers the ligand endocytosis and activates the signalling pathway. On the other hand, Neur is a downstream ligase of Mib that promotes directly the lysosomal degradation of ligands and regulates their levels (Song *et al.,* 2006).

#### 1.1.4.2 Glycosylation

O and N-glycosylation occurs in conserved sequences of Notch receptors and ligands, in specific EGF- like repeats. Until now, only O-fucose and O-glucose modifications were related with effects on Notch signalling, while N-glycan additions do not appear to have an impact in normal function of this pathway (Panin *et al.,* 2002). Also, glycosylation of the ligands does not appear to be involved in signalling activity.

### 1.1.5 Notch signalling and disease

Given that the Notch pathway is involved in the development of tissues and organs, it is not surprising that its malfunction is connected to many diseases. It was first associated with T-cell acute lymphoblastic leukaemia (T-ALL) in 1991 and since then it has been linked to a large variety of pathologies, like Alagille syndrome, a hereditary human disease caused by mutations in one of the ligands of Notch receptor - *Jag1* (Li *et al.,* 1997).

#### 1.1.5.1 Notch as an oncogene

T-ALL is an aggressive type of cancer that generally affects children and teenagers. In 1991, when the first case of T-ALL concerning Notch1 was studied, the authors proposed that the normal Notch gene is involved in normal lymphoid development, but its rearranged form may be related with transformation and progression of some of these neoplasms (Ellisen, 1991). Nowadays, it is known that the Notch1 receptor is fundamental for the development of T cell progenitors (Koch *et al.,* 2001), and the growth of T-ALL cell lines that lack chromosomal translocation depend on Notch transducing signals. Moreover, more than a half of T-ALL cases are related to Notch1 mutations involving the PEST domains (Weng *et al.,* 2004b). Also, this oncogenic function of Notch receptors has been extended to solid tumours and it was possible to link both receptors and ligands to neoplasms development or progression (vanEs *et al.,* 2005; Koch and Radtke, 2007; Demehri *et al.,* 2009, Mittal *et al.,* 2009). Despite the many evidences that link Notch pathway to an oncogenic behaviour, in some cases the scenario can be totally different. In murine skin models, it was observed that Notch1 had a tumour suppressor effect (Radtke and Raj, 2003). This observation corroborates with the idea that Notch expression and function is dependent on the cellular context and on the interaction with other pathways.

#### 1.1.5.2 Angiogenesis

The process by which new blood vessels are formed from an existing net of vessels is called angiogenesis. It is complex and it starts with a *stimuli*, and the primary driver of angiogenesis are cells under conditions of hypoxia. These cells secrete many proangiogenic factors and the best studied is the vascular endothelial growth factor (VEGF) (Sharma *et al.,* 2011). Notch is important to maintain the vascular homeostasis, by repressing the proliferation of endothelial cells. In response to VEGF levels, tip cells (non-proliferative cells) begin to express high levels of DLL4 that activates Notch signalling in adjacent cells (Claxton and Fruttiger, 2004). Stalk endothelial cells that have a highly proliferative capacity, downregulate the VEGF receptors´ expression in response to Notch activation, and consequently, inhibit excess formation of sprouts that allow new vessels to grow. On the other hand, Jag1 does the opposite and stimulates new vessels growth, antagonizing DLL4 action (Benedito *et al.,* 2009). Since DLL4, Jag1 and Notch1 are involved in vasculature formation and homeostasis it is normal that aberrant expression of any of these genes plays an important role in tumour progression and survival, which makes these proteins good therapeutic targets. Blockage of Notch signalling using a DLL4 antibody led to regression in different types of tumours (Noguera-Troise *et al.,* 2006; Ridgway *et al.,* 2006). However, other studies proved that long-term inhibition of Notch signalling can have bad consequences to the organism (Wu *et al.,* 2010). So, probably, Notch inhibition has different effects depending on the type of tumour. Finally, several findings suggest that the Notch pathway may have a role helping the tumour to adapt to the hypoxic environment present in cancer, through interaction with hypoxia inducible factor-1 alpha (HIF-1α), whose regulation promotes cells adaptation to low oxygen levels (Gustafson *et al.,* 2005; Saison and Harris, 2006).

#### 1.1.5.3 Cancer stem cells

Cancer stem cells (CSCs) are a sub-population of cells with highly proliferative potential and self-renewal ability. Their division is asymmetric, giving rise to stem cells and differentiated cancer cells (Li *et al.,* 2014). CSCs have also a great invasive capacity and apparent resistance to many cancer treatments, and have been associated to metastatic events and relapse of some patients (Creighton *et al.,* 2009; Singh *et al.,* 2014).

Notch receptors 1 and 4 have been described as more activated in CSCs of breast cancer (Weng *et al.,* 2004a). Other studies proved that Jag1 is an inducer of stem cells phenotype and the main ligand in Notch signalling activation of CSCs, in different types of cancer, including breast cancer (Li *et al.,* 2014).

### 1.1.5.4 Breast cancer

In our days, breast cancer represents the most common cause of death from cancer in women all over the world. Because it has a lifetime risk of one in nine and its incidence continues to increase, many efforts in the science field have been taken trying to find out what triggers this type of cancer, in order to develop efficient treatments. Recently, several groups have linked abnormal expression of Notch signalling receptor and ligands to breast cancer. Mittal and his team showed that a crosstalk between Notch and Ras/mitogen activated protein kinase (MAPK) signalling pathways apparently leads to a poor prognostic of the patients (Mittal *et al.,* 2009). Moreover, Notch has been related to the invasive behaviour of cancer cells. Breast cancer metastases in the bones are the most common ones, leading to severe fractures and pain, among other complications (Mundy *et al.,* 2002). The linkage of Jag1 and transforming growth factor beta (TGF-β) pathways is able to create a positive feedback loop between tumour and bone cells promoting osteolytic bone metastasis (Sethi *et al.,* 2011). Another important feature of metastatic behaviour is the Epidermal - to - mesenchymal transition (EMT), phenomena that occurs during development, but can be reactivated by cancer cells. EMT is described as being important for tumour metastasis and progression, in which Notch may play a critical role. It can modulate down regulation of E-cadherin by TGFβ and, consequently interfere with normal cell-cell adhesion (Timmerman *et al.,* 2004; Zavadil *et al.,* 2004).

### 1.1.5.5 Notch inhibition as a treatment for cancer

Normally, it is easier to develop inhibitors against enzymes. As mentioned before, in the canonical Notch pathway, there are two proteolytic steps where enzymatic reaction occurs, first with alpha-secretase complex and second with γ-secretase complex. So, investigators have designed small molecules in order to inhibit Notch signalling, and gamma-secretase inhibitors (GSIs) were the first to be used in research and clinic. However, these molecules are not very specific since gamma-secretase interacts with other targets like E-cadherin, nectin-1 alpha or even APP (amyloid precursor protein). On the other hand, if we think that these targets are also described as candidates for cancer therapy, maybe the use of GSIs can, in fact, be very helpful (Purow *et al.,* 2012). However, the lack of specificity of GSIs and consequent inhibition of other pathways, as well as their ability of blocking both Notch1 and Notch2, has been associated with intestinal toxicity (vanEs *et al.,* 2005). To better understand the role of both receptors and create less toxic inhibitors, Wu and his team have developed antibodies against Notch1 and Notch2 receptors using the phage display technology. Co-crystallization of these highly specific antibodies with both receptors, revealed the therapeutic potential of inhibiting Notch1 and Notch2 individually by unveiling relevant interactions (Wu *et al.,* 2010).

### 1.2 Phage display: antibodies development

In 1985, Smith presented for the first time the phage display technology (Smith *et al.,* 1985). This technique uses genetic engineering of filamentous bacteriophages to display peptides and proteins (e.g. antibody fragments) at their surface. The DNA of interest is cloned into a specific region of the bacteriophage's genome resulting in the "display" of proteins or peptides at the surface, in fusion with one of the phage coat proteins (Azzazy and Highsmith, 2002). By carrying out several rounds of selection against a target it is possible to develop *in vitro* a specific antibody fragment that can after be reformatted into a complete monoclonal antibody (mAb) and further used in diagnosis, research and/or therapeutics (Barbas *et al.,* 2004; Lee *et al.,* 2007).

#### 1.2.1 The antibody molecule

Antibodies (Abs) play a crucial role in immune response by targeting antigens for destruction by other cells. They are "Y-shaped" glycoproteins part of immunoglobulins (Ig) family and are divided into five classes: IgG (γ), IgM (μ), IgA (α), IgD(δ) and IgE(ε), being IgG the most abundant antibody in the serum. These five classes share the same structure with two heavy chains (HC) with at least 50 kilo Daltons (kDa) each and two light chains (LC) with 25 kDa each. The LCs can be subdivided into two forms, known as kappa (κ) and lambda (λ), and these are linked to each HC by a disulfide bond. HCs are linked between them by several disulfide bonds. The HC and LC connection generates the Ab molecule, which is joined by a flexible polypeptide chain – the hinge region (Murphy, 2011; Delves *et al.,* 2006).

The Ab class or isotype is defined according to the constant region carboxy-(C) terminal of HC, which determines the biological function of the Ab. On the other hand, the variability of the Ab is present in the region composed by the first 100 amino acids, in the amino-(N)-terminal regions of both LC and HC, and this constitutes the variable (V) region of an Ab molecule. Inside, there are hypervariable regions, often referred as complementary determining regions (CDRs), divided into three segments - CDR1, CDR2 and CDR3, and these are the regions responsible for Ab specificity. The remaining portions of the V region are called the framework regions (FR) and are less variable than the CDRs. As for the constant (C) region it is referred as CL for light chain and CH for heavy chain. It presents a similar sequence between Abs of the same class, and the HCs can contain three or four domains namely CH1, CH2, CH3 and CH4 (Murphy, 2011; Delves *et al.,* 2006; Elgert, 2009).

The Ab molecule is composed by two distinct fragments. The first results from the non-covalent interaction of VL with VH, and CL with CH1, originating the "antigen binding Fragment" (Fab), which contains the antigen binding activity. The other is the "crystallisable Fragment" (Fc), and is composed by the remaining CH regions (CH2 and CH3). This portion is responsible for the interaction with other cells and effector molecules of the immune system (Delves *et al.,* 2006) (Figure 1.4).

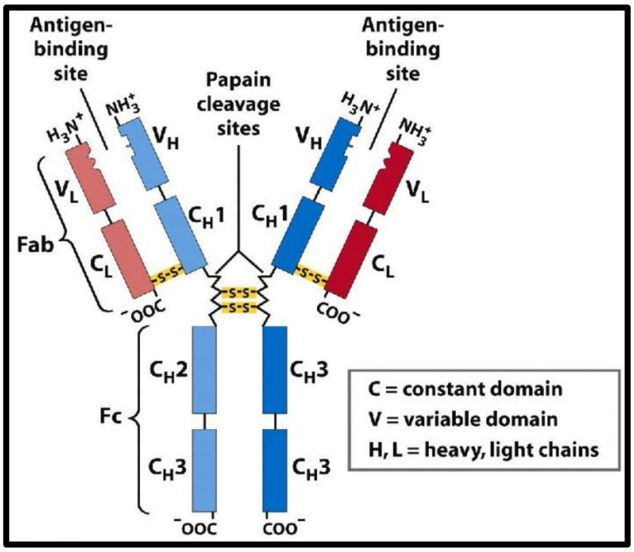


**Figure 1.4 - Antibody structure.** The antibody is divided into two chains (heavy and light chain) which have two regions: the variable and the constant regions. In the centre of the molecule there is the hinge region, represented here as "papain cleavage site". Papain is an enzyme that digests the molecule and divides it into three - two Fab fragments and one Fc fragment. Figure from *Legninger, 5$^{th}$ edition*.

From the genetic point of view, each HC is encoded by four gene segments: $V_H$, $D_H$, $J_H$ and $C_{H,}$ while the LC is encoded by $V_{L,}$ $J_L$ and $C_L$ segments. The combination of the $V_H$-$D_H$-$J_H$ with the $V_L$-$J_L$ regions creates the paratope which is the antigen-binding region and recognizes a single site of the antigen – the epitope (Azzazy and Highsmith, 2002). Diversity is achieved through a highly regulated and ordered process called V(D)J recombination that occurs during B cells development. Rearrangement of the $D_H$-to-$J_H$ segments of the HC is the first step in V the (D)J recombination process. Next, the $V_{H}$-to-$D_HJ_H$ rearrangement occurs on precursor B cells giving rise to the $VDJ_H$ HC genes that bind to the $C_H$ gene. Finally, the $V_L$-to-$J_L$ rearrangement takes place, by binding to the $C_L$ gene, and the LC genes are produced. (Figure1.5) (Schatz, 1992).

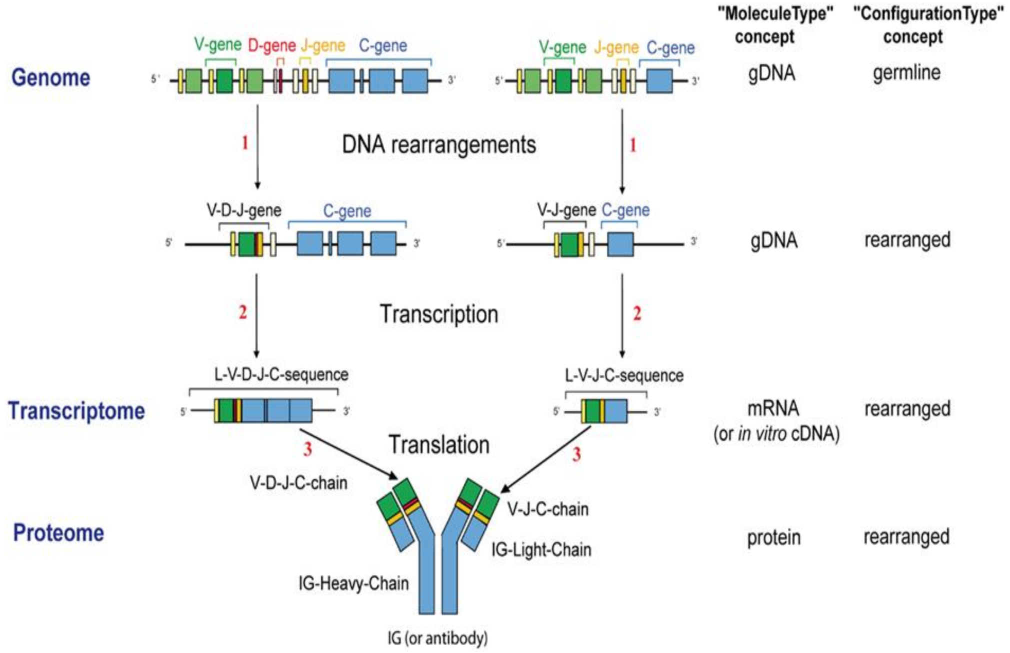


**Figure 1.5 - The V(D)J recombination.** The process begins with the rearrangement of the VDJ fragments of the heavy chain, followed by the light chain. Figure from Giudicelli and Lefranc, 2012.

### 1.2.2 Generation of an antibody library

The first step of phage display is the generation of an antibody library. Different libraries include libraries for Ig isotypes (e.g., IgG, IgA, and IgE) or libraries of mAbs – Fab fragments or single-chain variable fragments (scFv) (Figure 1.6) (Hammers and Stanley 2013).

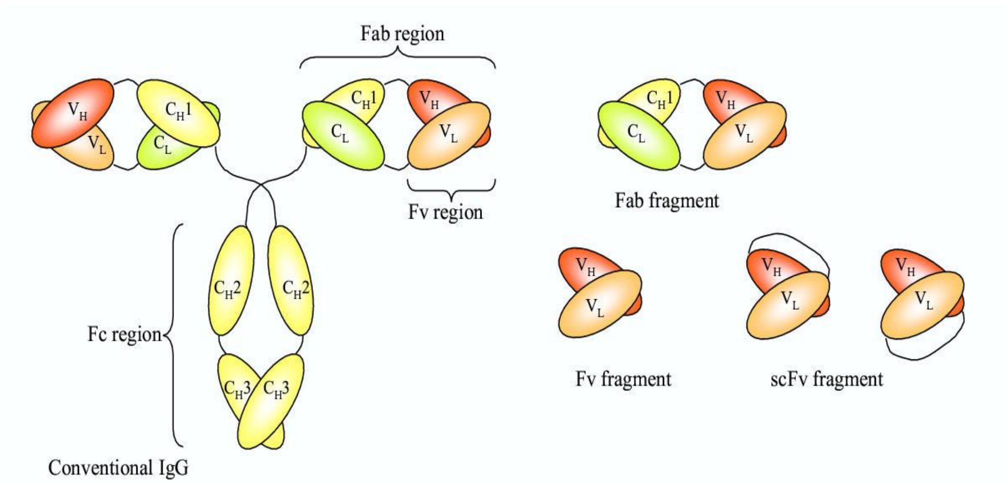


**Figure 1.6 - Representation of antibody structure and fragments.** Figure from Joosten *et al.,* 2003.

Library preparation begins with the collection of messenger Ribonucleic acid (mRNA) from a cell source, like peripheral blood mononuclear cells. After isolation, the mRNA is converted into complementary DNA (cDNA) and the VH and VC genes are amplified by Polymerase Chain Reaction (PCR). The DNA amplification is achieved using sets of primers that are specific for all the conserved

V-genes of the IgG repertoire of a given individual (Hammers and Stanley 2013). Libraries can be divided into "single pot" and immune, depending if the donor was previously immunized with the antigen or not. "Single-pot"¨ libraries include naïve, semi-synthetic and synthetic libraries, and are designed to produce Ab against a large number of antigens (Hoogenboom, 2005; Shirrmann *et al.,* 2011). Immune libraries are constructed using IgG mRNA of B cells from an immunized donor. These libraries are enriched in Abs specific for the chosen antigen, allowing the selection of high-specific antibodies with small libraries (Bazan *et al*., 2012; Hoogenboom *et al.,* 1998). However, the use of immune libraries can be a very laborious process when the goal is to produce specific Abs against distinct targets, since it is necessary to create a new library for every antigen, although more comprehensive sources are often used i.e. donors in specific conditions with high expression of diverse targets (e.g. cancer patients) (Watkins and Ouwehand, 2000).

### 1.2.3 Filamentous bacteriophages and phagemid vectors

Bacteriophages are viruses that can infect Gram-negative bacteria through interaction of Fl filamentous phage particles with the bacterial F Pili receptor. These phages express around 2700 copies of gene 8 protein (g8p or pVIII), often called "the major capsid protein", and 3 to 5 copies of the gene III (g3)-encoded adsorption protein (g3p or pIII). Ab fragments produced by phage display are normally fused to g3p and, consequently displayed at the surface of the phage (Figure 1.7) (Azzazy and Highsmith, 2002; Dente *et al.,* 1994).

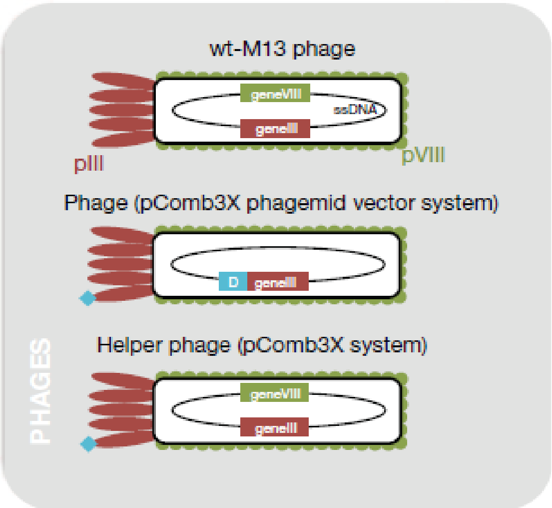


**Figure 1.7 - M13 use in phage display.** In wild type M13 (WT) the single-stranded DNA (ssDNA) codifies for both capside proteins – pIII and pVII. In phage display phagemid vectors can be used, i.e. like pComb3X bearing the gene of interest (D) fused to gene III, but lacking gene VIII, that is provided later by the helper phage essential for phage replication. Figure from Hammers and Stanley, 2013.

Cloning of the Ab fragments fused with g3p protein is often achieved using phagemids that contain both M13 phage and *Escherichia coli* (*E.coli*) origins of replication, the g3p gene (gene III), appropriate multiple cloning sites and an antibiotic resistance (Mead and Kemper, 1998). Nevertheless, phagemids differ from phage vectors since they lack the rest of the genes required to produce a complete phage, so in this case a helper phage is needed. Helper phages like M13KO7 or

VCSM13 contain and supply all the remaining genes necessary to generate the phage particles (Figure 1.7), and once they are built inside the bacteria (e.g. *E.coli* TG1) they are secreted (Azzazy and Highsmith, 2002).

### 1.2.4 Pannings

Following the library construction, it is necessary to screen against the chosen target. This technique is called panning and is characterized by several rounds of phage binding to the target (antigen), washing to eliminate the non-binders, elution to recover the binders and re-amplification of the eluted phages in *E.coli* (the TG1 bacterial strain is normally used in this step) (Figure 1.8). In each round, the phage pool from the previous round is used for selection. Normally, a depletion step using a non-target is performed before the selection step to retain the non-specific binders. After three or four rounds of selection the phage population is enriched with highly specific clones that can be detected by phage Enzyme-Linked Immunosorbent Assay (ELISA) (Barbas *et al.,* 2004). This technique allows the detection of the clones that express Fabs specific for the antigen. It begins with antigen coating, incubation of the phage pool with the coated antigen, and washing of the non-binders. Detection is commonly carried out using an antibody against the major capsid protein (M13) conjugated with an enzyme (e.g. Peroxidase). Eventually, if the antibody used in non-conjugated a second incubation with a different antibody might be required using a secondary conjugated-antibody that binds the first.

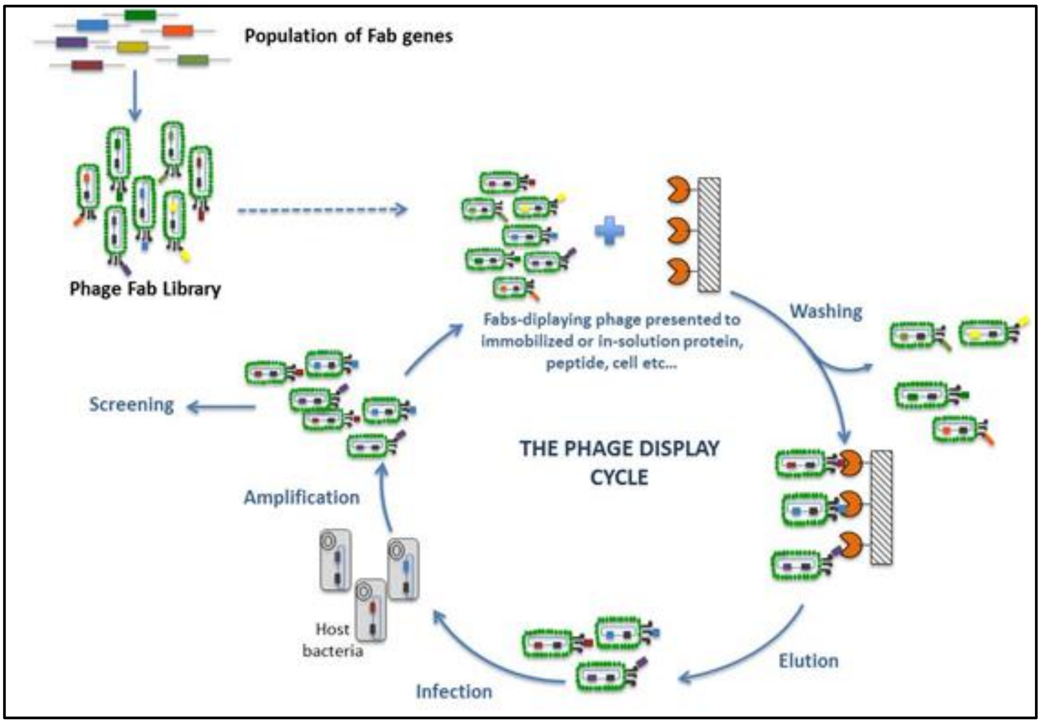


**Figure 1.8- Phage display cycle for selection of Ab fragments**. Figure from *FairJourneyBiologics*. (http://www.fjb.pt)

### 1.3 Goals

The first goal of this thesis is to optimize the conditions for expression and purification of Notch ligands, in order to obtain a good quality target. The second and main goal of this thesis is to develop a function blocking antibody against the ligands produced, using the phage display technology. Aiming at the inhibition of the interaction between the notch receptor and its ligands, it is expected that the produced antibodies can be used in therapeutics for breast cancer, since this disease has been related with an abnormal function of the Notch signalling pathway. Finally, we also pretend to gain some structural insights by solving the 3-D structure of the Notch ligands alone and in complex with the specific antibody, in order to understand the interactions between them and contribute to the knowledge of how the inhibition specifically takes place.

# 2- Materials and methods

## 2.1 Molecular Biology

All primers were all designed using CloneManager Suite 7 software and synthesized by StabVida. PCR steps were performed in the Thermal cycler - MyCycler (Bio-Rad). For DNA extraction, Miniprep kit from Thermoscientific was used. DNA purifications were made using either ThermoScientific GelPure Kit or NzyTech Gel Pure kit. Quantification of the pure DNAs was performed by spectrophotometry using NanoDrop ND-1000 spectrophotometer (Alfagene). All steps of cloning were monitored by electrophoresis using 1% agarose gels. To transform DNAs in cloning steps, electrocompetent DH5α (see Section 5.2 for strains genotype) were used and transformed by electroporation (2500 volts shock), using the Eletroporer (Eppendorf).

### 2.1.1 Notch ligands cloning

#### 2.1.1.1 pET-47b (+) (*E.coli*) and pHL-sec (mammalian – HEK293T)

Twelve different constructs of three of the Notch I ligands – DLL1, Jag1 and Jag2, were previously cloned in pET47b (+) and pHL-sec vectors by Margarida Silva in her MSc (Silva, 2014) as summarized in Table 2.1.

#### 2.1.1.2 pETfh8

In order to increase the expression of the ligands in the soluble fraction in the *E.coli* strain used, a different vector was chosen, pETfh8, containing *Fasciola hepatica* antigen 8kDa (Fh8) tag. hDLL1_MNNL-DSL and hDLL1_MNNL-EGF3 constructs were cloned in this plasmid.

Amplification of the fragments was achieved using the following PCR mix: hDLL1 cDNA (dilution 1:100), 0.4 mM of deoxynucleotides tri-phosphate (dNTPs), 0.4µM of primers forward and reverse (see table 2.1), 1x *Pfu* buffer, 1.25 units of *Pfu* polymerase and RNase free water to a final volume of 50µL. The program used began with a denaturing cycle at 95°C during 4 minutes, followed by 35 cycles of a denaturing step (95°C) of 30 seconds, annealing step (54-62°C) for 30 seconds and extension step (72°C) for 2 minutes. Finally 1 additional extension step was carried out for 10 minutes at 72°C. Amplified fragments were purified from the agarose gel and both fragments and plasmid were digested during 4 hours at 37ºC. hDLL1_MNNL-DSL and pETfh8 were digested with *Nco*I/*Xho*I, while hDLL1_MNNL-EGF3 was digested with *Pci*I/*Xho*I. *Nco*I enzyme was not used for the second fragment because it cuts inside the fragment. So, in alternative, a complementary restriction enzyme, *Pci*I, was chosen. After heat inactivation of the enzymes at 85ºC and purification of the digested DNA, ligation was carried out using 2.5 units of T4 DNA ligase together with 1x Buffer T4 Ligase and two different proportions vector:insert, namely 1:3 and 3:1. The mixture was incubated overnight (o/n) at 16°C, transformed in DH5α and plated in LB agar plates with 50µg/mL of kanamycin. On the next day, colony PCR was carried out to evaluate the ligation outcome. The reaction mix components were:

1mM of dNTPs, 0.4mM of the same primers mentioned before, 1.25 units of *Taq* DNA Polimerase and respective buffer (1x), 2 mM of $MgCl_2$, 4% dimethyl sulfoxide (DMSO) and RNase free water to achieve a final volume of 25µL per reaction. The program was similar to the one used in the amplification step with the following alterations: the first denaturing cycle was at 95°C, and 30 cycles were used with 59ºC for annealing. After analysing the colony PCR results, DNA of the positive hits was extracted and digested with *Xho*I/*Hind*III to recheck if the colonies presented the correct fragment. DNA of the positive colonies was also sent for sequencing by Stabvida or GATC. Finally, DNA from the chosen colonies was transformed in BL21(DE3)Star/pRARE2 and plated in LB Agar with chloramphenicol at 30µg/mL and kanamycin at 50µg/mL for further protein expression tests.

**Table 2.1 - Primers used to amplify Notch ligands.** R.E. – Restriction enzymes. The letters in bold represent the restriction enzymes sites. The underlined letters represent the linker between the ligand and the tag. (F) – forward primer; (R) – reverse primer.

| Plasmid | Ligand | Domain | R.E. | Primer |
|---|---|---|---|---|
| **pET47-b (+)** | **hJag1** | MNNL | ***Eco*RI** | 5'- GAGTATCA**GAATTC**CGTGACCTGTGATGAC - 3' (F) |
| | | DSL | ***Eco*RI** | 5'- GCAGGC**AAGCTT**AGCCTATTCACAGTTGG - 3' (F) |
| | | EGF3 | ***Hind*III** | 5'- GCAGT**AAGCTT**TCAGTTATGAGCAGTTCTTG - 3' (R) |
| | | EGF9 | ***Hind*III** | 5'- GTGCA**GAATTC**ACGTCCGATGGGTTATTTTG - 3' (R) |
| | **hJag2** | MNNL | ***Eco*RI** | 5'- CTGCA**GAATTC**TGTTCGCTGCGATGAAAAC - 3' (F) |
| | | DSL | ***Eco*RI** | 5'- CGTGCAGGC**AAGCTT**CGCTTATTCACAGTTGC - 3' (F) |
| | | EGF3 | ***Hind*III** | 5'- CACGGT**AAGCTT**GGCTAGCTACAGTTTTTAC - 3' (R) |
| | | EGF9 | ***Hind*III** | 5'- CCTT**GAATTC**TCAGGTCTGGAGCTC - 3' (R) |
| | **hDLL1** | MNNL | ***Eco*RI** | 5'- CTCAA**GAATTC**CTACCGCTTCGTGTGTG - 3' (F) |
| | | DSL | ***Eco*RI** | 5'- CTCGTC**AAGCTT**CAGCTAGCAGGTGGCACC - 3' (F) |
| | | EGF3 | ***Hind*III** | 5'- CGTC**AAGCTT**GTCCTAACAGTGCCTCCC - 3' (R) |
| | | EGF6 | ***Hind*III** | 5'- CCAAGGTG**ACCGGT**GCCTCGGGTCAGTTCG – 3' (R) |
| **pHL-sec** | **hJag1** | MNNL | ***Age*I** | 5'- CCAAGGTG**ACCGGT**GCCTCGGGTCAGTTCG - 3' (F) |
| | | DSL | ***Age*I** | 5'- GCATGATCAACCCC**ACCGGT**CAGTGGC - 3' (F) |
| | | EGF3 | ***Kpn*I** | 5'- GCAGGC**GGTACC**AGCAATTTCACAGTTGG - 3' (R) |
| | | EGF9 | ***Kpn*I** | 5'- GCTGCG**GGTACC**GTCTTTCAGGTGTGAGC - 3' (R) |
| | **hJag2** | MNNL | ***Age*I** | 5'- GCACTG**ACCGGT**CAGGCACGACGTCCG - 3' (F) |
| | | DSL | ***Age*I** | 5'- ATGATC**ACCGGT**GAAGACCGCTGGAAATCACTGC - 3' (F) |
| | | EGF3 | ***Kpn*I** | 5'- CGGGTTAGA**GGTACC**GGCATGTTCCGC - 3' (R) |
| | | EGF9 | ***Eco*RV** | 5'- CGACAGGCACCACCC**GATATC**GGTTCACG - 3' (R) |
| | **hDLL1** | MNNL | ***Age*I** | 5'- GTGTCAG**ACCGGT**AGCTCTGGGGTGTTCG - 3' (F) |
| | | DSL | ***Age*I** | 5'- CGGTCGGC**ACCGGT**TGGTCCCAGGACC - 3' (F) |
| | | EGF3 | ***Kpn*I** | 5'- GGTGACACTC**GGTACC**CCCCAGCTCGC - 3' (R) |
| | | EGF6 | ***Kpn*I** | 5'- GCGCA**GGTACC**CTCGTTGTCGTCACAGTGC – 3 ' (R) |

| | | | | |
|---|---|---|---|---|
| **pETfh8** | **hDLL1** | MNNL | ***Nco*I or *Pci*I** | 5'- GCT**CCATGG**CATCCATGGGCTCCCAGGTCTGGAGCTCTGGGTGT- 3' (F)<br>5'- GCT**ACATGT**TGTCCATGGGCTC CAGGTCTGGAGCTCTGGGTGT - 3' (F) |
| | | DSL | ***Xho*I** | 5' -TGA**CTCGAG**CAGCAGTAGGGCCCTTTCCAG - 3' (R) |
| | | EGF3 | ***Xho*I** | 5'- GCGCA**GGTACC**CTCGTTGTCGTCACAGTGC - 3' (R) |

## 2.2 Protein expression in *E.coli*

### 2.2.1 Expression tests

In order to achieve an optimal expression in *E.coli*, several conditions were tested for nine of the constructs of pET47(b)+. Bacteria strains BL21Star (DE)/pRARE2 or BL21(DE3) were transformed with pET47(b)+ cloned with Notch ligands and also with pGRO7, a plasmid that contains two molecular chaperones GroEL and GroES.

First, a pre-inoculum was prepared with 5mL of Luria-Bertani broth (LB) medium with the appropriated antibiotics, inoculated with a loop of bacteria and incubated overnight at 37ºC and 250 rotations per minute (rpm). On the next day, the cultures were prepared using 20mL medium, antibiotics and pre-inoculum in a certain volume that the final starting $OD_{600nm}$ was approximately 0.05. The culture was grown until the chosen $OD_{600}$ for induction and 0.1 or 0.5mM of Isopropyl β-D-1-thiogalactopyranoside (IPTG) and L-arabinose (to induce pGro) at 4mg/mL were added. A sample of non-induced culture was taken before induction to be used as a negative control. After induction (culture with $OD_{600nm}$ = 0.8-1) two samples of the culture corresponding to 1OD (optical density), together with the non-induced sample, were centrifuged at 13200x*g* and 4ºC, during 15 minutes. Pellets from the non-induced sample and of one of the samples taken after induction were resuspended in 1x Loading buffer (see Section 5.3). The remaining pellet was used for cell lysis to separate the soluble fraction from the insoluble one. The pellet was resuspended in BugBuster 10xProtein-Extraction-Reagent (Millipore) supplemented DNase I, incubated during 15 minutes on ice and centrifuged at 13200x*g* and 4ºC, during 15 minutes. After centrifugation, the supernatant was transferred into a new tube and 4x Loading Buffer was added to premake the same final volume of the other samples. Pellet was resuspended in 1x Loading Buffer and all the samples prepared were stored at – 20ºC. All the results were monitored by Sodium Dodecyl Sulphate Polyacrylamide Gel electrophoresis (SDS-PAGE) and/or Western Blot analysis using Penta-His as primary antibody (dilution 1:2000) and anti-mouse horseradish peroxidase (HRP)-conjugated as secondary antibody (dilution 1:3000). Expression tests for pETfh8 were performed following the same protocol.

### 2.2.2 Expression and purification of hDll1-DE3 – *E.coli*

The protein was obtained from refolding of inclusion bodies and for that, two different protocols were used. All the steps from expression to purification were monitored by SDS-PAGE and Western blotting, and protein quantification was measured by UV spectrophotometry at A280.

#### 2.2.2.1 Solubilisation with Guanidine-HCl and L-arginine refolding

The first protocol was adapted from previous tests made by Margarida Silva, MSc (Silva, 2014). Buffers composition is described in Appendix 5.3.1.1. First, 2L of culture (BL21 Star(DE)/prare2 transformed with pET47(b)+_hDLL1-DE3) were grown in Power Broth (PB) medium with kanamycin (50µg/mL) and chloramphenicol (30µg/mL) and when the $OD_{600nm}$ was 0.9 the culture was induced using 0.5mM IPTG and incubated o/n at 20°C. The bacterial pellet was obtained by centrifuging the culture at 7500x*g*, at 4ºC for 30 minutes and stored at -80ºC. Cell lysis was performed resuspending the pellet in Lysis Buffer A and sonicating the cells for 3-4 minutes (10 seconds on; 10 seconds off) with an amplitude of 35%. Then the culture was centrifuged at 10 000x*g*, at 4ºC during 30 minutes. Inclusion bodies were then washed with two washing solutions – Wash IA and Wash IIA. The pellet obtained was resuspended in Wash IA on ice and centrifuged 15 minutes at 30 000x*g* and 4ºC. This procedure was repeated four times and finally the pellet was resuspended in 15mL of Wash IIA on ice and centrifuged during 15 minutes at 30 000x*g* and 4ºC. The supernatant was discarded and the pellet, containing the pure inclusion bodies, was resuspended in 10mL of Solubilisation Buffer A, that was prepared with guanidine-HCl to denature (solubilise) the inclusion bodies, and incubated o/n at 4ºC and gentle agitation. After incubation, the solution was centrifuged for 30 minutes at 4ºC, and 16 000x*g*. The supernatant was collected into a new tube and stored at -20ºC before proceeding with refolding. The total amount of protein was measured in order to calculate the volume of refolding buffer in which the inclusion bodies had to be diluted. The refolding was achieved diluting the protein to a final concentration of 0.1mg/mL. For that, the denatured inclusion bodies were added dropwise to the Refolding Buffer A, at 4ºC, and gentle agitation, and the mixture was incubated for 48h. After, the refolded inclusion bodies were filtered (0.22µm filter) and the protein was concentrated in a Diaflow (Molecular weight cut-off (MWCO) of 10 kDa).

Purification was achieved by performing a desalting step to remove the components present in the Refolding Buffer, where two HiPrep 26/10 Desalting columns were used in series. The columns were first equilibrated with the Desalting Buffer and after, the refolded protein was injected at 1-2mL/min. 2 peaks of each injection step were collected - $1^{st}$ peak corresponding to the protein in the new buffer and the $2^{nd}$ peak corresponding to the old buffer. The selected fractions were pooled and concentrated using Diaflow and AMICON (MWCO 10KDa). Finally, the protein aliquots were froze in liquid nitrogen and stored at -80ºC.

#### 2.2.2.2 Solubilisation with urea and refolding

In order to improve the yield of purified protein, a new protocol adapted from Zhao *et al,* 2009 was followed. The expression of the protein was the same mentioned before (Section 2.2.2.3). Cell lysis was performed in Lysis Buffer B using three cycles in French Press followed by centrifugation at

10 000x*g*, at 4ºC during 30 minutes. The pellet was initially resuspended 4 times in solution Wash IB and centrifuged at 15000x*g*, for 15 minutes at 4ºC, and secondly resuspended 1 time in solution Wash IIB and centrifuged in the same conditions. Solubilisation was achieved with urea by resuspending the pure inclusion bodies in Solubilisation Buffer B (9mg pellet - 81 mL buffer) and incubating in agitation for 1 hour at 37ºC. The mixture was centrifuged at 4ºC, 16 000x*g* for 15 minutes. The supernatant was added dropwise to 800mL of Refolding Buffer IB with agitation at 4ºC and after that 800mL of the Refolding Buffer IIB was added dropwise to the mixture in order to adjust the pH to 9.1. The mixture was incubated at 4ºC with gentle agitation during 24h and the solution containing the refolded protein was filtered and stored at 4ºC before purification.

All the purification steps were performed at 4ºC in Akta Prime (GE Healthcare). The first step of purification was an anionic exchange chromatography (AIC) using a HiPrep Q HP 16/10 that was pre-activated with 1 column volume (CV) of Buffer AIC-B and then equilibrated with Buffer AIC-A. The protein was injected o/n and was eluted using a NaCl gradient (0-100% in 200mL) with Buffer AIC-B. After, a 5mL Histrap FF column was used, equilibrated with Buffer Histrap A and injecting o/n. Two injections were made. Before the first injection the column was washed with 10 CVs of Buffer Histrap B and the protein was first eluted with an imidazole gradient using Buffer Histrap C (0-100% in 100mL) and with Buffer Histrap D using 3 steps – 25%, 50% and 100%. On the second injection, the elution was made with a gradient of imidazole using Buffer Histrap D (0-100%). All pools obtained were concentrated and changed to a final Buffer – 20mM Tris-HCl, 300mM NaCl. Finally, the protein was distributed in aliquots and froze with liquid nitrogen to store at -80ºC.

## 2.3 Protein expression in mammalian cells HEK293T

### 2.3.1 Cell culture

To express Notch ligands in mammalian cells Human Embryonic Kidney 293T cell line - HEK293T was used. These adherent cells were maintained using Dulbecco's Modified Eagle Medium (DMEM) supplemented with 10% Fetal Bovine Serum (FBS) at 37ºC with 95% humidity and 5% $CO_2$ atmosphere. Sub-culturing was performed when the cells reached 85-95% confluency using PBS for to the wash step, and 0.05% Trypsin-EDTA for 5 minutes to detach them. To inactivate the trypsin DMEM supplemented with 10% FBS was used. The cells were diluted 1:10 or 1:20 depending on the interval between sub-cultures. To keep track on the efficiency of sub-culturing, cells were counted using the heamacytometer with Tryptan Blue Dye and the appropriate dilution to allow counting 20-50 cells per square (4 diagonal squares were counted in each site of the heamacytometer).

### 2.3.2 Expression tests in HEK293T

Transient transfection of HEK293T cells using the constructs hDLL1-DE3, hDLL1-DE6, hJag1-ME3, hJag2-DE3, hJag2-ME3 and hJag1-ME9 in pHL-sec was carried out. The empty pHL-sec vector (i.e. no fragment cloned) was always included as negative control. Cells were seeded using DMEM supplemented with 10% FBS and 100 mg/ml penicillin and 100U/ml streptomycin and were incubated o/n at 37ºC with 95% humidity and 5% $CO_2$ atmosphere. On the next day, cells medium was discarded and replaced by fresh DMEM with serum. Cells were transfected using polyethylenimine (PEI) at 1µg/µL and a 3:1 or 2:1 PEI:DNA ratio, depending on the PEI batch. Also, different final concentrations of DNA were also tested. Transfection efficiency was evaluated using as a positive control the pAAVPURO kindly provided by Gabriela Silva, PhD. This vector has the green fluorescent protein (GFP) cloned that allows the visualization of transfected cells by fluorescence microscopy (Leica Microsystems GmbH). After transfection, the medium was removed, centrifuged at 13 200x*g* for 5 minutes at 4ºC and the supernatant was collected to a new tube. A sample of the collected supernatant was mixed with 4x Loading Buffer and was analysed by Western blot.

### 2.3.3 Expression and purification of hDLL1-DE3 in HEK293T

Production and purification of the protein was achieved using T225cm$^2$. Two purifications were performed and all the buffers are described in Appendix 5.3.2. All the steps from expression to purification were monitored by SDS-PAGE or Western Blot.

#### 2.3.2.1 First strategy

Ten 225cm$^2$ t-flasks were used to produce the protein. To seed each T-flask, a 4x10$^4$ cells/cm$^2$ cell density was used. On the next day, cells were at 75% confluence approximately and were transfected using a PEI:DNA ratio of 2:1 (45µg of DNA per T-flask) and subsequently incubated for 72h in DMEM + 2%FBS at 37ºC and 5% $CO_2$. Transfection efficiency was evaluated using pAAVpuro with GFP at 48h post-transfection. After 72h, the culture media from each T-flask (45mL x 10 = 450mL) was removed and centrifuged at 2000x*g* for 20 minutes. The supernatant was collected, filtered (0.22µm filter), concentrated in a Vivaflow 200 (MWCO 10kDa) and washed with DMEM until a final volume of 80mL. The medium was again filtered, froze using liquid nitrogen, and stored at -80ºC.

Purification was achieved performing a Histrap affinity step followed by Size Exclusion Chromatography (SEC) step using an Akta Purifier system (GE Healthcare). A Histrap FF 5mL column was equilibrated with Buffer Histrap 1A and the sample was filtered and injected at 1 mL/min. The column was then washed with 10 column volumes (CV) of Buffer Histrap 1B and when the UV line was stable, the protein was eluted with 3 steps of imidazole using Buffer Histrap 1C – with 20%, 50% and 100%, respectively, finalized by 100% of Buffer Histrap 1D. The pool collected from the Histrap was concentrated in an Amicon Ultra Centrifugal Filter (MWCP 10kDa) to a final volume of 2,5mL, and subsequently injected in a HiLoad 16/600 Superdex 75 pg column. The SEC column was previously equilibrated with Buffer SEC 1 and the protein was injected at 1mL/min. Finally the protein was concentrated using an Amicon (MWCO 10kDa) and quantified using Bradford method. Protein was aliquoted and froze in liquid nitrogen to store at -80ºC.

#### 2.3.2.2 Second strategy

In a second production, thirty three 225cm$^2$ t- flasks were seeded and transfected using the same conditions mentioned for batch 1. The culture medium was collected after 48h and treated the same way that in Section 2.3.2.1 with the exception that a cocktail of protease inhibitors was added to the medium after centrifugation. After concentration in a Vivaflow 200 (MWCO 10kDa) the volume was 45mL and the medium was filtered and froze in liquid nitrogen to store at -80ºC.

This purification was made at 4ºC using both an Akta Prime and Akta Purifier systems (GE Healthcare). Two steps were carried out – a Histrap affinity followed by SEC. The Histrap FF column was equilibrated with Buffer Histrap 2A and the sample was filtered and injected at 1,5mL/min. Washing was performed using Buffer Histrap 2A and when the UV line was stable, the protein was eluted with 3 steps of imidazole using Buffer Histrap 1B – 20%, 50% and 100%, respectively. Protein collected from the Histrap was pooled and concentrated using an Amicon (MWCO 10KDa) until a final volume of 4mL. The column used for SEC was HiLoad 16/600 Superdex 75 pg that was previously equilibrated using Buffer SEC 2. Protein eluted from the Histrap was injected at 1mL/min. The pure protein was concentrated using an Amicon (MWCO 10KDa) and quantified by Bradford method. Then, the aliquots were froze in liquid nitrogen and stored at -80ºC.

## 2.4 Phage display

### 2.4.1 Fab Library – IBET λ immune library

Phage display library used for pannings was formerly constructed by Maria Jardim, Msc and Ines Barbosa, MSc using pCOMB3XSS vector as part of the Research Project FCT– PTDC/SAU-ONC/121670/2010. This library is an immune library and it was prepared using serum from breast cancer patients.

### 2.4.2 Pannings on microplates

Panning on microplates was performed using 96-well Nunc Maxisorp plates and hDLL1-DE3 purified from HEK293T as target. The protocol used was adapted from Rader *et al*., 2001. Three rounds of selection were carried out and all the incubations were made at room temperature (RT) with gentle agitation. On the first round, one well was coated with the target at 5µg/mL in DPBS in a final volume of 100µL and the plate was incubated for 1 hour at RT. Also, a depletion step was added, using uncoated wells to eliminate unspecific and plastic phage binders. Then, both wells were washed 3 times with 1x PBST and blocked with 250µL of 3% Milk Powder in 1x PBST for 1 hour. After blocking, $1x10^{11}$ phages ( of the IBET λ immune library) (2µL library in 98µL of 1x PBS ) were added to the uncoated well (depletion step) and incubation was made for 1 hour. Selection step was performed by adding 90µL of the phage solution from the depletion well, mixing with 10µL of DPBS and incubating 1 hour. Then, the well was washed 3 times with 1x PBST and 1 time with DPBS, and after washing the phages were eluted by adding 100µL of TEA at 100mM for 10 minutes. Finally the eluted phages were transferred into a new tube with 100 µL of Tris-HCL pH 7.5 for neutralization.

Round two was made with the same protocol of round three, but the washing steps after selection were as follows: 3 times with 3% Milk in 1xPBST, 3 times with 1xPBST and one time with DPBS. For round three, the antigen concentration was decreased, and coating of the wells with the target was made using 2.5µg/mL in DPBS.

### 2.4.3 Glycerol stock

In order to store the selected phages, a glycerol stock was made for each round. After infecting the culture of TG1 with the phages, 500µL of that culture were removed and centrifuged at 5000xg at RT for 5 minutes. After centrifugation, the pellet was resuspended in LB medium, plated on two plates of LB Agar with ampicillin at 100µg/mL and incubated at 37ºC, o/n. On the next day, all the biomass was removed by scraping from the plates and mixed in 6mL LB medium with glycerol to a final concentration of 15%. The mixture was then divided into three cryovials and stored at -80ºC.

### 2.4.4 Input and Output titration

In order to analyse how many phages entered in the selection step, "inputs" were prepared using 12 wells of a 96-well plate. To each well, 90µL of LB medium was added and 10µL of phages from depletion step were pipetted to the first well. Serial dilutions 1:10 were performed on the 12 wells by transferring 10 µl from the previous well to the next. After that, 90 µL of mid-logarithmic phase TG1 ($OD_{600}$=0.5) were added to each well and the plate was incubated for 30 minutes at 37ºC and 50 rpm. Finally 10 µL of each dilution was plated in LB Agar with ampicillin at 100µg/mL and plates were incubated o/n at 37ºC

To analyse the selected phages, "outputs" were prepared following this protocol: 180µL of LB were added to 4 wells of a 96-well plate; 20µL of TG1 infected with the phages (from selection step) were added to the first well and serial dilutions (1:10) were performed. 100 µL of each dilution was plated in LB Agar with ampicillin at 100µg/mL and plates were incubated o/n at 37ºC.

### 2.4.5 Phage Amplification

In order to proceed to a following round of panning the selected phages have to be amplified. A bacterial culture is prepared by inoculating the glycerol stock (from section 2.4.3) in 30 mL of LB medium to a starting $OD_{600nm}$ of 0.05-0.07. The culture is then incubated at 37ºC and 250 rpm until it reaches an $OD_{600nm}$ of 0.5 (approximately 1h20). At this stage 4.5 mL of the bacterial culture are infected with M13KO7 helper phage using an MOI (mulplicity of infection) of 50:1 (helper phage:bacteria), and the culture is incubated for 15 minutes at 37ºC and 50 rpm. After, the culture was centrifuged for 5 minutes at 4000 rpm at RT, and the pellet was resuspended in 30 mL of LB with kanamycin at 50µg/mL and ampicillin at 100µg/mL. Phages were amplified o/n at 30ºC and 250 rpm. The next day phage recovery was achieved by centrifuging the culture at 4500x*g* for 15 minutes at 4ºC. Then, the supernatant was filtered with a 0.22µm filter and 1/5 of the initial volume (supernatant's volume) of PEG precipitation buffer (20% PEG (6000) + 2.5M NaCl) was added to precipitate the phages and the mixture was left 1 hour on ice. The precipitated phages were centrifuged at 6200x*g*, at

4ºC for 30 minutes and the pellet obtained (when dry) was resuspended in 200µL of 1xPBS and stored at 4ºC in order to be used on the next round.

### 2.4.6 Phage pools analysis by Fab-on phage ELISA

To evaluate if the phage pools from round 2 and 3 from the pannings showed a dose response towards the target a Fab-on-Phage ELISA was carried out. First, the wells of a 96-well Maxisorp plate were coated with the target hDLL1-DE3 at 5µG/mL, and incubated for 1 hour at RT. After the coating was complete the wells were washed 3 times with 1x PBST and blocked with PBST + 5% Milk Powder for 1 hour. In parallel, in a non-treated plate, twelve dilutions (1:2) of phages from both pools were prepared and transferred to two plates: one previously coated with the target, and a second non-coated blocked plate to be used as the negative control. Phages were incubated for 1 h RT, and after, the wells were washed 3 times with 1x PBST. Finally for detection incubation with an anti-M13-HRP conjugated antibody at 5µg/mL for 1 hour was pursued. Finally, for development 50 µL of RT colorimetric substrate for horseradish peroxidase 3,3',5,5'-tetramethylbenzidine (TMB) were added to the wells and incubated in the dark before the colour reaction became saturated, or until negative controls started to react. Reaction was stopped by addition of 50 µL of 2N $H_2SO_4$ per well. Plates' absorbance was measured at 450 nm in Multiskan$^{TM}$ FC (Thermo Scientific).

### 2.4.7 Individual clones analysis

#### 2.4.7.1 Clones rescue (5mL amplification)

To guarantee that the phages amplification was enough to have a good ELISA signal, amplification using 5mL of culture was carried out. First, 30 clones from round 3 (chosen randomly from output plates) were pre-inoculated in falcons containing 5mL of 2YT medium supplemented with 100µg/mL ampicillin. After incubation o/n at 37ºC and 250 rpm, inoculums for each clone were prepared using 60-75µL of pre-inoculum (to a starting OD=0.05) in 5mL of 2YT medium with 100µg/mL ampicillin and incubation was carried out at 37ºC and 250 rpm until OD= 1.0. After, each culture was infected with helper phage M13KO7 using an MOI of 500: 1 (helper phage: bacteria), incubation was made for 2 hours at 37ºC, 250 rpm and kanamycin was added at a final concentration of 50µg/mL. Cultures were then incubated o/n at 37ºC and 250 rpm. The following day the amplified phages were recovered using the same protocol described above (2.4.5 Phage Amplification), but in this step the phages were resuspended in 225µL of DPBS.

#### 2.4.7.2 Fab-on-Phage ELISA

In order to evaluate the specificity for the target and the display of the individual clones, the Fab-on-Phage protocol similar to that described in section 2.4.6.1 (Screening of phage pools by Fab-on-Phage ELISA) was followed. The only alterations were that in this case four plates were used for each round, a non-coated, and three which were coated during the night with target at 5µG/mL, anti-

M13 at 5µG/mL and anti-Fab at 5µG/mL respectively. Also, 50uL from each amplified phage preparation were transferred to each well of the blocked plates and incubated for one hour.

### 2.4.8 Pannings on immunotubes

Panning on immunotubes was performed using hDLL1-DE3 purified from inclusion bodies as target. The protocol used was identical to the one described for the microplates. Three rounds of selection were also performed and all the incubations were made at RT with gentle rotation.

On the first and second rounds coating was made with 100µg of target in 1mL of 1x PBST. On the third round 50µg of target were used in 1mL of 1xPBST. Blocking was made with 3mL of 3% Milk in 1xPBST. The number of phages used in round 1 was $1x10^{12}$ and in rounds 2 and 3, 500µL of the amplified phages were added. To elute the phages after each selection, 500µL of TEA was added and incubated 10 min with gentle rotation, followed by addition of 500µL Tris-HCl 100mM pH 7.5. For amplification, 9.5mL of each bacterial stock culture containing the phagemid were infected with helper phage at an MOI of 50:1. After o/n amplification and PEG precipitation phages were resuspended in 1mL of 1xPBS, and stored at 4ºC until further use.

The preparation of the glycerol stock, Input and Output titration and phage amplification were performed with the same protocol described in Sections 3.3.3, 3.3.4 and 3.3.5, respectively. Also, the selected phage pools analysis was made using the same protocol described in Section 2.3.6.1.

### 2.4.9 Individual clones analysis

#### 2.4.9.1 Fab-on-phage expression plates and glycerol stocks

Fab-on-Phage expression plates of 88 randomly picked clones were prepared as follows: 200µL LB was added on each well of a 96-well plate, and each well was inoculated with an individual colony from the output plates from rounds 2 and 3. After, plates were incubated o/n at 37ºC and 250 rpm. On the next day, 20µL of the pre-inoculum were used to prepare the clone plates that were previously filled with 150µL of fresh LB medium supplemented with the ampicillin at 100 µg/mL. Bacteria were grown at 37ºC during 3 hours and then amplification was promoted by adding helper-phage and incubating overnight at 30ºC, 200 rpm. Fab-on-phage ELISA was performed using the same protocol described above (Section 2.3.5.2). To the remaining volume of the expression plates glycerol was added to a final concentration of 15%, and the plates were froze at -80ºC, giving origin to the glycerol stocks plates.

### 2.4.10 Characterization of the positive clones

Positive Fab-on-phage ELISA clones were confirmed by colony PCR (same conditions used in pETfh8 – Section 2.1.1.2) using pCOMB3XSS forward and reverse primers, 5' AGTGGACTGGCTGGTTTCGC 3' and 5' CCATGGTGATGGTGATGGTGC 3', respectively. The annealing temperature used was 54ºC. Clones considered positive after colony PCR were sequenced by StabVida using the same primers mentioned before. Also, these clones were digested with *Spe*I/*Sac*I for 3 hours at 37°C and analysed in a 1% agarose gel.

.

### 2.4.11 Soluble Fab (sFab) expression in pCOMB3XSS

For sFab expression in pCOMB3XSS, a protocol adapted from Barbas *et al*., 2004 was used. Clones were transformed in a nonsupressor strain, namely TOP 10 F'. Pre-inoculum was prepared in 10mL of Super Broth (SB) medium (see Appendix 5.3), supplemented with ampicillin at 100µg/mL and was incubated at 37°C overnight, 250 rpm. Inoculum was prepared by using 1mL of pre-inoculum in 25mL of SB medium with ampicillin and glucose at 1%, and the culture was incubated at 37°C until final $OD_{600nm}$ = 0.8. The culture was centrifuged at 5000xg, for 20 minutes (to remove the glucose) and the pellet was resuspended in fresh SB medium supplemented with ampicillin. After, the culture was incubated at 37ºC for 1 hour (250 rpm) and then induction was made with 2mM of IPTG for 3 hours and 4 hours at 37ºC or overnight at 30ºC. All samples for analytics were prepared according to Section 2.2.1. The detection of the Fab was made by Western Blot using Anti-Fab-HRP conjugated antibody at a dilution of 1:5000 in 1xPBS.

### 2.4.12 sFab Cloning and expression tests in pT7

The DNA extracted from a few clones (pCOMB3XSS) and pT7 vector were both digested with *SfiI* for 3 hours at 50ºC. After analysing by gel, ligation of the positive clones took place. For that, 2.5 units of T4 DNA ligase were used and using two different proportions vector:insert was used, namely 1:2 and 2:1. The mixture was incubated for 10 minutes at 20ºC and overnight at 16°C. After, ligations were transformed in DH5α and plated in LB agar plates with 100µg/mL. The DNA was extracted and colony PCR was performed as described before (Section 2.1.1.2). Annealing temperature was 55ºC and the primers used were pT7 forward and reverse (universal primers). After selecting the positive colonies and extracting the DNA, the clones were digested with *Sfi*I for 4h at 50ºC and transformed in three strains: BL21(DE3), BL21Star (DE3)/pRARE2 and Shuffle T7 express.

Expression of the Fab using pT7 was tested using the same protocol mentioned for pCOMB3XSS. Several conditions were tested: medium – PB, 2YT, LB; IPTG concentration – 0.5mM,1mM and 2mM; Time of induction – 3h, 5h and overnight; Temperature – 20ºC, 25ºC, 30ºC and 37ºC. Also, the Overnight Express Auto Induction System from Merck was tested.

### 2.4.13 Protein titration

In order to access the optimal concentration of target to be used in the Phage ELISA, the protein was serial diluted (1:2) using 12 wells from a 96-well plate, starting at 10µg/mL or 20 µg/mL. Then, dilutions were transferred into a Maxisorp plate and incubated for 1h. The wells were washed three times with 1xPBST and blocking was made for 1h using 250µL of 3% Milk powder in 1xPBST. After washing the wells again, plates were incubated with the primary antibody Anti-penta-histidines (QIAGEN) at 2.5µg/mL and anti-mouse-HRP conjugated. ELISA plates were developed using 3,3′,5,5′-

Tetramethylbenzidine (TMB) and sulphuric acid 2M to stop the reagent. The signal was analysed using Skan it Multiskan software at 450nm.

## 2.5 SDS-PAGE electrophoresis and Western Blot

For SDS-PAGE electrophoresis, Invitrogen and Bio-Rad pre-cast gels were used. Before running the gels all the samples were boiled 5-10 minutes at 99ºC. Running was pursued with 1xMES buffer at 150-200 volts and during approximately 1 hour. After the run, staining was made using Instant Blue (Expedeon) or with Silver Staining (Bio-Rad) following the manufacturers protocol.

Western blot technique was carried out using the same gels and protocol mentioned before. After running the gel, it was transferred onto nitrocellulose membrane using a NuPAGE Transfer Buffer and the Trans-Blot SD Semi-Dry Transfer Cell (BioRad) following the manufacturer's instructions, specifically at 25 volts during 35 minutes. The membrane was further blocked with 3% Milk Powder in 1xPBST for 45 minutes, washed 3 times with 1xPBST during 10 minutes and 1 time with 1xPBS for a few seconds. The primary antibody was incubated during 1-2 hours and the secondary HRP-conjugated antibody was incubated during 1 hour. Between these two incubations, a washing step was performed following the same protocol mentioned before. After the secondary antibody incubation, another washing step was made and finally the signal was developed using a Western Lightning Plus-ECL Enhanced Chemiluminescence Substrate (PerkinElmer) and the images were obtained in ChemiDoc (Bio-Rad). In this work, to detect the histidine tag fusion a Penta-His (Anti-His) was used at a dilution of 1:2000 and anti-mouse-HRP conjugated at a dilution of 1:3000. Also, an Anti-Fab-HRP conjugated antibody (dilution 1:5000) was also used for a direct Fab detection.

## 2.6 Protein quantification

To access protein's concentration two methods were used: Bradford and spectrophotometry at 280nm (A280). The first was performed using a calibration curve with BSA prepared in the same buffer of the protein. The protein was diluted in a way that the concentration was within the range of the calibration curve. All the samples were prepared in duplicates on a 96-well plate and 5µL of each sample was used. After pipetting the samples, 150µL of Reagent (Bio-Rad Protein Assay Dye Reagent Concentrate) was added to each well and the plate was incubated for 30 minutes protected from the light. Absorbance was measured at 595nm and blank-subtracted absorbance readings were averaged to compare with the calibration curve prepared. A280 method was made in NanoDrop using the parameters of the protein – Molecular Weight (MW) and extension coefficient, or by a direct measurement.

## 2.7 Thermal shift assay (TSA)

In order to evaluate the thermal stability of the purified proteins, TSA was performed in a iQ5 Real Time PCR Detection System from Bio-Rad, equipped with a charge-coupled device camera and a Cy3 filter with excitation and emission wavelengths of 490 and 575 nm, respectively.

The samples were prepared in 96-well plates (low profile plate, Bio-Rad). Reagents were added to the well, to a final volume of 20µL or 50µL, following this order: protein buffer; 5-fold SYPRO Orange dye concentration and the protein (20, 40 or 60µg). In experiments using additives, the last were added to the plate in first place, followed by the protein in appropriate buffer and incubation of 30 minutes, followed by the addition of dye at 5-fold final concentration. Before each assay, the plates were covered with optical quality sealing tape (Bio-Rad) and centrifuged at 2500*g* during 2 minutes to remove air bubbles. The plates were subsequently heated from 20 to 90ºC with stepwise raises of 1ºC on the temperature with 10 seconds equilibration time, followed by fluorescence reading.

Protein denaturation was monitored using the fluoroprobe SYPRO Orange dye, which is quenched in aqueous environment, but it emits fluorescence when it binds to protein hydrophobic residues. This increase can be measured as function of the temperature. Melting temperature (Tm) was determined using the first derivative (d(Rfu)/dT) in order to extract the accurate inflection point on each observed transition.

## 2.8 Protein Crystallization

Crystallization experiments were prepared using CrystalQuick$^{TM}$ 96 Well, Greiner (Hampton Research) plates in a Cartesian MiniBee Robot, available in the host lab, with commercial screens from Molecular Dimensions or Hampton Research. The drops were made with 0.1µL protein + 0.1µL crystallization solution and one control drop per condition was made with protein buffer + crystallization solution. Each reservoir contained 35µL of crystallization solution. After making the drops, the plates were covered and stored at 4ºC or 20ºC. Also, the reported crystallization condition for hDLL1-ME6 (Kershaw *et al.*, 2015), was used to prepare a grid screen around the published crystallization. Hanging-drop method was used and the drops were made on a 24-wells plate as follows: 0.5 µl of protein and 0.5 µl of mother liquor; Precipitant was varied between 14% and 19% PEG 3350 in 100mM Bis-Tris propane, pH 7.5, 400mM potassium thiocyanate and 5mM $CaCl_2$. The plate was kept at 20ºC and analysed periodically.

## 2.9 Functional assay for hDLL1-DE3

### 2.9.1 Cell culture and treatments

Human induced pluripotent stem cells (hiPSCs, Stemcell technologies) and breast cancer line HCC1954 (American Type Culture Collection (ATCC)), were used to assess the biologic activity of produced recombinant protein. Human induced pluripotent stem cells were inoculated at $4{,}5\times10^5$ cells/well of a 6-well plates in 2mL of complete mTeSR™1 medium (Stemcell technologies). HCC1954 cells ($4\times10^4$ cells/$cm^2$) were seeded in T25 flasks in 4-6 mL RPMI media supplemented with 2mM L-glutamine, 1% Hepes buffer, 0.01% beta-mercaptoethanol and 10% heat inactivated fetal bovine serum (FBS)(all from Gibco). All cells were cultured at 37ºC and 5% $CO_2$. On the next day, cells at 60-70% confluence were treated with 1.0, 2.5, 5.0 and 10µg/ml of hDLL1-DE3 and further incubated for 2h to 24h. For each incubation period, control cells were treated with vehicle. After the incubation periods the culture medium was removed, cells were washed once with 1x phosphate saline buffer (PBS) and detached with 1x trypsin/EDTA solution (Gibco) by incubating them at 37C for 3min. The breast cancer cell line MDA-MB-468 from ATCC was cultured in DMEM media (Gibco) supplemented with 2mM L-glutamine, 10% FBS and 100 mg/ml penicillin and 100U/ml streptomycin (LifeTechnologies).

### 2.9.2 RNA purification, cDNA synthesis and gene expression analysis by real-time quantitative polymerase chain reaction (qRT-PCR)

Total RNA was isolated from cells using the miRNeasy Mini kit (Qiagen) or the GeneJet RNA Purification kit (Thermo scientific) according to the kits manufacturer's instructions. Isolated, purified RNA was analysed and quantified by UV spectroscopy using the NanoDrop spectrophotometer. For each cell type/experiment cDNA was generated from equal amounts of RNA (1.5-4 µg) by reverse transcription using the Advantage RT-for-PCR kit (Clontech Laboratories) or the Transcriptor First strand cDNA Synthesis kit (Roche) as per manufacturer's instructions.

The mRNA expression levels of the *HES-1, HEY-1*, *HEY-L*, *hJag1*, *hJag2*, *hDLL1, and hNotch1* genes in the different cDNA samples was quantified by real time PCR on the Roche LightCycler 480 (LC480) apparatus using gene specific primers (listed in table 2.2) and the FastStart DNA SYBR Green I mix (Roche). qRT-PCR reactions mixes were prepared in 96-well plates (Roche)(20µL/well) using 7µl of cDNA (previously diluted 3x in molecular biology grade $H_2O$), 5pmol/µL of each gene specific forward and reverse primers and 10µL of SYBR Green master mix. All experiments were performed in triplicate as per the manufacturer's instructions. Conditions for cDNA amplification were 95°C (10min), followed by 45 cycles of 95°C (10 s), 59°C (20 s), and 72°C (20 s). All reactions underwent a post-amplification dissociation curve determination to ensure a single PCR product at the correct melting temperature according to LC480 recommendations. For each sample, mRNA transcripts were normalized to the house-keeping hypoxanthine-guanine-phosphoribosyltransferase (HPRT1) levels and calculated using the advanced relative quantification method as per LC480 software manufacturer´s recommendations. Results are expressed as relative mRNA expression or as fold change relative to control cells treated with vehicle.

**Table 2.2 - Primers used in qRT-PCR reactions.** PrimerBank IDs from http://pga.mgh.harvard.edu/primerbank

| Gene | Primer | | Reference |
|---|---|---|---|
| | Foward | Reverse | |
| ***hDLL1*** | 5' CTTCCCCTTCGGCTTCAC 3' | 5' GGGTTTTCTGTTGCGAGGT 3' | Falk *et al.*, 2012 |
| ***HES-1*** | 5′ CCTGTCATCCCCGTCTACAC 3' | 5′ CACATGGAGTCGCCGTA A 3' | PrimerBank ID: 325652058c3 |
| ***HEY-1*** | 5' GTTCGGCTCTAGGTTCCATGT 3' | 5' CGTCGGCGCTTCTCAATTATTC 3' | PrimerBank ID: 105990527c1 |
| ***HEY-L*** | 5´ GGAAGAAACGCAGAGGGATCA 3' | 5´ CAAGCGTCGCAATTCAGAAA 3' | PrimerBank ID: 105990530c1 |
| ***hJag1*** | 5' GAATGGCAACAAAACTTGCA 3' | 5' AGCCTTGTCGGCAAATAGC 3' | Falk *et al.*, 2012 |
| ***hJag2*** | 5' TGGGACTGGGACAACGATAC 3' | 5' ATGCGACACTCGCTCGAT 3' | Falk *et al.*, 2012 |
| ***hNotch1*** | 5' CGCACAAGGTGTCTTCCAG 3' | 5' CCCTGGCAATGTACTTGTGA 3 | Falk *et al.*, 2012 |

## 3 - Results and Discussion

The results obtained in this thesis will be presented in this section in a chronological fashion. Firstly, we will present the feasibility tests performed to choose the best targets for production and purification. Secondly, we describe, step by step, each strategy, outcomes and consequently whether a new approach was used to tackle the project goals. At each sub-section, strategies are justified based on the results obtained throughout the experimental work.

### 3.1 Notch ligands Expression in *E.coli*

#### 3.1.1 Expression screening in pET47 (b) +

Constructs of the three Notch ligands (Jag1, Jag2 and DLL1) were built to contain a different domain composition but always maintaining the ligand's minimal binding region - DSL to EGF- like 2 (Shimizu *et al.*, 1999), as described in the introduction. For clarity Notch ligands constructs MNNL to EGF-like 3, 6 or 9, will be denoted as: – ME3, ME6 and ME9 while DSL to EGF-like 3, 6 or 9 constructs, will be designed as: DE3, DE6 and ME9.

To produce the Notch ligands using bacteria as host, two *E.coli* strains were used - BL21 (DE3) and BL21(DE3)/pRARE2. The choice of the first strain is due to its repertoire of successful recombinant protein expression in the literature (Daegelen *et al.*, 2009), while the second choice will be explained later. Since preliminary data had shown that these ligand constructs were mostly expressed as inclusion bodies (Silva, 2014), several tests were performed in order to increase protein solubility. Different expression conditions known to affect soluble protein expression were tested such as: the use different host strains (BL21(DE3) and BL21(DE3)/pRARE2), growth media (LB, PB and M9), induction time (2-6h, and o/n), induction temperature and IPTG concentration. All described conditions were simultaneously tested using bacteria that co-expressed the target protein and also two chaperones – GroEL/GroES complex encoded by the pGro plasmid. Chaperones, and more specifically the well-studied system in *E.coli* GroEL and GroEs, are a special class of heat shock proteins that assist protein folding (Chen *et al.*, 2013).

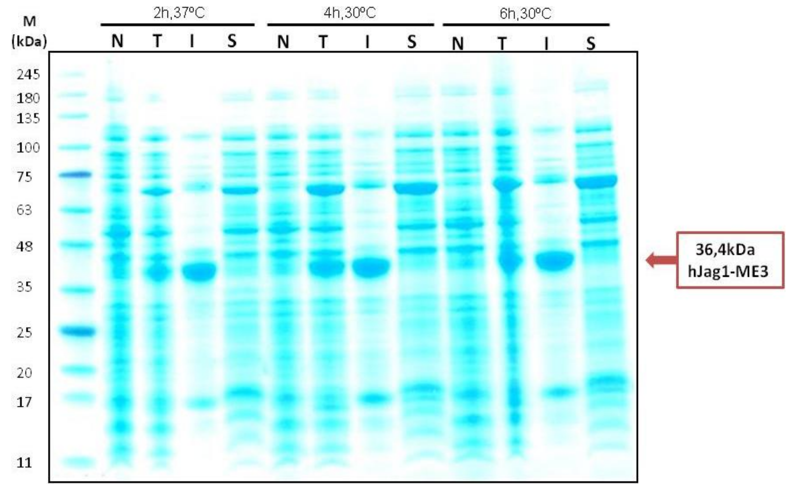


**Figure 3.1 - SDS-PAGE of expression tests in hJag1-ME3.** Expression tests using PB medium and 2h, 37ºC; 4h, 30ºC and 6h, 30ºC with 0.1mM IPTG. M- Marker; N- Non-induced culture; T- Total induced culture; I- Insoluble fraction; S- soluble fraction. Red arrow indicates the induced protein band with the predicted molecular mass for this construct.

The tested expression conditions for the nine studied target constructs are summarized in Table 3.1. As an example, Figure 3.1 shows the results for *homo sapiens* (h) Jag1-ME3 protein expression in PB medium, using 30ºC and 37ºC, as induction temperature with different induction times (2, 3, 4 and 6h) where most of the produced protein is present in inclusion bodies. Similar results were obtained for most of the remaining target proteins and expression conditions (results not shown), except for hDLL1-DE3 (check bellow). Generally, inclusion bodies contain mostly over expressed protein in *E.coli* that undergo an intermediate state of partial folded protein, prone to aggregate *via* hydrophobic but also ionic interactions. In the case of the Notch ligands proteins, composed by several domains which contain many disulfide bonds, formation of these aggregates can be explained by the cytosolic bacterial reducing environment, which does not favour disulfide bonds formation. Also, the usage of strong promoters and high inducer concentrations, leads to high concentrations of protein in the bacterial cytoplasm. Under these conditions, the rate of protein production is normally much higher than the time needed for proper folding (Baneyx and Mujacic, 2004).

**Table 3.1 - Conditions tested for expression of Notch ligands cloned in pET47 (b) +**

| | | **Growth medium** | | | **Temperature (°C)** | | | **Time (h)** | | | | | | **[IPTG] (mM)** | | **OD$_{600nm}$** | ***E.coli* strain** | |
|---|---|---|---|---|---|---|---|---|---|---|---|---|---|---|---|---|---|---|
| | | **LB** | **PB** | **M9** | **20** | **30** | **37** | **2** | **3** | **4** | **5** | **6** | **o/n** | **0.1** | **0.5** | **0.8-1** | **BL21 DE3** | **BL21 pRARE2** |
| **pET-47 (b)+** | **hJag1-DE3, ME3,ME9; hJag2-DE9 and ME9** | | • | | | | • | • | | | | | | • | | • | • | |
| | | | • | | | • | | | | • | | | | • | | • | • | |
| | | | • | | | • | | | | | | • | | • | | • | • | |
| | **hJag2-ME3** | | | | | | • | • | | | | | | • | | • | • | |
| | | | • | | | • | | | • | | | | | • | | • | • | |
| | | | • | | | • | | | • | | | | | | • | • | • | |
| | **hDLL1-DE3** | | • | | | | • | • | | | | | | • | | • | • | |
| | | | • | | | | • | | | • | | | | | • | • | • | |
| | | | • | | | | • | | | | • | | | | • | • | • | |
| | | | • | | | | • | | | | | | • | | • | • | • | |
| | | | • | | | • | | | • | | | | | • | | • | • | |
| | | | • | | | • | | | • | | | | | | • | • | • | |
| | | • | | | | | • | • | | | | | | | • | • | • | |
| | | | | • | | | • | • | | | | | | | • | • | • | |
| | | | | • | | | • | | | • | | | | | • | • | • | |
| | | | • | | | • | | | | • | | | | | • | • | • | |
| | | | • | | • | | | | | | | | • | | • | • | • | |
| | | | • | | | • | | | | • | | | | | • | • | | • |
| | | | • | | • | | | | | | | | • | | • | • | | • |

| | | Growth medium | | | Temperature (°C) | | | Time (h) | | | | | | [IPTG] (mM) | | $OD_{600nm}$ | *E.coli* strain | |
|---|---|---|---|---|---|---|---|---|---|---|---|---|---|---|---|---|---|---|
| | | LB | PB | M9 | 20 | 30 | 37 | 2 | 3 | 4 | 5 | 6 | o/n | 0.1 | 0.5 | 0.8-1 | BL21 DE3 | BL21 pRARE2 |
| pET-47 (b)+ | hDLL1-ME3 | | • | | | | • | • | | | | | | • | | • | • | |
| | | | • | | | | • | | | • | | | | | • | • | • | |
| | | | • | | | | • | | | | • | | | | • | • | • | |
| | | | • | | | | • | | | | | | • | | • | • | • | |
| | | | • | | | • | | | • | | | | | • | | • | • | |
| | | | • | | | • | | | • | | | | | | • | • | • | |
| | | • | | | | | • | • | | | | | | | • | • | • | |
| | | | | • | | | • | • | | | | | | | • | • | • | |
| | | | | • | | | • | | | • | | | | | • | • | • | |
| | hDLL1-ME6 | | • | | | | • | • | | | | | | • | | • | • | |
| | | | • | | | • | | | • | | | | | • | | • | • | |
| | | | • | | | • | | | • | | | | | | • | • | • | |

In extreme cases, as the one shown in Appendix 5.5 (Figure 5.1) for hDLL1-ME6, no protein expression was detected neither in the soluble nor in the insoluble fraction, probably because the protein is toxic to the bacteria and so, the production of protein is impaired for its own survival (Corchero and Villaverde, 1998). As mentioned earlier, for hDLL1-DE3, expression of soluble protein was observed, using 2h at 37ºC, with 0.1mM IPTG induction or alternatively using 3h at 30ºC with 0.5mM IPTG induction (Figure 3.2 and 3.3). Nevertheless, the protein expression yield was not high and a clear detection of the presence in the soluble fraction was only obtained when using Western blot, which is a much more sensitive technique when compared with SDS-PAGE.

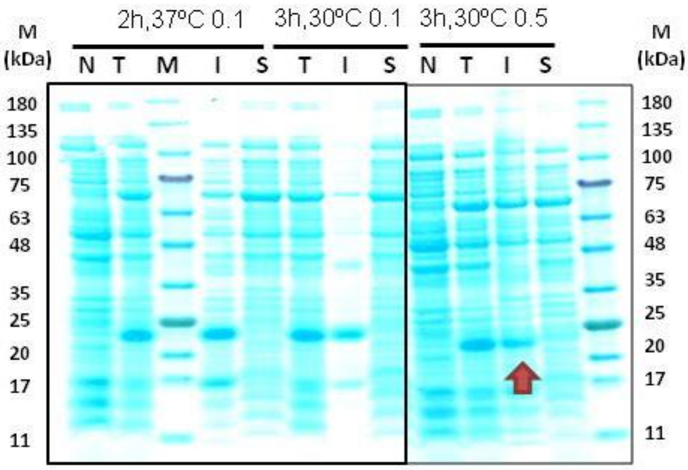


**Figure 3.2 - SDS-PAGE of expression tests in hDLL1-DE3.** Expression tests using PB medium and 2h37ºC with 0.1mM IPTG,3h30ºC with 0.1mM IPTG and 3h30ºC with 0.5mM IPTG. M - Marker; N - Non-induced culture; T- Total induced culture; I - Insoluble fraction; S - soluble fraction. Red arrow pointing the induced band with the molecular mass predicted for this construct (19,5 kDa).

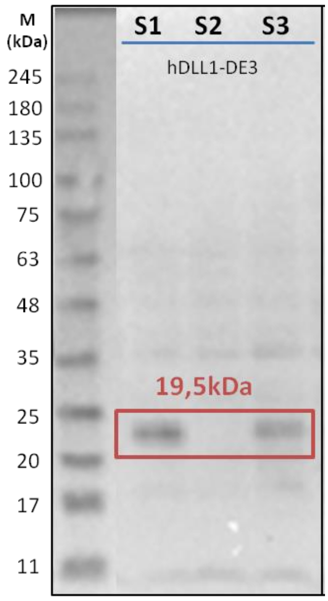


**Figure 3.3 - Anti-His Western blot results for hDLL1-DE3 soluble fractions.** M – Marker**;** S1 - Soluble fraction of 2h37ºC with 0.1mM IPTG; S2 – Soluble fraction of 3h30ºC with 0.1mM IPTG; S3 - Soluble fraction of 3h30ºC with 0.5mM IPTG. Red box highlights the band induced in the molecular mass predicted for this construct.

Based on these results additional expression conditions were tested for hDLL1-DE3, including M9 Minimal Medium and low induction temperatures (e.g. 20ºC) which may help decreasing aggregation. This is due to the fact that low temperatures decrease the rate of protein synthesis and folding kinetics, consequently diminishing the hydrophobic interactions that are involved in protein self-aggregation (Schumann and Ferreira, 2004; Costa *et al.*, 2014). Also, pRARE2 codon- transformed BL21 Star (DE) was tested for hDLL1-DE3. This vector co-expresses rare transfer RNAs (tRNAs) that bacteria are not able to produce and its use leads to an optimization in the gene sequence in *E.coli* resulting in an increase in protein quantity and quality (Sorensen and Mortensen, 2005; Jana and Deb, 2005). Unfortunately, the protein was again mostly in the insoluble fraction for all tested conditions. At this point, and as the soluble protein is scarce, a different strategy was considered.

### 3.1.2 Cloning and expression tests with a solubility-inducing fusion protein

In order to increase expressed proteins solubility, a plasmid containing a fusion tag was used - pETfh8. The fh8 tag, is a recently described solubility tag with approximately 8kDa (Costa *et al.*, 2013a). Fh8 consists of a *Fasciola hepatica* antigen and it has been recently reported to improve protein solubility for different proteins, representing a promising strategy to express difficult targets in *E.coli* (Costa *et al.*, 2014). To express Notch ligands using this new strategy, the tag was fused in the N-terminal of the expressed proteins, as depicted in Figure 3.4. A linker was added between the insert and the solubility tag because is well described that a link spacer favours correct protein folding (Esposito and Chatterjee, 2006; Malhotra, 2009). This linker was adapted from Costa *et al.*, 2013b.

Also, the vector presents a six-histidine tag in fusion with the tag that allows detection and purification of the protein.


**Figure 3.4 - Illustration of the constructs cloned in pETfh8.** Tag was cloned in the N-terminal. The linker used was threonine-glycine-glycine-serine (TGGS)

For the fh8 tag system, the solubility fused-tag was not sufficient to shift the equilibrium from the insoluble to the soluble fraction in both tested constructs (this was confirmed by Western blots in Figure 3.5 and 3.6). The tested conditions for this vector were: 3h at 37ºC, overnight at 18ºC and overnight at 20ºC using BL21Star(DE3)/pRARE2 in LB medium, and induction with 0.5mM IPTG at $OD_{600nm}$=0.7- 0.9.

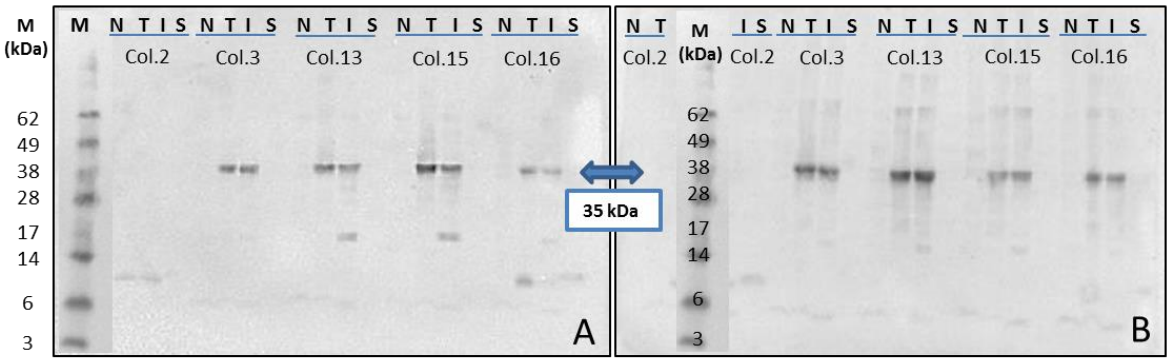


**Figure 3.5 - Anti-His Western Blot of expression tests in pETfh8 with hDLL1_DSL. A.** Expression at 37ºC for 3h. **B.** Expression at 18ºC overnight. M - Marker; N - Non-induced culture; T- Total induced culture; I - Insoluble fraction; S-Soluble fraction. Blue double-arrow points to the bands induced in the molecular mass expected for 6xHis-fh8-hDLL1_DSL fusion.

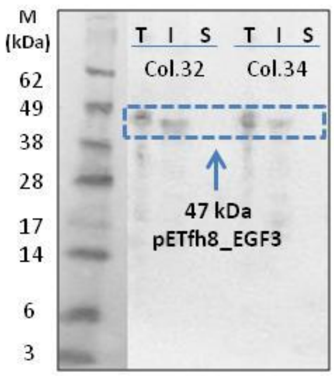


**Figure 3.6 - Anti-His Western Blot of expression tests in pETfh8 with hDLL1_EGF3. .** Results for expression at 30ºC overnight using colony 32 and 34. M- Marker; N- Non-induced culture; T- Total induced culture; I- Insoluble fraction; S-Soluble fraction. Blue box marks the bands induced in the molecular mass expected for 6xHis-fh8-hDLL1_EGF3 fusion.

At this point, both strategies based on pET47 (b) + and pETfh8 were shown to fail in expressing reasonable amounts of soluble protein for crystallography and phage display approaches, which forced us to test another expression system.

## 3.2 Expression in mammalian cells (HEK293T)

### 3.2.1 Expression tests in pHL-sec

After exhaustingly testing expression in bacteria, an alternative host-system was chosen. Expression of recombinant cells in mammalian is expensive and a very time-consuming task when comparing with expression in *E.coli*. However, mammalian cells represent the native environment of human recombinant proteins and it is more likely to obtain a protein with the correct native conformation and post-translational modifications (Aricescu *et al.*, 2006), which may be fundamental for the over-expression of these targets. HEK293T cells were selected for transient expression of Notch Ligands cloned in pHL-SEC. Cells from HEK293 lineage are known for their large use to produce several types of recombinant proteins, as they grow robustly and transfection using various types of reagents is normally easy (Dalton and Barton, 2014).

A small–scale feasibility study was performed using two different types of platforms (6-well plates and T25cm$^2$) to analyse if the expression levels were maintained. Also, different quantities of DNA and time post-transfection were tested. The expression of the protein was detected in the growth media, because the used vector, pHL-sec, contains a secretion signal fused with the recombinant protein (Aricescu *et al.*, 2006).

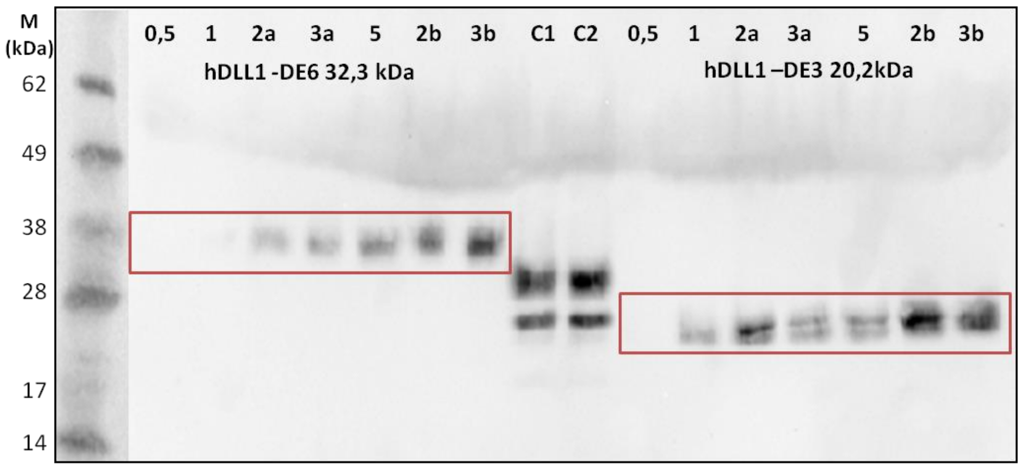


**Figure 3.7 - Anti-His Western Blot of expression tests for hDLL1-DE6 and hDLL1-DE3 in 6-well plates.** Five quantities of DNA were tested for each construct – 0.5,1,2,3 and 5µg of DNA. M-Marker; 2a and 3a – 15µL of extract loaded; 2b and 3b – 30 µL of extract loaded. Red box marks the bands induced in the molecular mass expected for hDLL1_EGF3 and hDLL1-DE6.

Six different ligands were tested and analysed conditions are summarized in Table 3.2. First, 6-well plates were used for hDLL1-DE6 and hDLL1-DE3 and the best conditions were 2, 3 and 5 µg of DNA after 72h post-transfection (Figure 3.7). These three quantities of DNA were also used to test the remaining four constructs but the protein expression was too low or absent (data not shown)

**Table 3.2 - Conditions tested for expression of Notch ligands cloned in pHL-sec**

| | Vessel | | Quantity of DNA (µg) | | | | | Seeding (cells/cm$^2$) | | Time Post-transfection (hours) | |
|---|---|---|---|---|---|---|---|---|---|---|---|
| | 6-well plate | T25 cm$^2$ | 0,5 | 1 | 2 | 3 | 5 | $3x10^4$ | $4x10^4$ | 48 | 76 |
| hDLL1-DE3<br>hDLL1-DE6 | ● | | ● | | | | | ● | | ● | ● |
| | ● | | | ● | | | | ● | | ● | ● |
| | ● | | | | ● | | | ● | | ● | ● |
| | ● | | | | | ● | | ● | | ● | ● |
| | ● | | | | | | ● | ● | | ● | ● |
| | ● | | ● | | | | | | ● | ● | ● |
| | ● | | | ● | | | | | ● | ● | ● |
| | ● | | | | ● | | | | ● | ● | ● |
| | ● | | | | | ● | | | ● | ● | ● |
| | ● | | | | | | ● | | ● | ● | ● |
| | ● | | | | ● | | | | ● | ● | ● |
| | ● | | | | ● | | | | ● | ● | ● |
| hJag2-DE3<br>hJag2-ME3<br>hJag1-ME3<br>hJag1-ME9 | ● | | | | ● | | | ● | | ● | ● |
| | ● | | | | | ● | | ● | | ● | ● |

For hDLL1-DE6 and hDLL1-DE3 proteins the next step was to scale-up into 25cm$^2$ T-flasks, and Western blot analysis showed similar expression levels of the two proteins when compared to the 6-well plates experiment (Appendix 5.5 – Figure 5.2). These results are concordant with the ones obtained when evaluating transfection efficiency using pAAVPURO vector as control, which contains the GFP and allows detection of transfected cells. Figure 3.8 shows the results for hDLL1-DE3 in 6-well plate, obtained by fluorescence microscopy, where 70-80% of the cells were transfected. Also, in T25cm$^2$ the percentage of transfected cells appears to be similar. The protein expressed in these small scales was confirmed to be hDLL1 by mass spectrometry (Appendix 5.4). At this point, for hDLL1-DE3, we were ready to further scale-up into 225 cm$^2$ T-flasks.

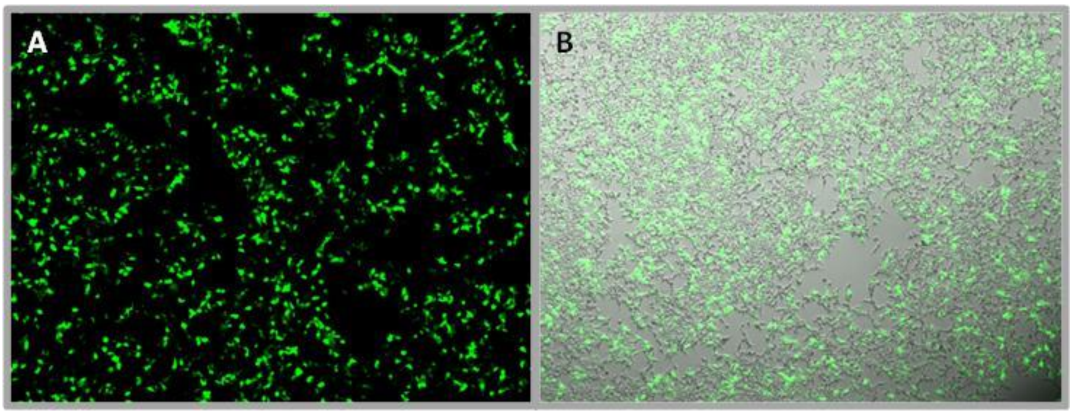


**Figure 3.8 - pAAVPURO control for expression tests in hDLL1-DE3. A.** 6-well plate. **B.** T25cm$^2$

### 3.2.2 hDLL1-DE3 expression and purification

#### 3.2.2.1 First strategy

In the initial batch, ten T-225cm$^2$ were transfected with 2.5µg of DNA and the media was collected after 72h. The media looked yellow and contained many detached cells however, the successful protein secretion to the growth medium was confirmed by Western Blot (See Appendix 5.5 – Figure 5.3).

After centrifuging the media, the supernatant was concentrated and injected into a Histrap column. The chromatogram depicted in Figure 3.9 shows a first eluted peak, which corresponds to BSA (bovine serum albumin – originated from the FBS) and a second peak corresponding to other contaminants also present in the growth media. The third eluted peak corresponds to the Notch ligand elution, as confirmed by SDS-PAGE (Figure 3.10). hDLL1-DE3 protein fractions were pooled together and concentrated, and during this procedure some protein precipitation was observed.

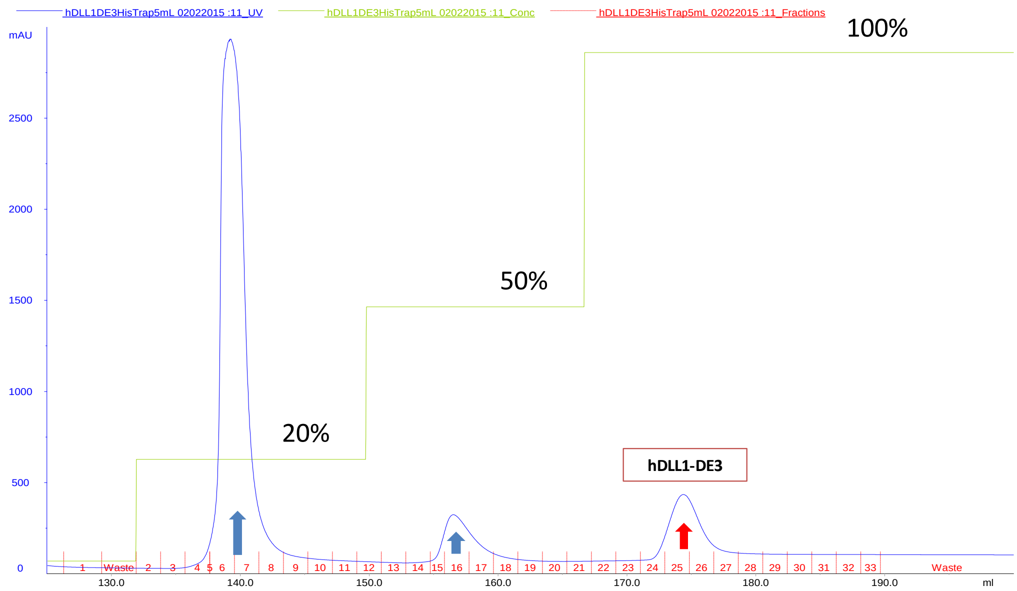


**Figure 3.9 - Chromatogram of elution of hDLL1-DE3 from the HisTtrap column –first strategy.** Blue arrows – contaminant peak; Red arrow- hDLL1-DE3 peak (Fractions 24 to 27). The steps of imidazole are marked in black – 20% -116mM Imidazole; 50% - 260mM imidazole; 100% - 500mM Imidazole. Column – Histrap FF 5mL.

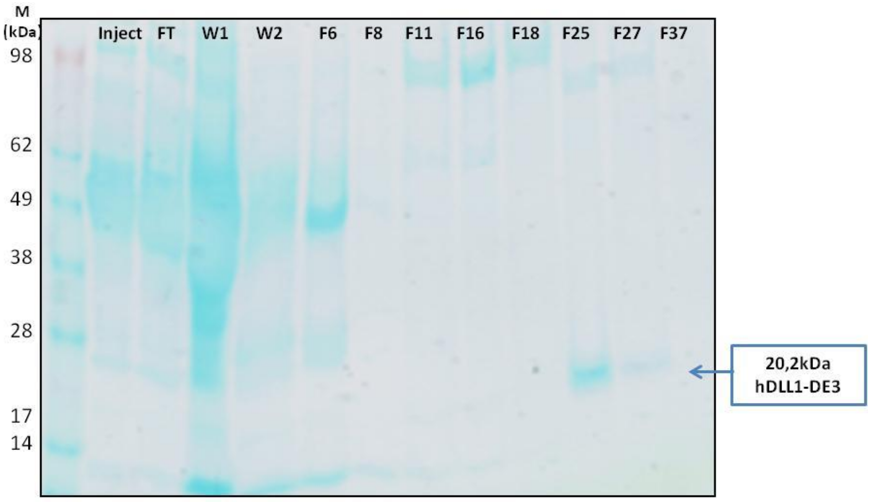


**Figure 3.10 - SDS-PAGE of hDLL1-DE3 elution from the Histrap column – first strategy.** M- Marker; FT – flow-through; W1 – wash step 1; W2- wash step 2; F –fractions. Blue box – molecular weight expected for hDLL1-DE3.

In order to further purify the protein from remaining contaminants, a SEC was performed. The results shown in Figure 3.11 indicate an elution volume of 110mL for hDLL1-DE3, in three inseparable peaks, which nevertheless, corresponds to a molecular mass higher than predicted, based on the column calibration curve. This can be explained by the protein overall rod shape while the column calibration curve was prepared using globular proteins. SDS-PAGE analysis confirmed that all three peaks correspond to the target protein, which may be explained by the presence of different isoforms or protein degradation (Figure 3.12 and 3.13). In accordance, Figure 3.16 shows the final sample (after concentration of SEC pool), where it is possible to see multiple bands, all confirmed by Mass spectrometry to correspond to hDLL1 Notch ligand.

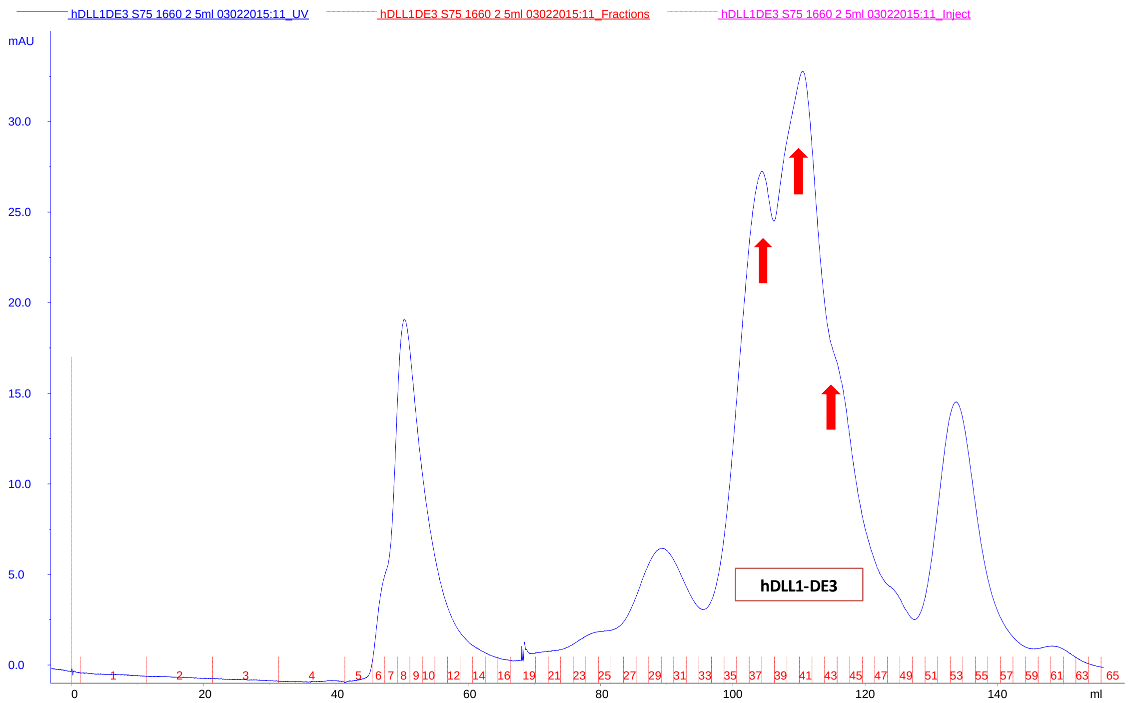


**Figure 3.11 - SEC chromatogram for hDLL1-DE3 – first strategy.** Red arrows correspond to the peaks of DLL1-DE3 elution (F34-44). Column – HiLoad 16/600 Superdex 75 pg.

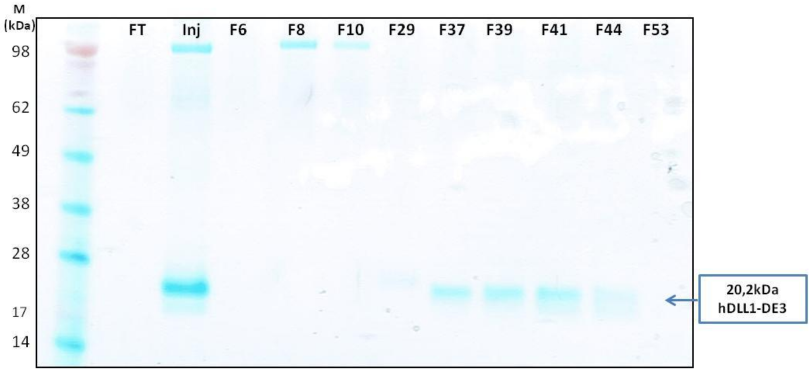


**Figure 3.12 - SDS-PAGE of elution of hDLL1-DE3 from SEC – first strategy.** Pool – Fractions 34 to 44. M- Marker; Blue box – molecular mass expected for hDLL1-DE3.

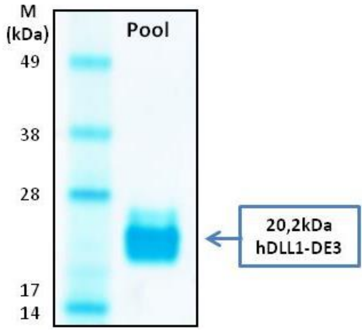


**Figure 3.13 - SDS-PAGE hDLL1-DE3 final pool – first strategy.** M- Marker; FT – flow-through; F - fractions. Blue box – molecular mass expected for hDLL1-DE3.

### 3.2.2.2 Second strategy

In order to increase protein yield and to possibly separate the observed different isoforms of hDLL1-DE3, a new batch was produced. Higher number of T-flasks were used and the culture medium was collected after 48h, to ensure cells were still healthy and, consequently that no protein degradation could occur. To further improve protein stability and prevent any degradation, the purification was now performed at 4ºC and protein stabilizers were used as additives to supplement buffers. One example is tris (2-carboxyethyl) phosphine (TCEP), a strong and stable (more stable than Dithiothreitol (DTT) and Beta-mercaptoethanol (BME)) reducing agent that reduces the disulphide bonds present in proteins thus preventing their aggregation (Bondos and Bicknell, 2003, Janson, 2011). Also, glycerol and Brij35 were added to improve the stability of the protein during purification (Bondos and Bicknell, 2003). The Histrap chromatogram showed a different profile than the one observed previously, where the first large peak corresponds to BSA and the second peak corresponds to fractions containing hDLL1-DE3 (Figure 3.14) confirmed by SDS-PAGE (Figure 3.15). Fractions containing the protein were pooled and concentrated previous to the injection in the SEC column.

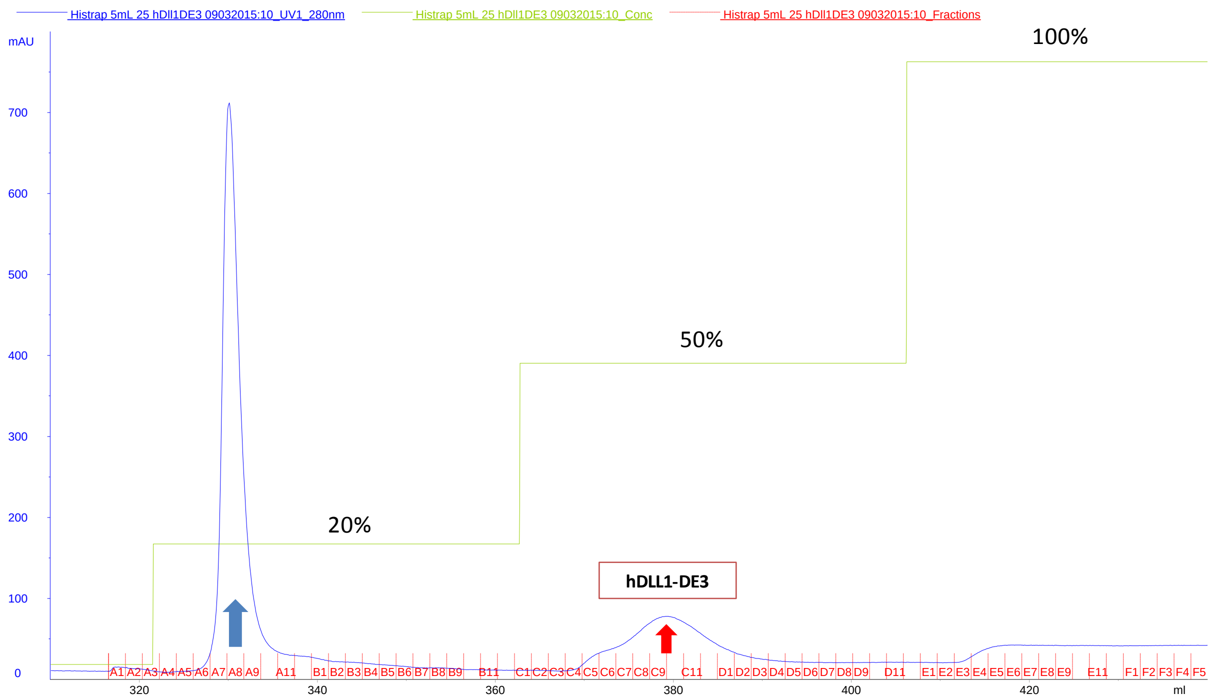


**Figure 3.14 - Chromatogram of elution of hDLL1-DE3 from the Histrap column – second strategy.** Blue arrow –contaminant peak; Red arrow - hDLL1-DE3 peak (fractions C6 to D6). The steps of imidazole are marked in black – 20% -116mM Imidazole; 50% - 260mM imidazole; 100% - 500mM Imidazole. Column – Histrap FF 5mL.

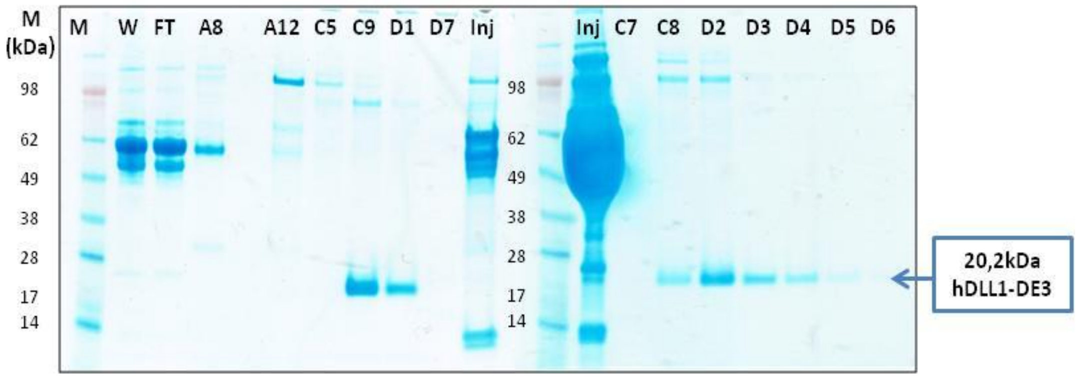


**Figure 3.15 - SDS-PAGE of elution of hDLL1-DE3 from the Histrap column – second strategy. .** M- Marker; FT – flow-through; W1 – wash step 1; W2- wash step 2; F –fractions. Blue box – molecular mass expected for hDLL1-DE3.

Despite all the modifications made in order to improve protein stability throughout purification, precipitation was detected during the concentration step leading to product loss. SEC results showed a completely different elution profile, where two main hDLL1-DE3 peaks could be isolated. Thus, two separate pools were prepared – pool 1 and pool 2 (Figure 3.16 and 3.17). After concentration, pool 1 target protein was considered to be pure, while pool 2 was still slightly contaminated with one smaller molecular mass protein (Figure 3.18).

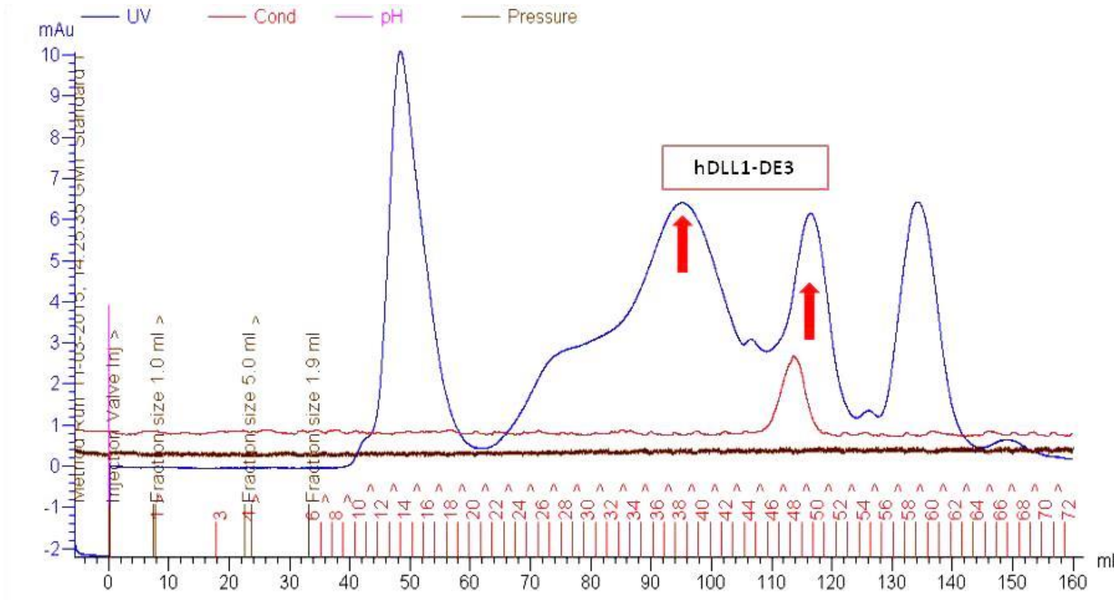


**Figure 3.16 - SEC chromatogram for hDLL1-DE3 – second strategy**. Red arrows correspond to the peaks of hDLL1-DE3 elution. The numbers represent the collected fractions. Column – HiLoad 16/600 Superdex 75 pg.

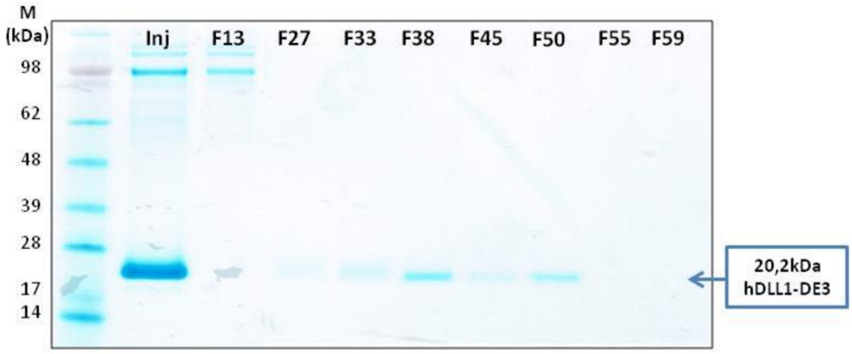


**Figure 3.17 - SDS-PAGE of hDLL1-DE3 elution from SEC – second strategy.** M- Marker; FT – flow-through; F –fractions. Blue box – molecular mass expected for hDLL1-DE3.

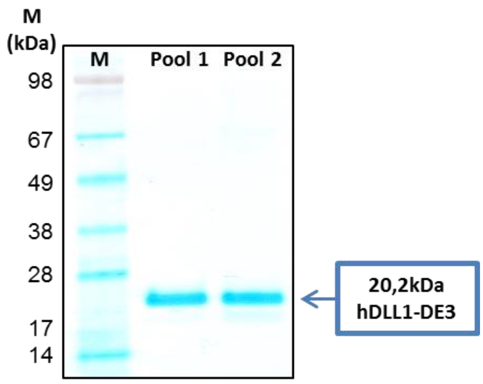


**Figure 3. 18 - SDS-PAGE hDLL1-DE3 final pools – second strategy.** Pool 1– Fractions 35 to 44; Pool 2 – Fractions 45 to 53; M- Marker; Blue box – molecular mass expected for hDLL1-DE3.

In the end of this second purification process highly pure protein could be obtained, but not without compromising the final protein yield (pool 1 - 90µg). One of the causes for the low yield may be the significant decrease in transfection efficiency obtained when scaling-up to T225cm$^2$. Figure 5.4 (Appendix 5.5) shows an example of one T225cm$^2$ transfected with the control plasmid (pAAVpuro-GFP), in which the percentage of transfected cells (green) is very low (only ranging from 10-20%) when compared to the one obtained in 6-well-plates or T25cm$^2$ (70-80%) (Figure 3.8). Furthermore and most importantly, recombinant protein expression when using mammalian cells as host is significantly lower when compared to *E.coli* and obtaining reasonable amounts of protein may be very challenging.

### 3.2.3 Assessment of target quality - hDLL1-DE3 titration

In order to evaluate the target quality to be used in panning, the hDLL1-DE3 protein was titrated using 1:2 dilutions, starting at a concentration of 10µg/mL and the detection was made using an Anti-His antibody (Ab). Figure 3.19 shows a good dose response for hDLL1-DE3 which suggests that the target quality is acceptable for further experiments.

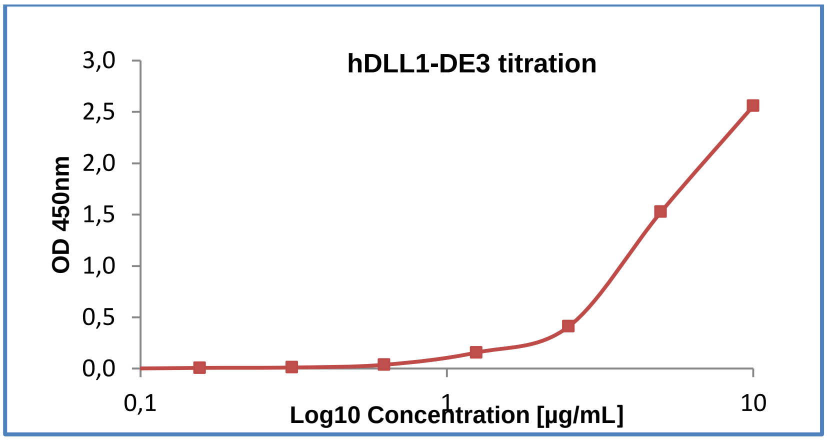


**Figure 3.19 - Titration of hDLL1-DE3**. Concentrations are represented in Log$_{10}$. The background signal was subtracted for each value represented.

### 3.2.4 Selection of specific Fabs for hLL1-DE3 - Panning

Due to the reduced protein quantities obtained in the previous section, the panning procedure was adapted from Rader *et al.*, 2001 and selection was performed using 96 well microplates. Three rounds of selection were carried out using the same target concentration for the first and second rounds (5µg/mL), which was then reduced for the third round (2.5µg/mL) in order to perform a more tight selection step. Furthermore, a depletion step was added previously to each selection to decrease the number of non-specific binders. Normally, the objective of the depletion steps is to redirect the selection specifically towards our antigen. In some cases, for example when the target has a fusion tag (i.e present for purification purposes) a different molecule with the same tags should be used simply to eliminate phage binders specific to that moiety of the protein. Another important feature of depletion is when the aim is to find phages for a specific protein domain. In this case, an ideal depletion molecule would be one is very similar to the target but different in the region that is to be targeted. For the specific case of the panning with hDLL1 no ideal molecule was available at that time in the host lab, so the depletion step was merely carried out using the uncoated wells of the plate. This strategy is also very commonly used since the coating of 96 well plates might not be 100% efficient, and by depleting on uncoated wells all plastic phage binders can be removed before selection with the target proteins.

All three rounds of selection were monitored by evaluating the Inputs and Outputs results. Inputs represent the number of phages that entered in the selection step. As for Outputs, they represent the number of phages that were selected. After plating the inputs and the outputs, colonies were counted and the following formula was used to obtain the number of colony forming units per mL (cfu/mL):

$$\frac{cfu}{mL} = \frac{number\ of\ colonies\ \times\ dilution\ factor}{plated\ volume\ (\mu L)} \times 1000$$

**Formula 3.1 – Calculation of colony forming units per mL (cfu/mL).**

Also, Formula 3.2 was used to calculate the percentage of phage recovery in each round and the enrichment between rounds was estimated using Formula 3.3.

$$phage\ recovery\ (\%) = \frac{output\ phages}{input\ phages} \times 100$$

**Formula 3.2 – Percentage phage recovery.** Formula adapted from *Arbabi-Ghahroudi et .al, 2009*.

$$Enrichment = \frac{phage\ recovery\ in\ round\ x}{phage\ recovery\ in\ round\ x-1}$$

**Formula 3.3 – Enrichment of recovered phages from one round to another.** Formula adapted from *Arbabi-Ghahroudi et al., 2009.*

The results for the three selection rounds are summarized in Table 3.3. The cfu/mL values obtained for the Outputs are in accordance to Rader *et al.*, 2012 that described that values should range between $10^4$ and $10^7$. Phage recovery increased from round 1 to round 2, which indicates an increase of target-specific phages, which was confirmed by the value of enrichment – 15,18x. As for Input values, in the first round they are higher than previously estimated – from $10^{11}$ to $10^{12}$, and this can be due to an error during titration or during library dilution when performing the depletion step. Unfortunately, it was not possible to obtain the Input values on the third round in order to evaluate if the enrichment in specific binders was higher or not. Nevertheless, the results obtained indicate that the panning using the microplate protocol was successful.

**Table 3.3 - Summary of hDLL1-DE3 panning.**

| Round | Input (cfu/mL) | Output (cfu/mL) | Phage recovery (%) x 1000 | Enrichment |
|---|---|---|---|---|
| 1 | $2,1 \times 10^{13}$ | $1,4 \times 10^6$ | 0,007 | – |
| 2 | $8,4 \times 10^{12}$ | $8,5 \times 10^6$ | 0,101 | 15,18x |
| 3 | – | $3,6 \times 10^7$ | – | – |

### 3.2.5 Assessment of Phage Pools Reactivity

In order to assess if the pools from rounds 2 and 3 presented a target dose response, phages from both rounds were analysed by Phage ELISA, by being serial diluted and incubated in a plate previously coated with the hDLL1-DE3 protein target. The typical dose response fingerprint should be an increase of the signal for higher number of phages until saturation is observed and the signal is kept at a plateau. As depicted in Figure 3.20, it is possible to observe a dose response for the more diluted samples - dilutions 1-4 for round 2 and 1-7 for round 3. However, and surprisingly when approaching higher phage concentration values the signal response clearly reduces. An hypothesis for this behaviour could be associated with the use of such high concentrations of phages in small volumes in the lower dilutions. It is known that phages are very sticky (Barbas *et al*., 2004) and for this reason, when in increased amounts the phages could be interacting among them impairing their ligation to the antigen. In such a case, because the phages would no longer be able to bind to their target, no dose response would be possible to detect. Moreover, this behaviour was also previously detected for two naïve libraries that were built in parallel with the one used in this work. Unfortunately, and since the expected result was not observed for the phage pools, individual clones were analysed to check whether the panning selected specific binders.

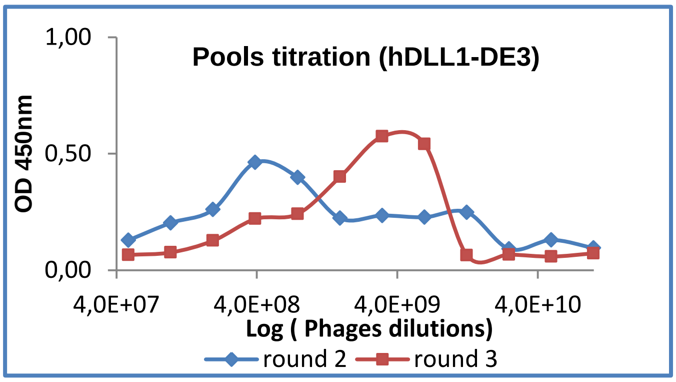


**Figure 3.20 - Titration of phages selected for hDLL1-DE3**. The background signal was subtracted for each value represented.

### 3.2.6. Assessment of selected individual clones reactivity

To evaluate whether panning-selected phages displayed target-specific Fabs, an ELISA assay was performed. With that goal in mind, 30 clones from round 3 Output plates were randomly chosen and amplified using the helper phage to produce Fabs-expressing phages. As the panning step was performed in a small scale (microplate), and therefore using a lower number of phages when comparing to other scales, the amplification was performed in 5mL in order to obtain enough phage copies that bind the target and give a detectable signal on ELISA.

For this assay, three types of coatings were used in order to evaluate: *i.* target specificity - using hDLL1-DE3 for coating; *ii.* Fab Display - using anti-Fab antibody for coating; *iii.* Phages production - using anti-M13 for coating, since this antibody recognizes the phage's surface protein 8 (Henry and Pratt, 1968). As a negative control an uncoated plate was used.

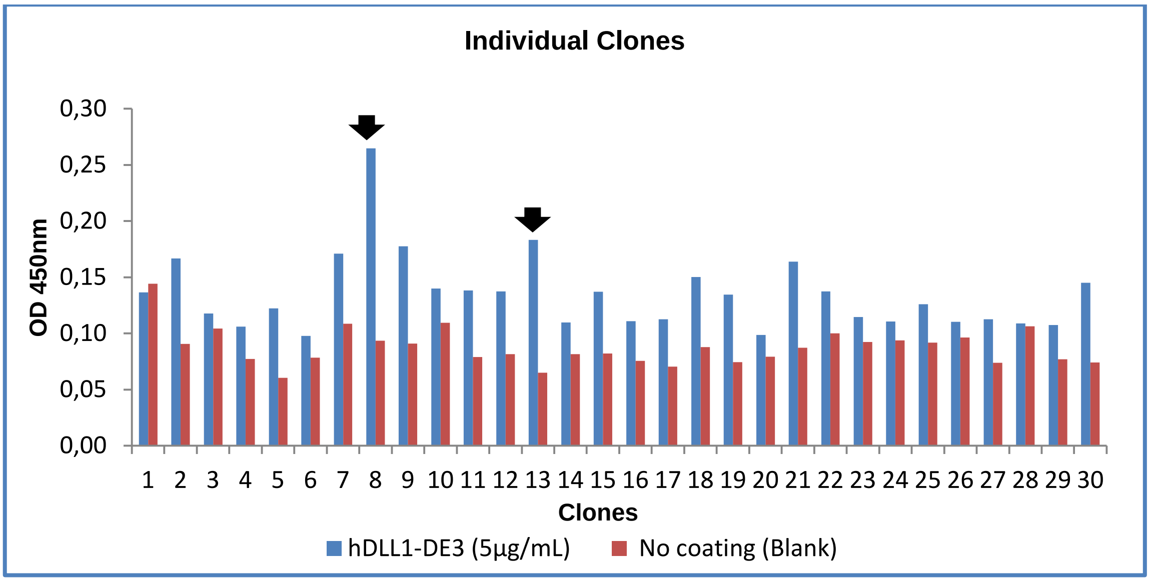


**Figure 3.21 - Fab-on-phage ELISA of individual clones selected against hDLL1-DE3.** Black arrows- highlight clones 8 and 13 that present an ELISA signal 2,8 times higher than the background ( non-coated well).

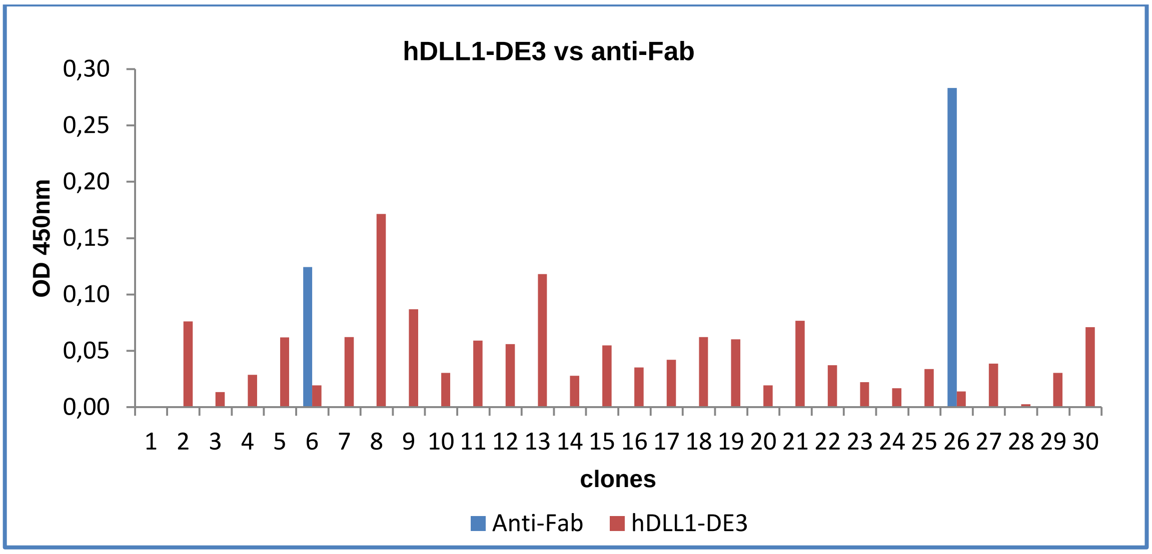


**Figure 3.22 - Fab-on-phage ELISA of individual clones. - Comparison of Anti-Fab with hDLL1-DE3.** The background signal was subtracted from the values obtain for the two types of coating.

In Figure 3.21, it is possible to observe that only two clones presented a signal approximately 3-fold higher than the background. On the other hand, Figure 3.22 shows the comparison between the signal using the target as coating and using anti-Fab Ab, where it is evident that the Fab expression was not ideal and the clones that present a good signal for Fab expression lack in specificity for the target. The signal for all clones when using anti-M13 Ab was good, confirming the presence of a high number of phages recovered after each round of panning (data not shown). The low number of target specific clones can in part be related with the limitations of the microplate technique. Normally, $1x10^{13}$ phages in 1mL should be used for panning (Sblattero and Bradbury, 2000). Although the standard concentration of phages was not suppressed ($1x10^{11}$ in 100µL were used), the confined space of a microplate's well when compared to other surfaces (e.g. immunotubes), may be related to a less efficient selection. Furthermore, due to limitations on the available target quantity only 30 individual clones were analysed. We cannot exclude that if a higher number of clones were analysed this may have resulted in the unveiling of more specific binders. So, in order to improve these results, it was crucial to repeat the selection procedure trying different panning strategies to obtain more target-specific clones.

### 3.3 Protein refolding from inclusion bodies in *E.coli* – hDLL1-DE3 (pET47(b)+)

According to the above described expression screenings results (Section 3.1.1), high levels of protein were expressed in the insoluble fraction. In order to make a better use of this protein material we followed the guidelines suggested by Rudolph and Lillie (1996) and also Zhao (2009), to refold protein from inclusion bodies. Inclusion bodies are dense electron-refractile particles composed by protein aggregates that can be formed in *E.coli* cytoplasm and periplasm (Carrió *et al.*, 2000; Palmer and Wingfield, 2004). Inclusion bodies are mostly composed of our target protein, which may be in two different forms; *i.* native protein, easily solubilised under mild conditions; or *ii.* misfolded protein, which is basically insoluble material requiring high concentrations of denaturants to be solubilised again. Therefore, the major hurdle to obtain native, active protein is to find the appropriate efficient refolding conditions (Clark, 1998). The refolding process and the two used solubilisation strategies are described below.

#### 3.3.1 Solubilisation with Guanidine-HCl and L-arginine refolding

After cell lysis, the inclusion bodies containing pellet, was well washed five times and centrifuged at high speed in order to separate all the remaining cell debris. The pellet presented a brownish colour when it was expected to be almost white, which may suggest the presence of unbroken cells. Samples were taken after each washing step and analysed by SDS-PAGE, as shown in Figure 3.23. In the first washing step (W1) many contaminants are washed away from the inclusion bodies fraction. The solubilisation step with denaturants was also well succeeded as it is possible to see in Figure 3.29 that the protein is almost pure. On this step Guanidine-HCl was used at high concentration (6M) to solubilize the insoluble protein fraction and DTT was used to maintain the disulphide bonds in the reduced state, consequently avoiding non-native intra or inter-molecular interactions between potential disulphide bonds (Janson, 2011). After this solubilisation the protein refolding was made using L-arginine, TMAO and GSSG/GSH. The first is used to help preventing aggregation during refolding (Arakawa and Tsumoto, 2003). TMAO, a known osmolyte, helps in folding by stabilizing proteins and counteracting the effect of the denaturant agent (Zou *et al.*, 2002). Finally, GSSG and GSH are both used to promote the right redox environment and, consequently to help in the right formation of the disulphide bonds that have been destroyed during the denaturation step by guanidine-HCl (Vallejo and Rinas, 2004).

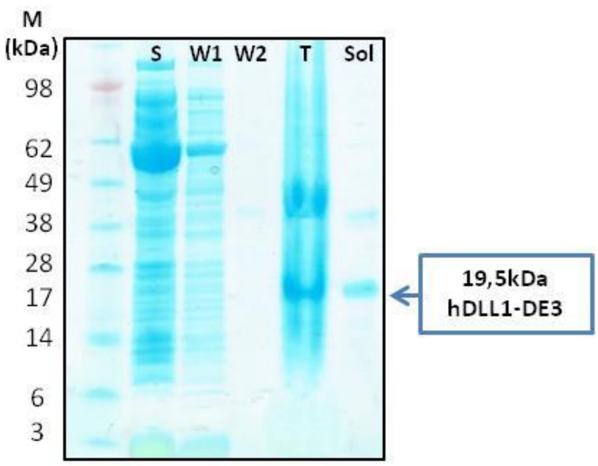


**Figure 3.23 - SDS-PAGE: washing and solubilisation of inclusion bodies.** M - Marker; S – soluble fraction after bacterial lysis; W1 – washing of the inclusion bodies with buffer Wash IA; W2 – washing of the inclusion bodies with buffer Wash IIA; T – Total after solubilisation; Sol – Sample after centrifuging the solubilised inclusion bodies. Blue box marks the molecular mass of hDLL1-DE3.

The refolding step was gently performed for two days with the protein diluted to a concentration of 0.1mg/mL. Low protein concentrations are here required to shift the equilibrium towards refolding, as aggregation is more likely to occur then refolding itself and more aggregation tend to happen when the concentration of protein is higher (Xie and Wetlaufer,1996). Also, dilution of the solubilized protein at a very slow rate (drop-wise) prevents aggregation and increases the likelihood of recovering a higher amount of refolded protein. After refolding, the protein was concentrated before proceeding to purification.

To change the refolding buffer to a simpler buffer, a desalting column was used and as observed in Figure 3.24, the first peak corresponds to the protein and the second to the refolding buffer. When one applies the protein into a desalting column pre-equilibrated with the new buffer, it will migrate faster than the old buffer's components – size exclusion principle, and will thus elute from the column under the new buffer (Porath and Flotin, 1959).

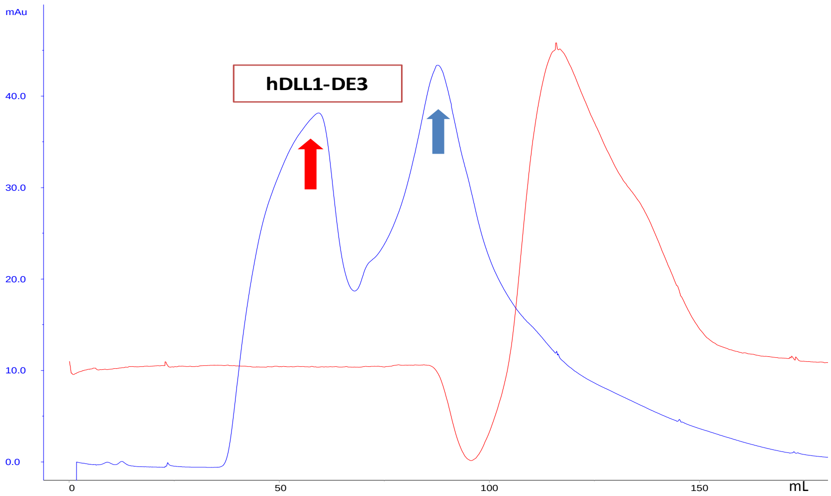


**Figure 3.24 - Chromatogram of Desalting – purification of hDLL1-DE3.** Blue line – UV; Red line – Conductivity; Red arrows – peak corresponding to hDLL1-DE3 elution; Blue arrows – peak corresponding to the refolding buffer elution. Column – HiPrep 26/10 desalting

After the desalting step, the purity of the protein was analysed by SDS-PAGE, using silver staining that due to its sensitivity allows the detection of low protein quantities. In Figure 3.25, it is possible to see that the eluted protein from the desalting column is more than 95% pure. So the protein was pooled and concentrated to be used for further experiments.

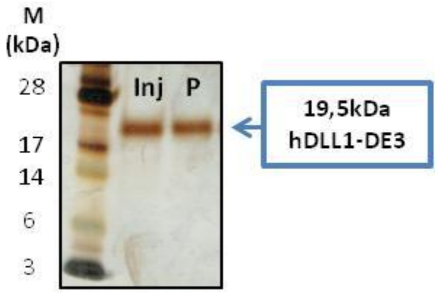


**Figure 3.25 - SDS-PAGE after desalting of hDLL1-DE3.** Silver staining. Inj– Inject; P – peak of hDLL1-DE3 elution. Blue box marks the bands induced in the molecular mass expected for hDLL1-DE3.

To assess the homogeneity of the purified protein, an analytical SEC was performed. The columns used for this analysis are composed by more theoretical plates than the ones used during preparative purification, which allows a better chromatography resolution. So, using this method one is able to confirm whether the protein is homogeneous and whether it is composed of only one isoform. In Figure 3.26, it is possible to see that, according to the analytical SEC, only one major peak is present, which suggests this sample to be fairly homogeneous.

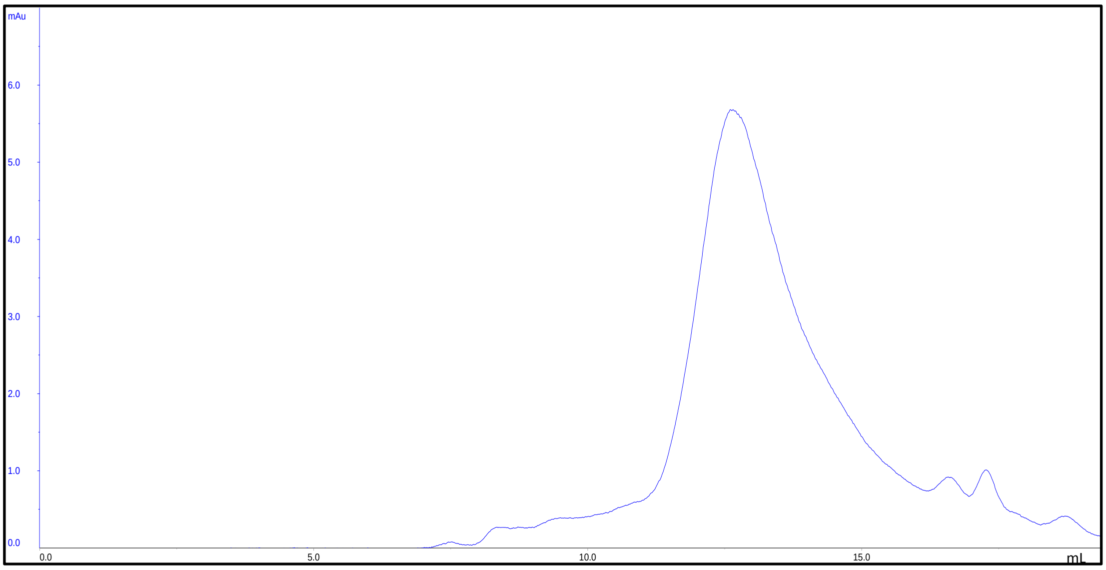


**Figure 3.26 -** Analytical SEC of hDLL1-DE3. Blue line – UV. Column - Superdex 75 10/300 GL.

#### 3.3.1.1 Protein thermal stability - Thermal shift assay

The hDLL1-DE3 was analysed by thermal shift assay (TSA), which is used to evaluate protein thermal stability using a specific The used fluorophore binds to the hydrophobic residues/patches of the protein that are normally hidden from solvent and are exposed upon protein thermal denaturation, exhibiting fluorescence that can be detected and measured (Pantoliano *et al.*, 2001).

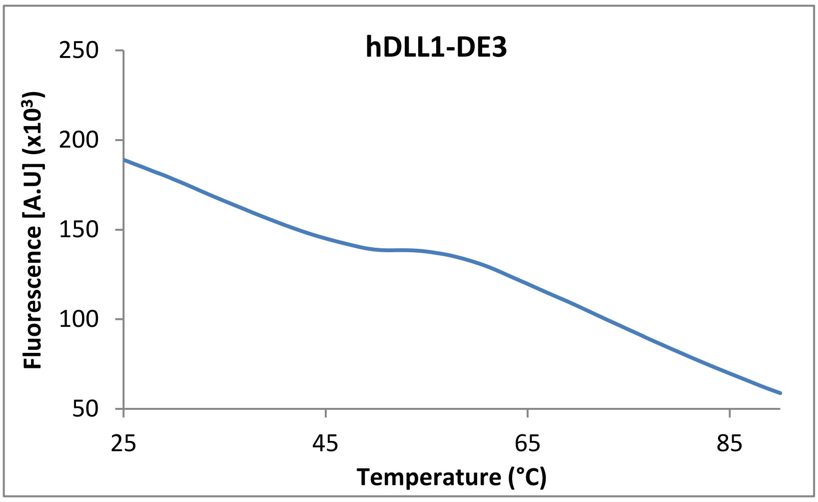


**Figure 3.27** - TSA for hDLL1-DE3. 20µg of protein were used. A.U – Arbitrary Units.

Although high initial fluorescence is observed for hDLL1-DE3, a small thermal transition can be detected masked by the intrinsic background fluorescence (Figure 3.27). According to previous studies, the conformation of hDLL1-DE3, expected to be elongated and composed by many loops (Kershaw *et al*., 2015), may help to explain these results. Based in the TSA literature (Pantoliano *et al.,* 2001,Ericsson *et al*., 2006), we may hypothesize that intrinsically, our target protein, may have some hydrophobic residues or regions slightly exposed where the fluorophore may bind. In spite of this, hydrophobic regions within the protein core region are still unexposed and are available for binding upon temperature increase and protein denaturation, thus generating the observed small transition. Using the derivative of the observed fluorescence increase transition, it is possible to estimate the melting temperature which corresponds to the temperature where the concentration of folded and unfolded protein is the equivalent (Niesen *et al.*, 2007). For this protein, the estimated Tm was 52ºC.

In conclusion, the final protein quality was considered good, and high purity was achieved as confirmed by silver staining gel. Also, the sample was found to be homogenous as only one peak was observed in the analytical SEC analysis. However, the amount of protein obtained from this first strategy was only 1mg. So, in order to obtain a higher yield of protein, a new strategy was adopted.

### 3.3.2 Solubilisation of the Inclusion Bodies with urea

Given that the yield of protein was not very high when using the refolding strategy with guanidine-HCl, a new protocol was tested in order to obtain more protein. This protocol was adapted from the work performed by Zhao and his team, in which an hDLL1 construct comprising the N-terminal and the DSL domain was successfully expressed and purified from inclusion bodies (Zhao *et al.*, 2009).

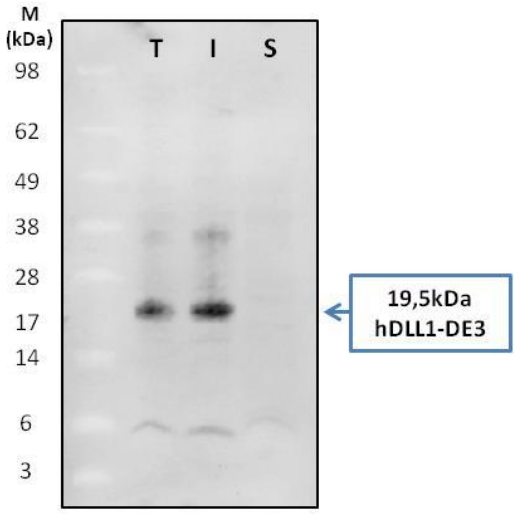


**Figure 3.28 – Anti-His Western Blot of hDLL1-DE3 large scale production.** M – Marker; T – Total induced culture; I – Insoluble fraction; S – Soluble fraction.

To confirm that the large scale expression of this protein was well succeeded, Western Blot was performed (showed in Figure 3.28). The pellet was washed in the same way as in batch I. In this strategy however, the solubilisation step was made using urea instead of Guanidine-HCl, and the refolding was achieved using two different buffers. The first buffer was used to dilute the protein and the second to adjust the pH to a more suitable value – pH 9.1. The refolding step was also performed using a low protein concentration to prevent aggregation.

After the refolding step, an anionic exchange chromatography (AIC) was performed in order to remove the endotoxins since they bind very tightly to this Q-sepharose (Lee *et al.*, 2003). This step was very important since the produced protein will be used to perform cell-based functional assays, where endotoxins can interfere with the results quality. Assuming an estimated hDLL1-DE3 isoelectric point of 5.8, the protein was diluted in a pH 9.1 buffer, in order to make its overall charge negative and thus able to bind a positively-charged resin. After injecting the protein, elution was carried out by slowly increasing the ionic strength of the elution buffer using increasing concentrations of sodium chloride. The SDS-PAGE analysis clearly shows that, surprisingly, the protein was also present in the flow-through possibly because the capacity of the column was exceeded. The protein was also detected spread over most of the elution profile. One hypothesis is that the injected sample is composed of a heterogeneous conformation population (Figure 3.29). A one step elution would have contributed to the elution of a more concentrated sample, although with a likely non-homogeneous sample, that could then be later analysed in a size-exclusion experiment. . Nevertheless, pure protein was obtained and two pools were prepared (Pool 1 and 2, as indicated in Figure 3.30).

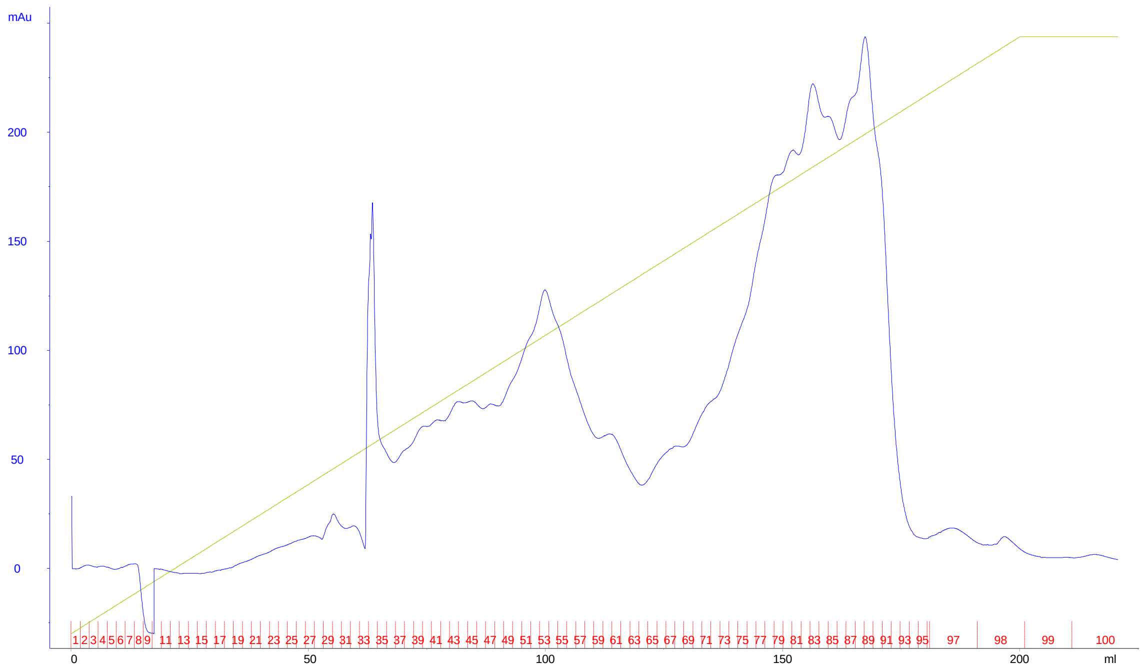


**Figure 3.29 - Chromatogram of AIC – elution step.** Blue line – UV; Green line – concentration of Buffer IEC B (1M of NaCl) and Red line – fractions. Column - HiPrep Q HP 16/10 column.

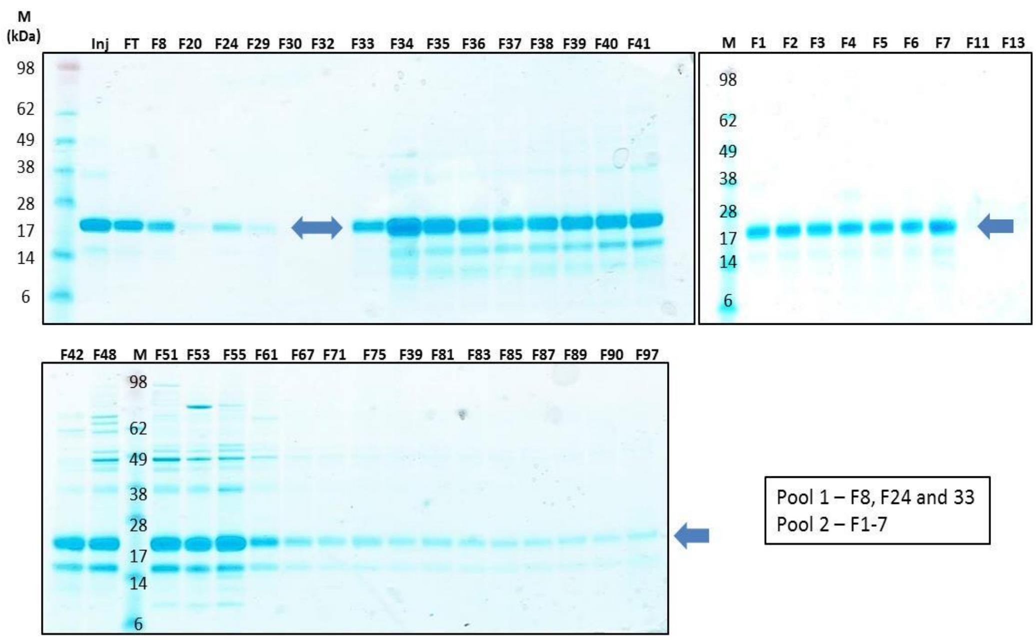


**Figure 3.30 - SDS-PAGE of AIC.** M – Marker; Inj – Inject; FT – Flow-through; F- Fractions. Blue arrows mark the molecular mass expected for hDLL1-DE3 (19,5kDa).

It was clear that this purification step was not suitable to properly remove contaminants. The remaining impure fractions, as well as the flow-through were re-injected in a Histrap column in two different injections. On the first injection, the elution was done in a gradient up to 0.2M imidazole (to remove contaminants), following *Zhao et al* protocol, followed by three steps of 25%, 50% and 100% of Buffer with 1M imidazole to assure all protein was eluted from the column (Figure 3.31). After analysis by SDS-PAGE gel, a third pool was prepared with the fractions that presented a band corresponding to the hDLL1-DE3 protein Figure 3.32. Part of the target protein was also eluted during the washing steps, which is in accordance with the heterogeneous behaviour previously observed in the AIC step.

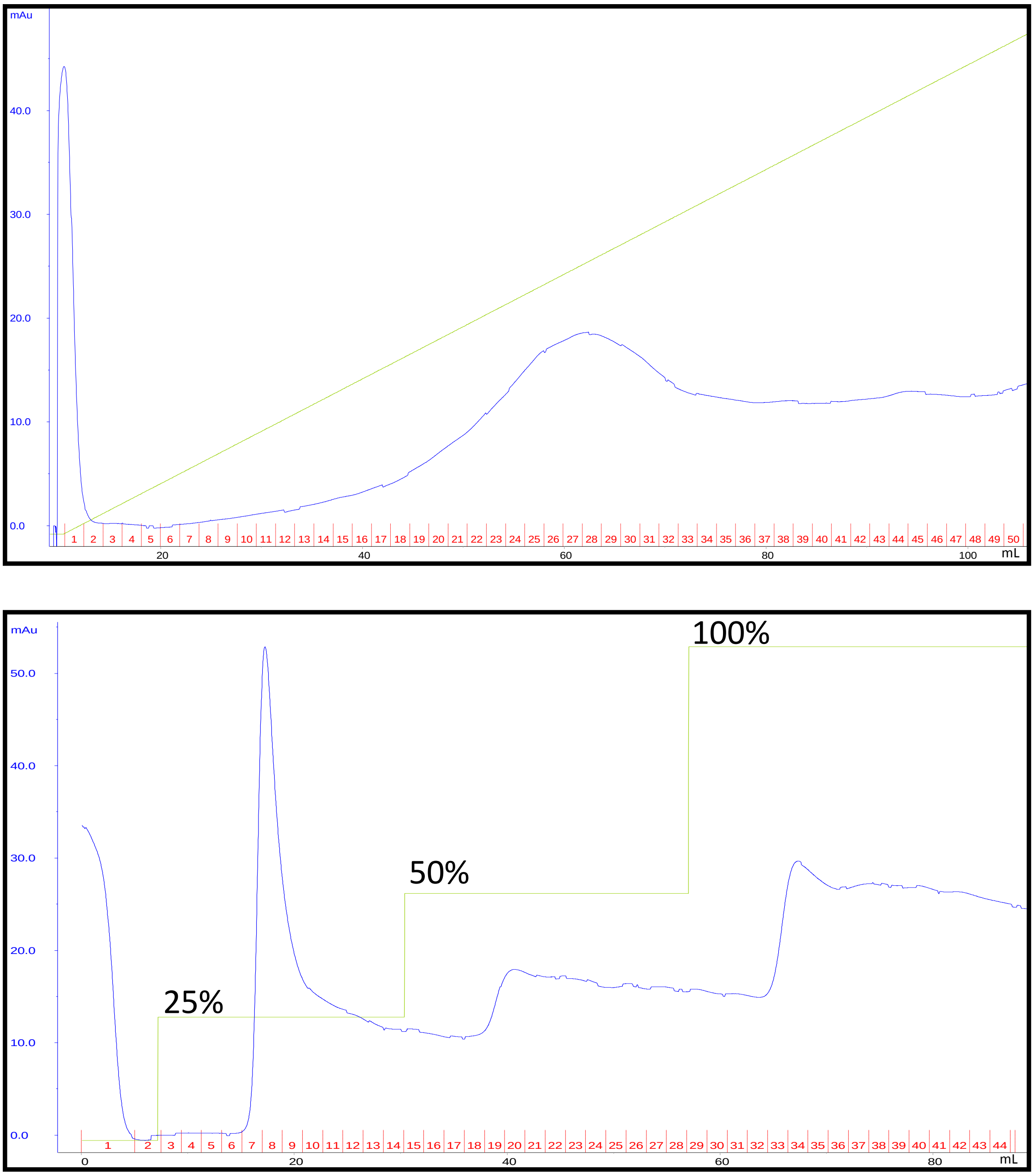


**Figure 3.31 - Chromatogram of Histrap 1st injection – elution step. First panel (top)**- first elution with a gradient of Buffer Histrap C. **Second panel (bottom) –** second elution with steps of Buffer Histrap D – 25% (287,5mM imidazole), 50% (525mM imidazole) and 100% (1M imidazole). Blue line – UV; Green line – concentration of Buffer Histrap C (0.2M imidazole) or Buffer Histrap D (1M imidazole); Red line – fractions. Column - HisTrap FF 5mL

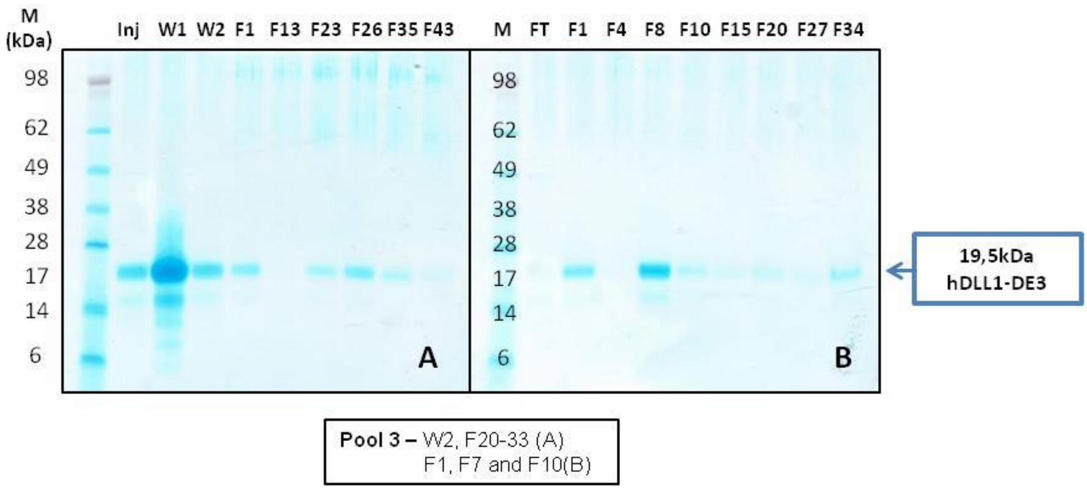


**Figure 3.32 - SDS-PAGE Histrap – 1st injection. A.** Elution with Buffer C gradient (0.2M imidazole). **B.** Elution with steps of Buffer D (1M imidazole). M – Marker; Inj – Inject; W – Wash; F – fractions; FT – Flow-through. Blue box – molecular mass expected for hDLL1-DE3; Black box: Description of pool 3.

In the second subsequent injection, the elution was now made with a gradient up to 1M imidazole and fixing the concentration of imidazole when a peak was observed (Figure 3.33). This strategy was used to ensure a simultaneously protein elution in a minimal volume. Once again the protein was still detected in the washing step, as well as in all the analysed fractions, regardless of used imidazole concentration,, , as observed in the first injection. From this step two extra pools (4 and 5) were prepared, in order to differentiate samples based on purity (Figure 3.34).

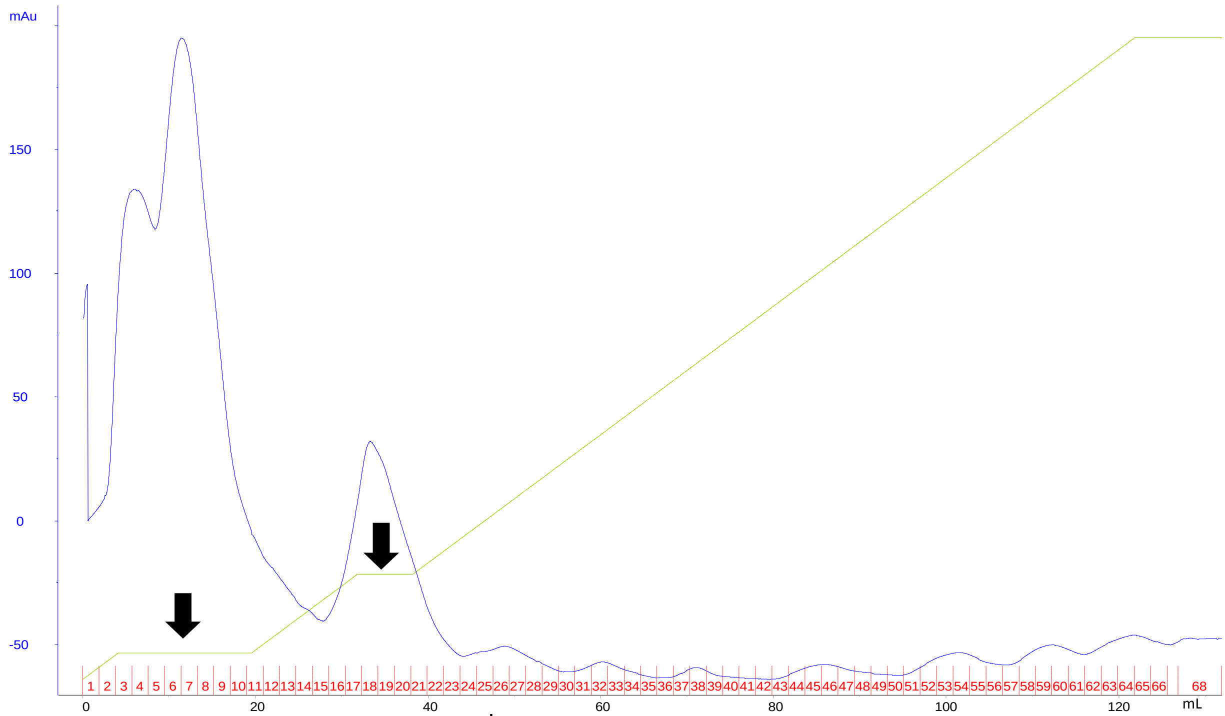


**Figure 3.33 - Chromatogram of Histrap 2nd injection – elution step.** Elution with gradient of Buffer Histrap D (1M Imidazole). Black arrow represents the steps where the concentration of Buffer D was fixed. Blue line – UV; Green line – concentration of Buffer Histrap D (1M imidazole); Red line – fractions. Column - HisTrap FF 5mL.

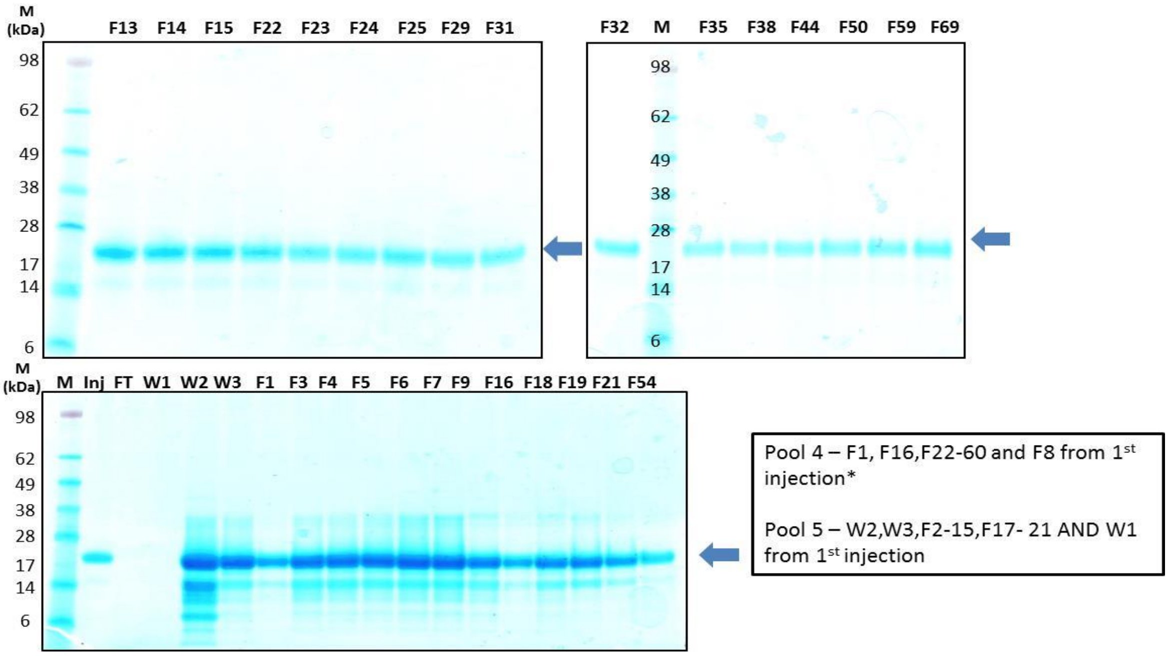


**Figure 3.34 - SDS-PAGE of Histrap – 2nd Injection.** M – Marker; Inj – Inject; FT – Flow-through; W – Wash; F- Fractions; *- elution with 1M imidazole Blue arrows mark the band correspondent to hDLL1-DE3 (19,5kDa).

All pools from anionic exchange and Histrap were concentrated and stored at -80ºC. A final SDS-PAGE was made in order to analyse the purity of each pool (Figure 3.35). It is possible to observe that, after concentration all the pools are equally pure, including pool 5 that was expected to contain the most contaminated sample. Contributing to this final good purification profile was also the concentration step using a cut-off of 10 kDa, where low molecular weight contaminants could be eliminated. However, we can observe the presence weak lower molecular mass protein band in the SDS-PAGE, which was confirmed, by mass spectrometry, to be a degraded form of hDLL1-DE3 protein.

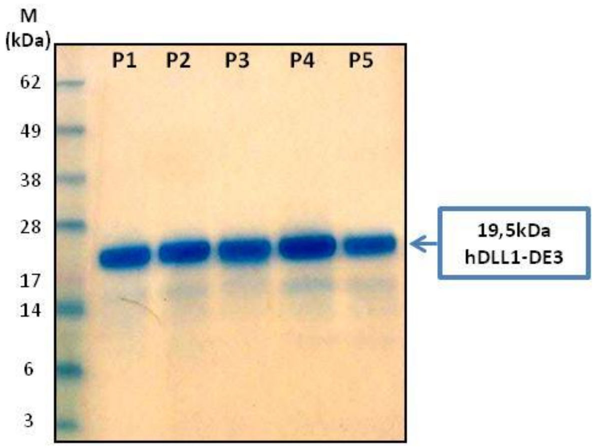


**Figure 3.35 - SDS-PAGE of hDLL1-DE3 purified from inclusion bodies.** M – Marker; P1- Pool 1; P2- Pool 2; P3- Pool 3; P4- Pool 4; P5- Pool 5.

In total, approximately 11 mg of pure protein were obtained with this new approach/protocol. Due to final protein quantities, we decided to use only Pool 5 for further experiences. Furthermore, this sample was analysed in terms of homogeneity in order to assess if it was in fact composed by proteins with different conformations. However, when performing an analytical SEC, it was possible to observe that this sample is apparently homogeneous; suggesting that only one conformation of this protein is present in the final sample (as depicted in Figure 3.36).

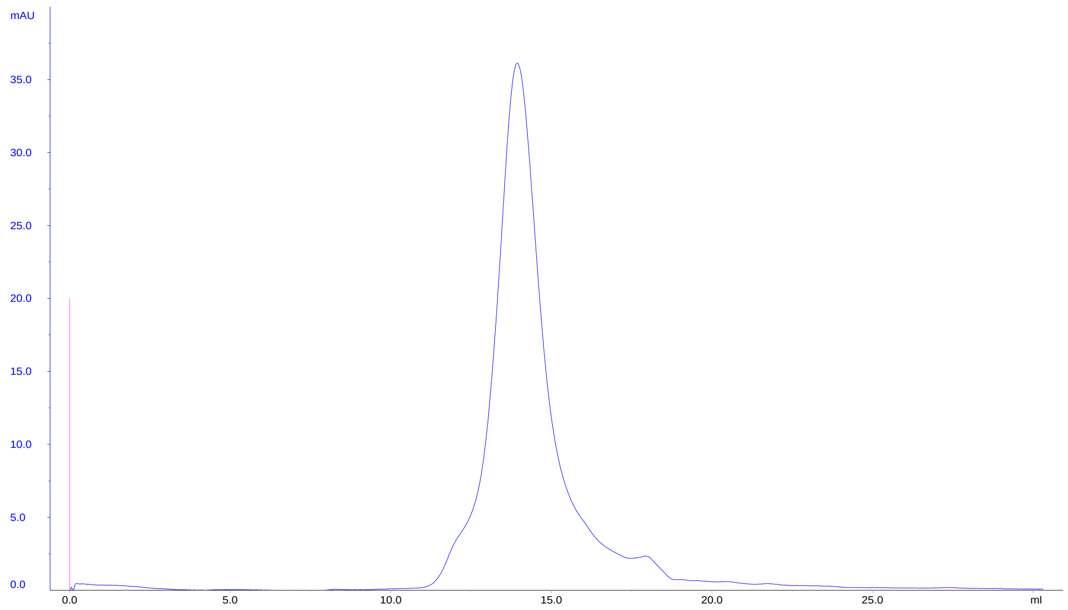


**Figure 3.36 - Analytical SEC hDLL1-DE3 pool 5.** Blue line – UV; Pink line – Inject. Column - Superdex 75 10/300 GL.

#### 3.3.2.1 Protein thermal stability - Thermal shift assay

The protein obtained from the second solubilisation strategy (using Urea) was analysed by thermal shift assay to assess the thermal stability of the sample. The result is depicted in Figure 3.37, and the curve obtained for this sample is comparable to the one obtained for the TSA performed for the protein from the first strategy (purified with Guanidine-HCl), where the initial fluorescence was very high but a small transition was nevertheless observed (Section 3.3.1.2). This high initial fluorescence seems to be a a fingerprint of this recombinant protein. However, the Tm value of 70ºC obtained for this second strategy, was considerably higher than the one obtained on the first strategy (52°C), which suggests that this new protein batch is more stable, given that this protein's denaturation occurs at higher temperatures.

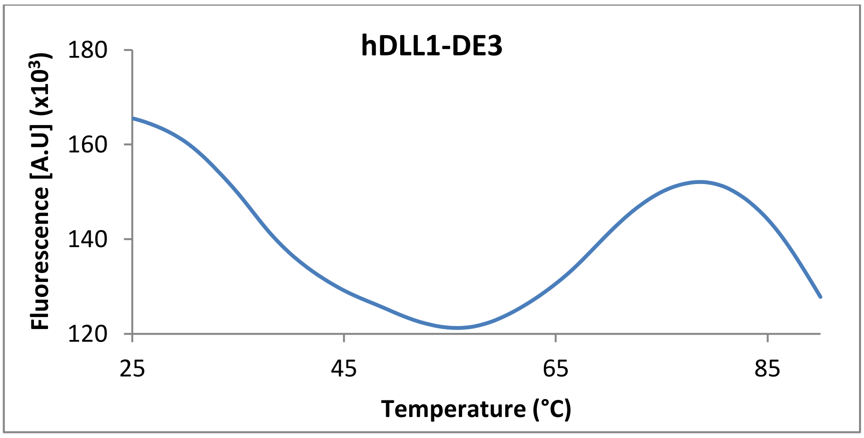


**Figure 3.37 - TSA for hDLL1-DE3 – pool 5**. 60µg of protein were used. A.U. – Arbitrary Units.

### 3.3.2.2 - Biologic activity or functional characterization of recombinant protein

#### 3.3.2.2.1 Cell line evaluation

To evaluate if the recombinant hDLL1-DE3 protein produced from refolding of inclusion bodies was biologically active, an *in vitro* assay was performed. For this purpose we first determined the basal mRNA levels of *hNotch1* and *hDLL1* in three different cell lines: human inducible pluripotent stem cells (iPSCs), and the breast cancer cell lines HCC1954 (low proliferative) and MDA-MB-468 (highly proliferative and metastatic). Total RNA was obtained from these cells, cDNA was generated and the expression levels of these genes were evaluated by real time PCR. The results presented on Figure 3.38, clearly show that the transcription levels of both *hNotch1* and *hDLL1* are significantly different amongst the three cell lines, being significantly higher in MDA-MB-468 cells. For *hNotch1*, the MDA-MB-468 cells presented mRNA levels about 470 times higher than HCC1954 cells and about 15 times higher than iPSCs. For *hDLL1*, the differences obtained between each cell line were lower. Nevertheless, MDA-MB-468 cells had transcription levels about 2 times higher than iPSCs and about 22 times higher than HCC1954.

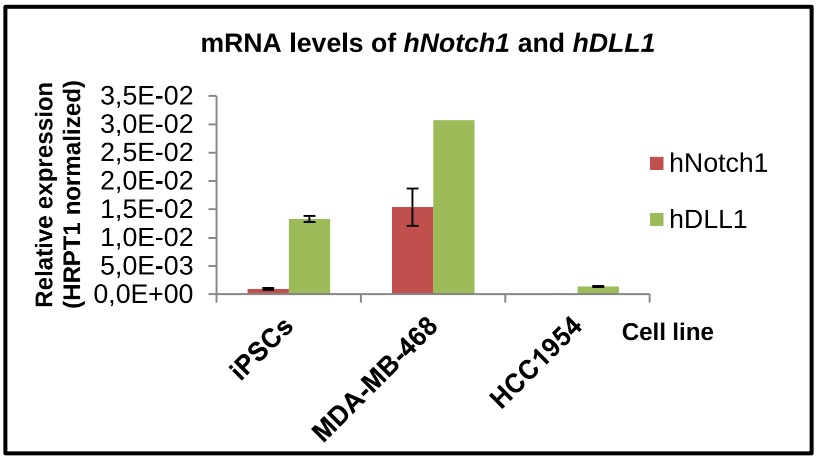


**Figure 3.38 - mRNA levels of *hNotch1* and *hDLL1* in different cell lines.** All values were normalized with HPRT1 (control gene). Error bars represent the standard deviation between replicates.

Hyper activation of the Notch signalling pathway has been related with carcinogenesis and more importantly with an invasive behaviour of breast cancer cells (Wang *et al.*, 2011b). Thus, given that MDA-MB-468 cells were isolated from a metastatic adenocarcinoma (Cailleau *et al.*, 1978) from the breast, with high-proliferative and invasive features it was expected that both Notch1 receptor and hDLL1 ligand were over-expressed in these cells. The HCC1954 cell line was obtained from a primary stage IIA, grade 3 invasive ductal carcinoma (breast cancer cells) with no metastases/invasive behaviour (Gazdar *et al.*, 1998). Therefore, when comparing the results for MDA-MB-468 with the ones obtained for HCC1954, a reduction of mRNA levels for both genes was anticipated in the last. Finally, iPSCs are reprogrammed embryonic-like pluripotent cells derived from adult cells (Takahashi *et al.*, 2007). Since Notch signalling pathway is involved in differentiation and is crucial during embryonic development (Artavanis-Tsakonas *et al.*,1999), it was expected to observe considerable levels of *hNotch1* and *hDLL1* mRNA on this cells, which was the case.

### 3.3.2.2.2 Modulation of Notch1-dependent genes by hDLL1-DE3

Given the results presented above, showing that Notch1 signalling is not hyper-activated in iPSCs and HCC1954 cells, contrary to MDA-MB-194 cells, these two cell lines were chosen to assess the bioactivity of the recombinant hDLL1-DE3 since, the activation of Notch signalling by this protein would be more easily detected. In these assays, the mRNA expression levels of genes belonging to Hes family Hes-1, Hey-1, Hey-L were evaluated, since their transcription depends on the activation of the Notch1 signalling pathway (Borggrefe and Oswald, 2009). The transcription levels of *hNotch,* and the Nocth-1 ligands *hDLL1*, *hJagged2, and hJagged1* were also evaluated in response to rDLL1-DE3. The assay was first performed in iPSCs treated with different concentrations of hDLL1-DE3 protein (0; 1,5; 2,5 and 5µg/mL).

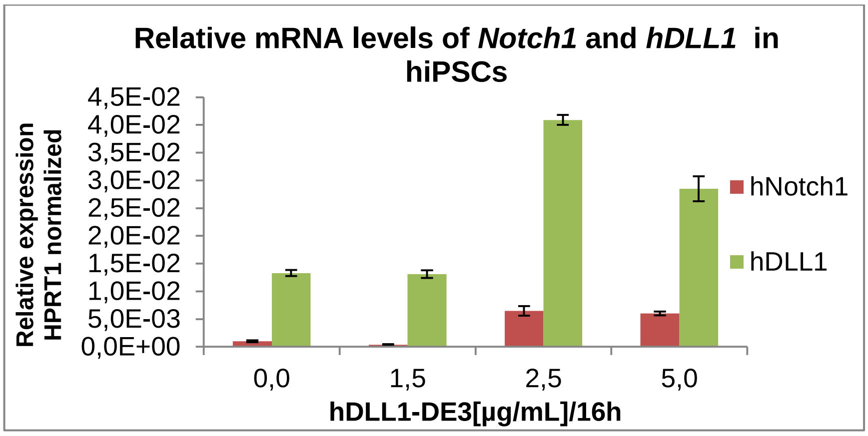


**Figure 3.39 - mRNA levels of *hNotch1* and *hDLL1* in iPSCs in response to hDLL1-DE3.** The values were normalized against the HPRT1 (control gene) mRNA levels in the same sample. Error bars represent the standard deviation between replicates.

As shown in Figure 3.39, treatment of iPSCs with rDLL1-DE3 (2,5 and 5µg/mL) for 16h increased significantly the mRNA levels of *hDLL1*, and a slight increment was also detected for Notch1, when compared to control cells to which only protein buffer (vehicle) was added. The *Hey-L, Hes-1, and Hey-1* genes showed a small inconsistent modulation of their expression levels in response to hDLL1-DE3 in these cells (data not shown). These results may suggest that these genes are not much regulated by DLL1-mediated Notch1 activation in the cell lines tested. However, another hypothesis is that the experimental conditions used were not ideal. Probably, the addition of more time points, including short periods of 2 and 4 hours, may represent a good option to achieve better results.

After observing the results for iPSCs, the expression of the target genes in response to rDLL1-DE3 in the HCC1954 cells was analysed at different times points (2, 4, 8 and 24h). Time course and dose response assays performed in these cells showed that rDLL1-DE3 caused a significant increase in the expression levels of some of the Hes family genes in a dose and time-dependent manner. The mRNA levels of *Hes-1* increased after 4h and 8h treatment with rDLL1-DE3, reaching expression levels 4 times higher when compared to the control cells (0µg/mL) (Figure 3.40).

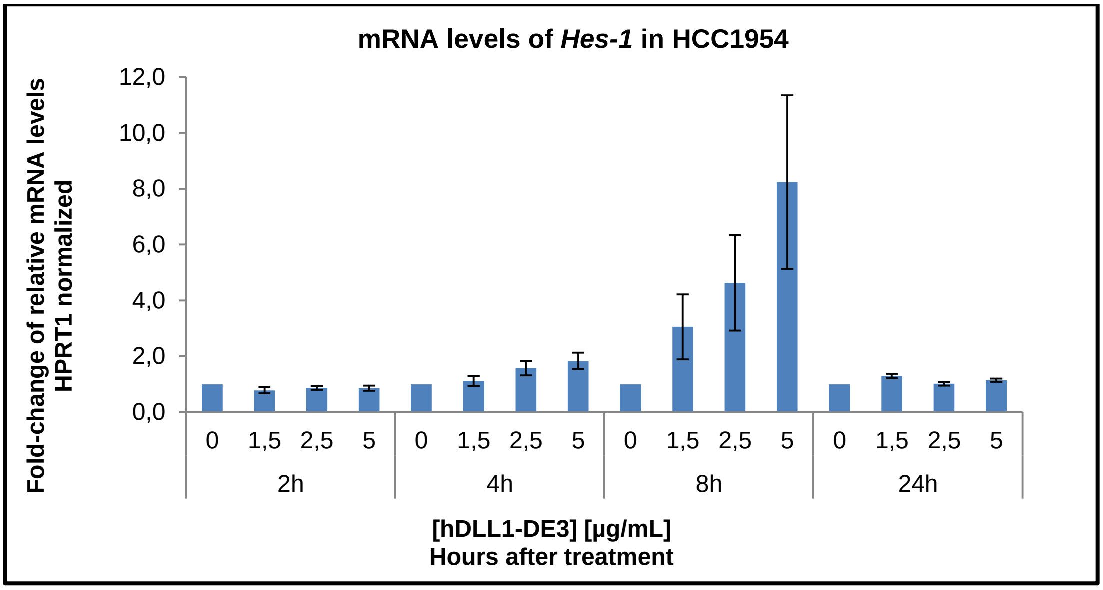


**Figure 3.40 - mRNA levels of *Hes-1* in HCC1954 in response to hDLL1-DE3 treatment**. All values were normalized against HPRT1 (control gene) mRNA levels in the same sample and are expressed as fold change relative to their levels in control cells treated with vehicle (0µg). Error bars represent the standard deviation between replicates.

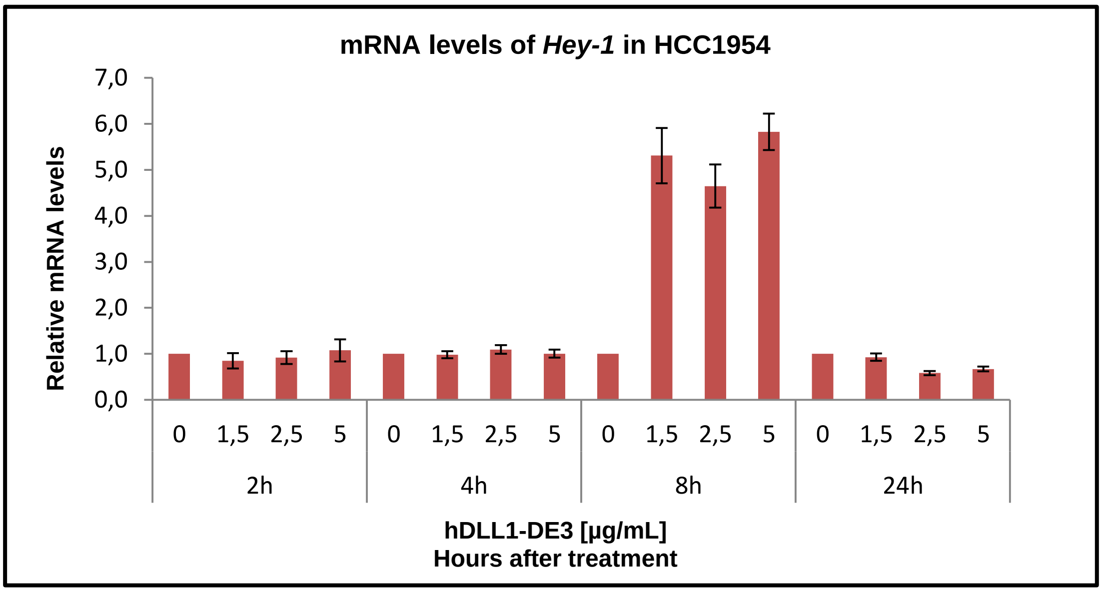


**Figure 3.41 - mRNA levels of *Hey-1* in HCC1954 in response to hDLL1-DE3 treatment**. All values were normalized against HPRT1 (control gene) mRNA levels in the same sample and are expressed as fold change relative to their levels in control cells treated with vehicle (0µg). Error bars represent the standard deviation between replicates.

For *Hey-1*, a modulation was also observed since its mRNA levels increased after 8h post-treatment by 5-fold when compared to control cells. However, no dose response effect of rDLL1-DE3 on Hey-1 expression was observed (Figure 3.41). When evaluating the expression of *hNotch1* an increase in its mRNA levels is visible only after 24h rDLL1-DE3 treatment, mostly with 2,5 and 5μg/mL of hDLL1-DE3 (Figure 3.42). Finally, addition of increasing doses of hDLL1-DE3 showed no effect in the transcription levels of the Notch1 ligands *hJagged1*, *hJagged2*, and *hDLL1,* and this was also true for *Hey-L* in HC1954 cells (data not shown).

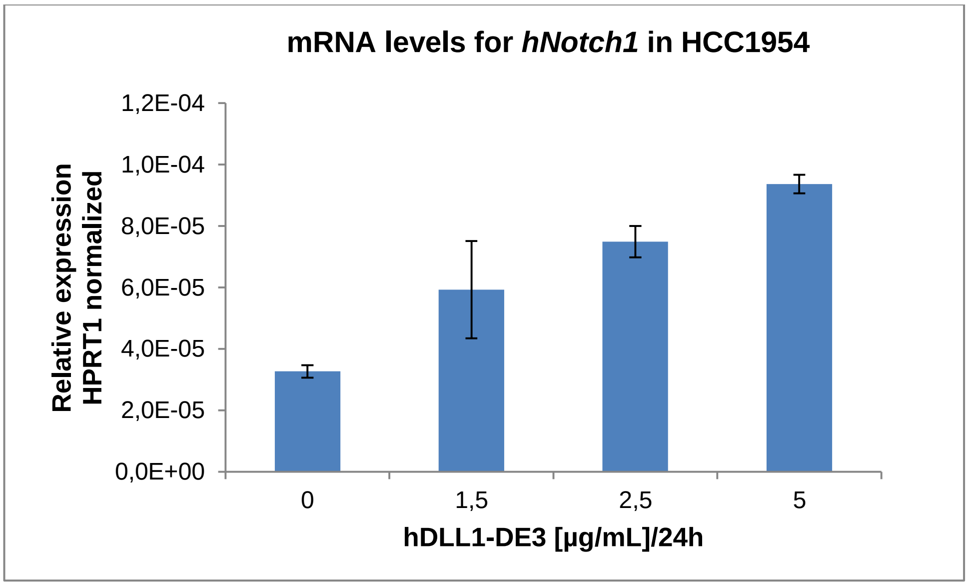


**Figure 3.42 - mRNA levels of hNotch1 in HCC1954 in response to hDLL1-DE3 treatment.** The values were normalized against the HPRT1 (control gene) mRNA levels in the same sample. Error bars represent the standard deviation between replicates.

The results for both iPSCs and HCC1954 cell lines show that rDLL1-DE3 modulates *hNotch1* in both cell lines. These findings are in agreement with previous studies described in the literature showing that *hNotch1* is a Notch-dependent gene itself (Bone *et al.*, 2014). On the other hand, the same study made by *Bone* and his team, suggests that *hDLL1* does not seem to be a Notch-dependent gene. Our result on modulation by rDLL1-DE3 shows an increase in the expression of hDLL1 in iPCSs but not in HCC1954 cells. Although it seems contradictory, these findings may be explained by the fact that modulation of Notch signalling pathway is cell-type specific and for the same cell type it depends on the cellular context (e.g. cellular differentiation stage, growth phase), and, consequently, different cell types may have different responses to a given *stimuli* (Cave, 2001).

Overall, our results show that the hDLL1-DE3 produced from inclusion bodies is bioactive and is capable of modulating the Notch1 signalling pathway, since it increased the expression levels of Hes-1, Hey-1, and Notch1 in breast cancer HCC1954 cells and Notch1 in iPCSs. As such, the recombinant protein can be used to generate hDLL1 antibodies with functional blocking activity against Notch1.

#### 3.3.2.3 Crystallization experiments to obtain hDLL1-DE3 3D structure

In order to solve the crystallographic structure of hDLL1-DE3 it was necessary to generate X-ray diffracting protein crystals. With that goal in mind, it was necessary to screen for crystallization conditions for the inclusion bodies refolded protein and the protein sample chosen for this purpose was pool 5 purified from the strategy in which the protein was solubilised with Urea. Different commercial screens were used and Table 3.4 summarizes all the tested conditions and screens.

**Table 3.4 – Commercial crystallization screens performed with hDLL1-DE3**

| Screen | [protein] [mg/mL] | Temperature (°C) | $CaCl_2$ (mM) |
|---|---|---|---|
| Index | 4.6 | 20 | 0 |
| | 3.0 | 4 | 5mM |
| Structure 1 + 2 | 4.6 | 20 | 0 |
| ShotGun | 3.2 | 20 | 0 |
| MIDAS | 3.0 | 20 | 0 |
| Pact Premier | 4.1 | 20 | 10mM |
| | 4.1 | 4 | 10mM |
| JCSG+ | 4.5 | 20 | 10mM |

Index and Structure I & II screens were tested initially. The first screen covers many different conditions and it is used to assess which precipitant reagent and pH is more effective for crystallization or to limit sample solubility. The second one comprises a group of conditions that allows the estimation of the solubility curve for one protein. These two screens were tested at 20ºC using a protein concentration of 4.2 mg/mL. The used protein concentration and incubation temperature was based on the available literature where Notch ligands structures are described, and in which protein concentrations ranging from 3.2-5.0 mg/mL were used for crystallization (Chillakuri *et al.*, 2013; Cordle *et al.*, 2008a; Kershaw *et al.*, 2015).

After analysing the two initial screen plates for several days, Index had 20% of the wells with amorphous precipitates and the remaining with crystalline precipitate, spherulites and phase separation. The presence of crystalline precipitate, spherulites or phase separation indicates that these conditions are not far from a crystallization condition (Luft *et al.*, 2011). As for structure I & II, the plate had many clear drops, and the presence of crystalline precipitates and spherulites was visible in the remaining drops. Given that the best conditions in Index and Structure 1 & 2 revealed a preference for PEG as precipitant agent, the Shotgun screen was tested, since it is composed mostly by PEG-based conditions. Furthermore, the MIDAS screen was also tested as it is mainly composed by rare crystallization solutions that are not covered by the remaining used screens. Unfortunately, both Shotgun and MIDAS, revealed similar results to those observed for Structure I & II.

In order to decrease protein solubility to achieve crystallization, 4ºC was tested as incubation temperature in two screens – Index and Pact Premier. The first was used again since it had shown the best results initially. The second (Pact Premier) is generally used to evaluate the effect of pH, anions and cation, with PEG as precipitant agent. In these conditions, $CaCl_2$ was added by buffer exchange because it was observed by TSA that the addition of $CaCl_2$ stabilizes hDLL1-DE3 (data not shown). Index was tested at 3mg/mL using 5mM $CaCl_2$ in the protein buffer formulation. After analysing the crystallization drops, the majority was clear or with a few crystalline precipitate. So, the protein concentration was increased up to 4mg/mL and the $CaCl_2$ concentration to 10mM, to prepare the Pact Premier screen. Also, 10mM of $CaCl_2$ were used to test Pact Premier and JSGC+ at 20ºC, since these two screens complement each other and this combination is described as “highly effective” to find new crystallization hits. After analysis of all performed screens, so far no crystals were obtained.

The reported crystallization condition used for hDLL1-ME6 was also tested (Kershaw *et al*., 2015). For that, a matrix of conditions around the original one was prepared in order to further test crystallization. Hanging-drop method using a grid screen around the published crystallization was prepared: 0.5 µl of protein and 0.5 µl of mother liquor; Precipitant was varied between 14% and 19% PEG 3350 in 100mM Bis-Tris propane, pH 7.5, 400mM potassium thiocyanate and 5mM $CaCl_2$. The plate was kept at 20ºC and analysed periodically. Unfortunately, all the drops were clear, suggesting that this condition is far from the right condition to promote crystallization of this protein.

Taken all together, no crystals were obtained so far using hDLL1-DE3. Protein ligands and inhibitors that bind the target protein are known to help protein stabilization and propensity for crystallization (Bergfors, 2009), being often used as crystallization tools. In that line of thought, our strategy focuses now on the usage of the hDLL1-DE3 specific Fab, selected by phage display to promote crystallization of a Fab:hDLL1-DE3 complex that would provide epitope structural insights and consequently the target protein structure.

### 3.3.3 Assessment of target quality for phage display - hDLL1-DE3 titration

In order to evaluate the quality of the new batch protein that was obtained from inclusion bodies, a titration ELISA was performed using 1:2 dilutions, starting at a concentration of 20µg/mL and using Anti- His Ab for detection. The results obtained in this titration revealed that a dose response was present but only above 2, 5µg/mL of target concentration (Figure 3.43).

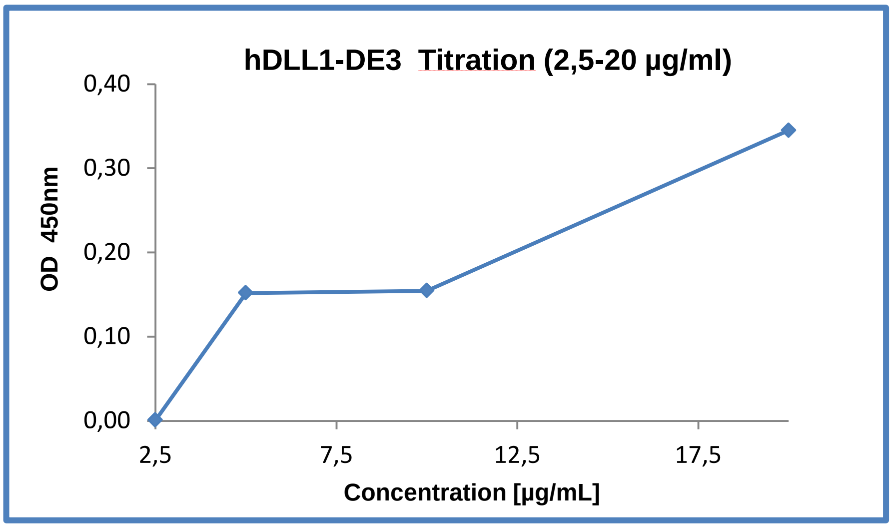


**Figure 3.43 - Titration of hDLL1-DE3 – results from 2.5 to 20µg/ml of target**. The background signal was subtracted for each value represented.

.

Since the ELISA titration results obtained for the first hDLL1-DE3 purified from mammalian cells gave a clear dose response, (Section 3.2.3), the result obtained now was not expected. However, since the protein was purified from a different host, using a completely distinct method for purification, it can behave differently. Nevertheless, a dose response was still observed and the quality of this target was found acceptable to proceed with panning aiming at finding specific Fabs against this antigen.

### 3.3.4 Panning for hLL1-DE3 obtained from inclusion bodies

The panning was performed with the aim of selecting a specific antibody against the hDLL1-DE3. Moreover, and since a higher amount of protein was produced, it was possible to use a different protocol for panning, and so immunotubes were used, in order to improve the selection efficiency in this panning. Three rounds were performed and were monitored by analysing the Input and Outputs as described in Section 3.2.4, and the results obtained were similar to those presented before (data not shown). Given that the results for Outputs ranged from $3.3 \times 10^5$ cfus and $8.3 \times 10^6$ cfus and Inputs were all between $10^{11}$ and $10^{12}$, the values were representative of an apparent well succeeded panning. However, no enrichment was detected from round 2 to round 3.

### 3.3.5 Assessment of Phage Pools Reactivity

As in Section 3.2.5., pools from round 2 and 3 were titrated and analysed by ELISA to access their response to the target. It was observed in Section 3.2.5 that the dose response did not present the typical pattern in which the signal starts to decrease when approaching high concentrations of phages. For round 2, similar results were obtained, while in round 3 no dose response was visible (Figure 3.44). The apparent absence of response in round 3 is probably related with the stringency applied in this selection, where half of the quantity of target was used (100µg in rounds 1 and 2; 50µg in round 3). The stringency is normally increased to promote the removal of nonspecific and low affinity binders, (Marks and Bradbury, 2004). However, in this case it was porbably too harsh and led to a decrease on the population of phages with affiinty for the target. Also, titrations of pools from round 2 and 3 were evaluated for their response to Anti-Fab. The test was included in order to evaluate the quality of the population of Fabs present on each pool. Figure 3.45 shows that a dose response is present in pool 2 and 3 but with the same pattern of the curves obtained for hDLL1-DE3. This result suggests that the response obtained for high amount of phages present in the lower dilutions, leads to aggregation and consequent impairment of the binding to the antigen.

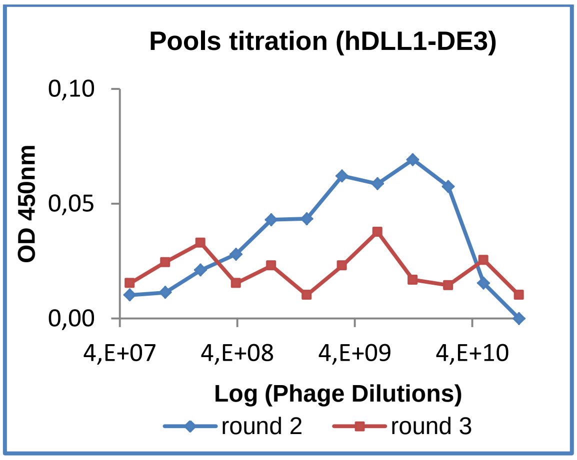


**Figure 3.44 - Titration of pools from round 2 and 3 - hDLL1-DE3.** The background signal was subtracted for each value represented.

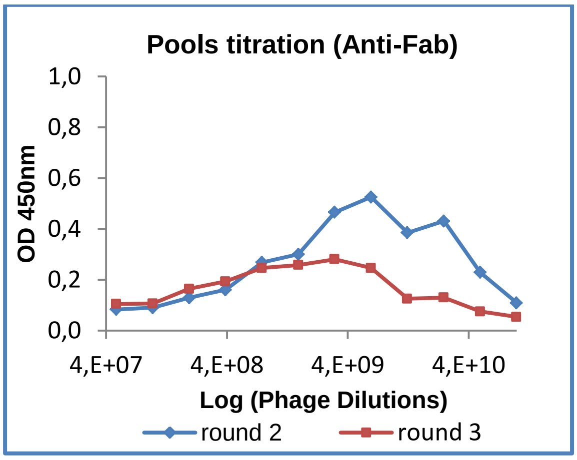


**Figure 3 45 - Titration of pools from round 2 and 3 - Anti-Fab**. The background signal was subtracted for each value represented.

#### 3.3.6 Assessment of selected individual clones reactivity

Focusing on the goal of finding positive binders for the target, individual clones were analysed. In this case, 88 clones from each round were analysed and the three points were evaluated using three different molecules for coating (same as in Section 3.2.6): target specificity using hDLL1-DE, Fab Display using anti-Fab and phages production using anti-M13. In Figure 3.46, it is possible to observe that for round two, 14 clones from round 2 had a signal that was at least 4-fold higher than the background signal (uncoated plate). However, in round 3, only 4 clones presented a signal 4-fold higher that the uncoated plate, which suggests that this round did not lead to a phage enrichment (Figure 3.47).

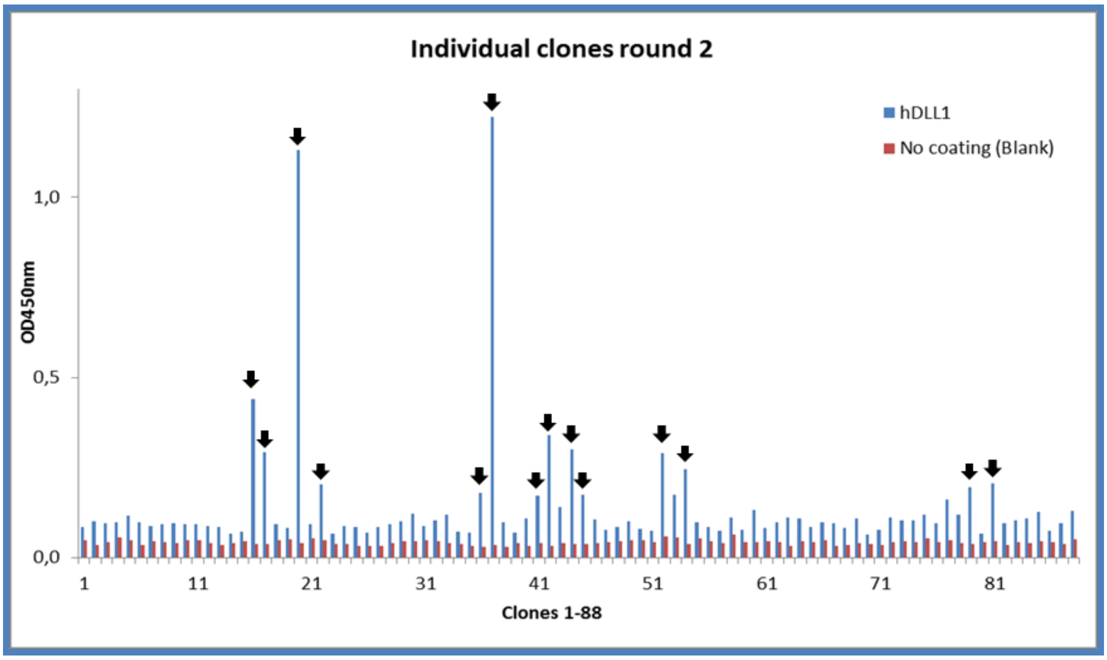


**Figure 3.46 – Individual clones selected with hDLL1-DE3 – round 2.** Black arrows - Clones with a signal with at least a 3-fold change from the background.

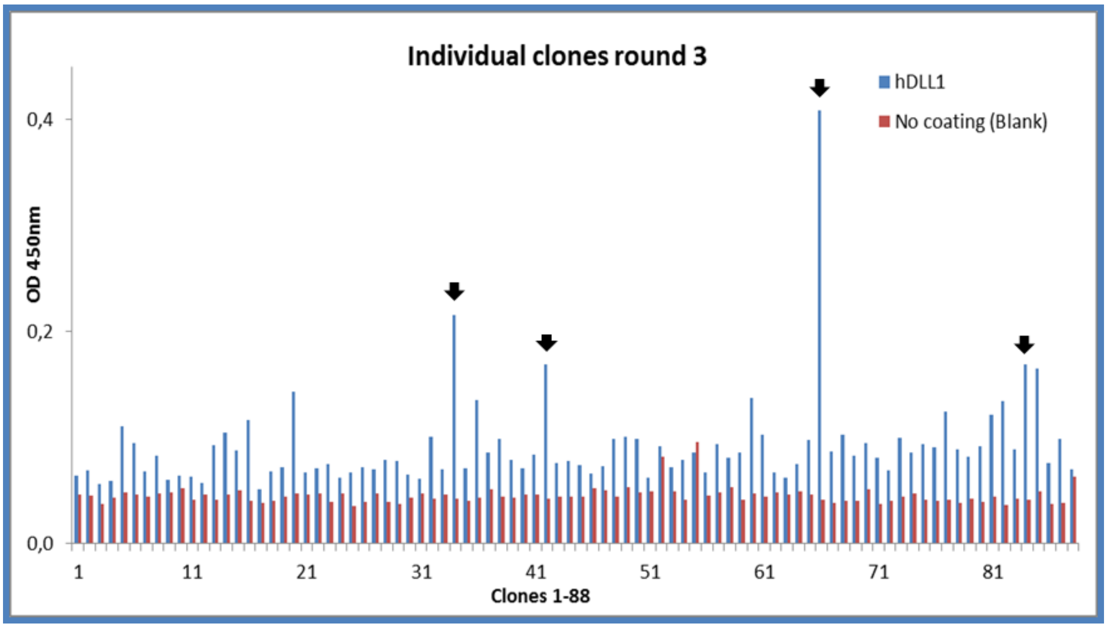


**Figure 3.47 - Individual clones selected with hDLL1-DE3 – round 3.** Black arrows - Clones with a signal with at least a 3-fold change from the background.

In round 2 the population of binders with affinity for the target was higher than in round 3, which may be related to the fact that in the last round, the selection was much more stringent since half of the concentration of target was used. Repeating the third round with less stringency or performing a fourth round in the same conditions could help in enriching the population of phages with affinity for the target. There are some cases in which a good enrichment and high diversity of clones is already obtained in a second round of selection, and an extra panning can result in a loss of diversity. However, this can only be confirmed by sequencing the clones obtained from both rounds 2 and 3.

Nevertheless, this new panning strategy with immunotubes allowed the selection of 18 clones, out of the 176 clones analysed (10.2%) that were considered for further expression and analysis in the soluble Fab format. The low number of clones recovered may be somehow related with two aspects: absence of a depletion molecule which allows a more efficient selection and the lack of enrichment from round 2 to round 3.

When comparing the results from this panning with the ones obtained for panning on microplate (performed with hDLL1-DE3 from HEK293T), it is possible to see that this new strategy showed clear improvements. Stronger ELISA signals were obtained for some of the clones analysed in this new selection, namely 2 clones revealed $OD_{450nm}$ values bigger than 1, while in the first panning strategy followed the higher value obtained was 0.27 approximately. These findings suggest that clones with higher affinity were selected this time. Finally, is important to refer that Fab expression was detected in all of the 176 clones and Anti-M13 reactivity was strong for all of them, suggesting that the correct formation of the Fab-displaying phages was achieved.

### 3.3.7 sFab characterization

In total, 12 clones were chosen to proceed with characterization. First, a colony PCR was made to analyse if amplification of the Fab was correct (data not shown), and simultaneously the DNA from these clones was sent for sequencing. After analysing the results from colony PCR, sequencing and digestion with *Sac*I and *Spe*I, only one clone out of the twelve presented the expected results and thus was chosen to move further. All the genetic tests mentioned above, suggests that clone 20 was correctly constructed, presenting both LC an HC. Together with the signal obtained on Fab-on-phage ELISA, where clone 20 presented a strong signal, these findings suggest that this clone constitutes a promising candidate to be used for further experiments.

### 3.3.8 sFab expression in pCOMB3xss – clone 20

In order to express the Fab in the soluble format, some optimization steps had to be performed. pCOMB3XSS contains an amber stop codon between the Fab and gene III sequences (Vector map in Appendix 5.5). With the intention of promoting expression of the soluble Fab alone and turn-off the expression of the pIII fusion protein, a nonsupressor strain (Top 10 F') had to be used to guarantee the reading of the stop codon. However, different conditions were tested and no Fab expression was detected (data not shown)

## 3.3.9 sFab expression in pT7 – clone 20

### 3.3.9.1 Expression tests

In order to promote soluble Fab expression, the fragment was digested from pCOMB3XSS with *Sfi*I and inserted in pT7 expression vector (previously digested with *Sfi*I). This vector contains T7 promoter which is stronger than the *lacz* promoter, present in pCOMB3XSS. This difference relies on the affinity of the promoter sequence for RNA polymerase. The T7 RNA polymerase is described as being very selective and with great efficiency, which often leads to a higher protein expression (Tegel *et al*., 2011). This vector also contains a six-histidine tag, allowing protein detection and purification.

After confirming the cloning success (data not shown), several conditions were tested to obtain expression in soluble (Table 3.4). First, BL21(DE3) was tested using different mediums, IPTG concentrations, temperatures and times of induction. Despite all the conditions tested, the expression of Fab was all in the insoluble fraction (data not shown).

**Table 3.4 - Conditions tested for expression of sFab (clone 20)**

| Growth medium | | | Temperature (°C) | | | | Time (h) | | | | [IPTG] (mM) | | | $OD_{600nm}$ | *E.coli* strain | | | Auto induction |
|---|---|---|---|---|---|---|---|---|---|---|---|---|---|---|---|---|---|---|
| LB | PB | 2YT | 18 | 25 | 30 | 37 | 3 | 6 | 16 | 24 | 0.5 | 1 | 2 | 0.8-1 | BL21 DE3 | Bl21 pRARE2 | Shuffle | |
| • | | | | | • | | • | | | | | • | | • | • | | | |
| | • | | | • | | | | • | | | | • | | • | • | | | |
| | • | | • | | | | | | • | | | • | | • | • | | | |
| | | • | • | | | | | | | • | | | | • | • | | | • |
| | | • | | | • | | | | • | | | | | • | • | | | • |
| | | • | | | | • | | | • | | | | | • | • | | | • |
| | | • | | | • | | | | • | | • | | | • | | • | • | |
| • | | | | | • | | | | • | | | | • | • | | • | • | |
| | | • | | | • | | | • | | | | • | | • | | • | • | |
| • | | | | | • | | | • | | | | • | | • | | • | • | |

The correct folding of a determined Fab maybe challenging due to the presence of multiple disulphide bonds that are required for their folding, stability and/or function (Jalalirad, 2013). As discussed before, disulphide bonds right formation requires a more oxidizing environment and the *E.coli* cytoplasm does not present such features, leading to a misfold of the protein and consequent formation of inclusion bodies (Carrió and Villaverde, 2006). With that in mind, we decided to choose to different strains in order to improve Fab's solubility – Shuffle T7 express (NEB) and BL21Star(DE3)/pRARE2. The first constitutes an engineered *E.coli* that allows the stable formation of disulphide bonds in bacteria cytoplasm, due to a mutation in two reductases - thioredoxin reductase and glutathione reductase (Lobstain *et al*., 2012). On the other hand, as explained in Section 3.1.1, the BL21Star (DE3)/pRARE2 contains the plasmid that allows the expression of rare codons often required for the right production of the protein. After testing different conditions with these two new strains, it was possible to detect Fab expression in the soluble fraction which was confirmed by Western blot. In Figure 3.48 is depicted the best expression condition obtained with Shuffle T7 express that was used to proceed with scale-up and purification.

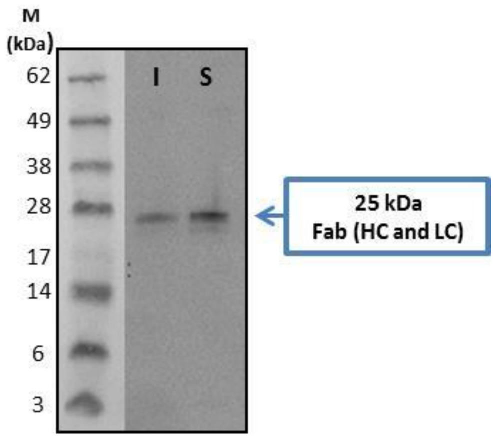


**Figure 3.48 - Anti-Fab Western blot of soluble Fab expression in Shuffle – clone 20.** Condition: 6h at 30ºC, 1mM IPTG in LB medium. M - Marker; I - Insoluble fraction; S - Soluble fraction. Blue box points the molecular mass expected for the Fab (LC and HC that appear as two fragments of 25kDa).

### 3.4 Conclusions and future perspectives

In this work we were able to optimize the expression and purification of an extracellular portion of human Delta-like 1 ligand, the hDLL1-DE3 construct.

The first choice when trying to express a recombinant protein is to use *E.coli* as a host. However, despite the different tested conditions, the studied target proteins were mostly expressed as inclusion bodies. The extracellular domains of these protein targets, with a rod-shaped conformation and many disulfide bonds, are most likely making expression and purification a challenging task. Taking this into account, we tried to obtain the recombinant protein using a different host system - mammalian cells (HEK293T). Although we were able to produce and purify the target protein, the obtained protein yield was not enough (approximately 60μg/L) for our purposes of obtaining a function-blocking antibody and the crystallographic structure.

The information acquired during the initial expression tests performed in *E.coli*, provided evidences that large amounts of protein were obtained in the insoluble fraction. Also, successful cases reported in the literature describing the refolding of these proteins, led to the decision of following this strategy moving back to the bacterial expression system. In fact, after optimization of the ideal expression conditions, we managed to produce one of the Notch ligand targets – hDLL1-DE3 construct that was also proved to be bioactive in cells by modulating the expression of some Notch dependent genes. In Table 3.5 and 3.6 a summary of the different used strategies for expression and purification conditions is presented.

**Table 3 5- Summary of Notch ligands expression strategies**

<table>
<tr><th>Host</th><th>vector</th><th>Tested constructs</th><th>Outcome</th></tr>
<tr><td rowspan="2">E.coli</td><td>pET-47(b)+</td><td>hDLL1-DE3, ME3 and ME6<br>hJag1-DE3, ME3 and ME9<br>hJag2-DE9, ME3 and ME9</td><td rowspan="2">Protein present in inclusion bodies</td></tr>
<tr><td>pETfh8</td><td>hDLL1_MNNL_DSL<br>hDLL1_ME3</td></tr>
<tr><td>HEK293T</td><td>pHL-sec</td><td>hDLL1-DE3 and DE6<br>hJag1-ME3 and ME9<br>hJag2-ME3 and ME9</td><td>Successful protein secretion to the growth medium</td></tr>
</table>

**Table 3.6 - Summary of hDLL1 – DE3 purification strategies. Condition with higher yield is marked in bold**

<table>
<tr><th>Host</th><th>vector</th><th>Construct</th><th>Method</th><th>Strategy</th><th>Yield of protein</th></tr>
<tr><td rowspan="2">E.coli</td><td rowspan="2">pET-47 (b) +</td><td rowspan="4">hDLL1-DE3</td><td rowspan="2">Refolding from inclusion bodies</td><td>Solubilisation with Guanidine-HCl</td><td>1 mg</td></tr>
<tr><td>Solubilisation with urea</td><td>11mg</td></tr>
<tr><td rowspan="2">HEK293T</td><td rowspan="2">pHL-sec</td><td rowspan="2">Soluble protein purification</td><td>First strategy</td><td>200µg</td></tr>
<tr><td>Second strategy</td><td>90µg</td></tr>
</table>

The produced hDLL1-DE3 protein was then used to select for Fab specific-binders, by using the phage display technology. From the several panning strategies performed one lead candidate clone was originated, and further used to determine the best expression conditions. After several attempts we were able to increase Fab solubility through expression on a modified *E.coli* strain – Shuffle T7 express. Furthermore, the hDLL1-DE3 protein was used also used for crystallization experiments, although no positive hits were detected so far.

In the future, we will perform a scale-up to express and purify the selected Fab fragment. Also, we plan to characterise the affinity of hDLL1-DE3 with the selected Fab molecule using different techniques such as BLItz and Surface Plasmon Resonance (SPR). These techniques will be used to study the affinity and kinetics of protein-Fab interactions. Further inhibition experiments on breast cancer cells will also be performed to assess if the transcription levels of Notch target genes are decreased by the addition of the antibody fragment. Also, cell proliferation assays will be conducted to study the effect of the selected Fab on the growth of breast cancer cells that exhibit high level expression of DLL1. One of our future goals is also to co-crystallize hDLL1-DE3 with the selected Fab fragment.

Several Notch ligands are associated with a pour outcome in breast cancer and so, the goal is to apply similar purification and expression conditions optimized here for hDLL1-DE3 construct to other similar proteins. The aim would be to select more specific binders for these proteins again using phage display technology, and validate selected candidates as potential therapeutic targets in breast cancer. Finally, crystallization of the Notch ligand proteins alone and in complex with Fab specific binders would be a final goal to structurally characterize the epitope-binding region. This will allow determining the molecular basis of anti-Notch1 ligands antagonistic activity in the Notch 1 signalling pathway.

## 4 References


- Ahimou, F., Mok, L. P., Bardot, B., & Wesley, C. (2004). The adhesion force of Notch with Delta and the rate of Notch signaling. *J Cell Biol, 167*(6), 1217-1229. doi: 10.1083/jcb.200407100
- Arakawa, T., & Tsumoto, K. (2003). The effects of arginine on refolding of aggregated proteins: not facilitate refolding, but suppress aggregation. *Biochem Biophys Res Commun, 304*(1), 148-152.
- Arbabi-Ghahroudi, M., Tanha, J., & MacKenzie, R. (2009). Isolation of monoclonal antibody fragments from phage display libraries. *Methods Mol Biol, 502*, 341-364. doi: 10.1007/978-1-60327-565-1_20
- Aricescu, A. R., Lu, W., & Jones, E. Y. (2006). A time- and cost-efficient system for high-level protein production in mammalian cells. *Acta Crystallogr D Biol Crystallogr, 62*(Pt 10), 1243-1250. doi: 10.1107/S0907444906029799
- Artavanis-Tsakonas, S., Rand, M. D., & Lake, R. J. (1999). Notch signaling: cell fate control and signal integration in development. *Science, 284*(5415), 770-776.
- Azzazy, H. M., & Highsmith, W. E., Jr. (2002). Phage display technology: clinical applications and recent innovations. *Clin Biochem, 35*(6), 425-445.
- Baneyx, F., & Mujacic, M. (2004). Recombinant protein folding and misfolding in Escherichia coli. *Nat Biotechnol, 22*(11), 1399-1408. doi: 10.1038/nbt1029
- Barbas, C.F., Burton, D.R., Scott, J.K., & Silverman, G.J. (2004). *Phage Display*: Cold Spring Harbor Laboratory Press.
- Bazan, J., Calkosinski, I., & Gamian, A. (2012). Phage display--a powerful technique for immunotherapy: 1. Introduction and potential of therapeutic applications. *Hum Vaccin Immunother, 8*(12), 1817-1828. doi: 10.4161/hv.21703
- Benedito, R., Roca, C., Sorensen, I., Adams, S., Gossler, A., Fruttiger, M., & Adams, R. H. (2009). The notch ligands Dll4 and Jagged1 have opposing effects on angiogenesis. *Cell, 137*(6), 1124-1135. doi: 10.1016/j.cell.2009.03.025
- Bergfors, T.M. (2009). *Protein Crystallization*: International University Line.
- Bondos, S. E., & Bicknell, A. (2003). Detection and prevention of protein aggregation before, during, and after purification. *Anal Biochem, 316*(2), 223-231.
- Bone, R. A., Bailey, C. S., Wiedermann, G., Ferjentsik, Z., Appleton, P. L., Murray, P. J., Dale, J. K. (2014). Spatiotemporal oscillations of Notch1, Dll1 and NICD are coordinated across the mouse PSM. *Development, 141*(24), 4806-4816. doi: 10.1242/dev.115535
- Borggrefe, T., & Oswald, F. (2009). The Notch signaling pathway: transcriptional regulation at Notch target genes. *Cell Mol Life Sci, 66*(10), 1631-1646. doi: 10.1007/s00018-009-8668-7
- Brou, C., Logeat, F., Gupta, N., Bessia, C., LeBail, O., Doedens, J. R., . . . Israel, A. (2000). A novel proteolytic cleavage involved in Notch signaling: the role of the disintegrin-metalloprotease TACE. *Mol Cell, 5*(2), 207-216.

- Cabral,M.J.C.D. 2014. Phage Display as a Tool for Development of Novel Therapeutics for Breast Cancer. Tese de Mestrado. Faculdade de Ciências e Tecnologia, Universidade Nova de Lisboa.
- Cailleau, R., Olive, M., & Cruciger, Q. V. (1978). Long-term human breast carcinoma cell lines of metastatic origin: preliminary characterization. *In Vitro, 14*(11), 911-915.
- Carrio, M. M., Cubarsi, R., & Villaverde, A. (2000). Fine architecture of bacterial inclusion bodies. *FEBS Lett, 471*(1), 7-11.
- Cave, J. W. (2011). Selective repression of Notch pathway target gene transcription. *Dev Biol, 360*(1), 123-131. doi: 10.1016/j.ydbio.2011.09.018
- Chen, D. H., Madan, D., Weaver, J., Lin, Z., Schroder, G. F., Chiu, W., & Rye, H. S. (2013). Visualizing GroEL/ES in the act of encapsulating a folding protein. *Cell, 153*(6), 1354-1365. doi: 10.1016/j.cell.2013.04.052
- Chillakuri, C. R., Sheppard, D., Ilagan, M. X., Holt, L. R., Abbott, F., Liang, S., . . . Lea, S. M. (2013). Structural analysis uncovers lipid-binding properties of Notch ligands. *Cell Rep, 5*(4), 861-867. doi: 10.1016/j.celrep.2013.10.029
- Chillakuri, C. R., Sheppard, D., Lea, S. M., & Handford, P. A. (2012). Notch receptor-ligand binding and activation: insights from molecular studies. *Semin Cell Dev Biol, 23*(4), 421-428. doi: 10.1016/j.semcdb.2012.01.009
- Clark, E. D. B. (1998). Refolding of recombinant proteins. *Curr Opin Biotechnol, 9*(2), 157-163.
- Claxton, S., & Fruttiger, M. (2004). Periodic Delta-like 4 expression in developing retinal arteries. *Gene Expr Patterns, 5*(1), 123-127. doi: 10.1016/j.modgep.2004.05.004
- Corchero, J. L., & Villaverde, A. (1998). Plasmid maintenance in Escherichia coli recombinant cultures is dramatically, steadily, and specifically influenced by features of the encoded proteins. *Biotechnol Bioeng, 58*(6), 625-632.
- Cordle, J., Johnson, S., Tay, J. Z., Roversi, P., Wilkin, M. B., de Madrid, B. H., Handford, P. A. (2008). A conserved face of the Jagged/Serrate DSL domain is involved in Notch trans-activation and cis-inhibition. *Nat Struct Mol Biol, 15*(8), 849-857. doi: 10.1038/nsmb.1457
- Cordle, J., Redfieldz, C., Stacey, M., van der Merwe, P. A., Willis, A. C., Champion, B. R., Handford, P. A. (2008). Localization of the delta-like-1-binding site in human Notch-1 and its modulation by calcium affinity. *J Biol Chem, 283*(17), 11785-11793. doi: 10.1074/jbc.M708424200
- Costa, S., Almeida, A., Castro, A., & Domingues, L. (2014). Fusion tags for protein solubility, purification and immunogenicity in Escherichia coli: the novel Fh8 system. *Front Microbiol, 5*, 63. doi: 10.3389/fmicb.2014.00063
- Costa, S. J., Almeida, A., Castro, A., Domingues, L., & Besir, H. (2013). The novel Fh8 and H fusion partners for soluble protein expression in Escherichia coli: a comparison with the traditional gene fusion technology. *Appl Microbiol Biotechnol, 97*(15), 6779-6791. doi: 10.1007/s00253-012-4559-1

- Costa, S. J., Coelho, E., Franco, L., Almeida, A., Castro, A., & Domingues, L. (2013). The Fh8 tag: a fusion partner for simple and cost-effective protein purification in Escherichia coli. *Protein Expr Purif, 92*(2), 163-170. doi: 10.1016/j.pep.2013.09.013
- Creighton, C. J., Li, X., Landis, M., Dixon, J. M., Neumeister, V. M., Sjolund, A., Chang, J. C. (2009). Residual breast cancers after conventional therapy display mesenchymal as well as tumor-initiating features. *Proc Natl Acad Sci U S A, 106*(33), 13820-13825. doi: 10.1073/pnas.0905718106
- D'Souza, B., Meloty-Kapella, L., & Weinmaster, G. (2010). Canonical and non-canonical Notch ligands. *Curr Top Dev Biol, 92*, 73-129. doi: 10.1016/S0070-2153(10)92003-6
- Daegelen, P., Studier, F. W., Lenski, R. E., Cure, S., & Kim, J. F. (2009). Tracing ancestors and relatives of Escherichia coli B, and the derivation of B strains REL606 and BL21(DE3). *J Mol Biol, 394*(4), 634-643. doi: S0022-2836(09)01139-5 [pii] 10.1016/j.jmb.2009.09.022
- Dalton, A. C., & Barton, W. A. (2014). Over-expression of secreted proteins from mammalian cell lines. *Protein Sci, 23*(5), 517-525. doi: 10.1002/pro.2439
- Deblandre, G. A., Lai, E. C., & Kintner, C. (2001). Xenopus neuralized is a ubiquitin ligase that interacts with XDelta1 and regulates Notch signaling. *Dev Cell, 1*(6), 795-806.
- Delves, P., Martin, S., Burton, D., & Roitt, I. (2006). *Roitt's Essential Immunology*: Wiley.
- Demehri, S., & Kopan, R. (2009). Notch signaling in bulge stem cells is not required for selection of hair follicle fate. *Development, 136*(6), 891-896. doi: 10.1242/dev.030700
- Dente, L., Cesareni, G., Micheli, G., Felici, F., Folgori, A., Luzzago, A., Delmastro, P. (1994). Monoclonal antibodies that recognise filamentous phage: tools for phage display technology. *Gene, 148*(1), 7-13.
- Dexter, John S. (1914). The Analysis of a Case of Continuous Variation in Drosophila by a Study of Its Linkage Relations. *The American Naturalist, 48*(576), 712-758. doi: 10.2307/2455888
- Elgert, K.D. (2009). *Immunology: Understanding The Immune System*: Wiley.
- Ellisen, L. W., Bird, J., West, D. C., Soreng, A. L., Reynolds, T. C., Smith, S. D., & Sklar, J. (1991). TAN-1, the human homolog of the Drosophila notch gene, is broken by chromosomal translocations in T lymphoblastic neoplasms. *Cell, 66*(4), 649-661.
- Ericsson, U. B., Hallberg, B. M., Detitta, G. T., Dekker, N., & Nordlund, P. (2006). Thermofluor-based high-throughput stability optimization of proteins for structural studies. *Anal Biochem, 357*(2), 289-298.
- Ersson, B., Ryden, L., & Janson, J. C. (2011). Introduction to protein purification. *Methods Biochem Anal, 54*, 3-22.
- Espinoza, I., Pochampally, R., Xing, F., Watabe, K., & Miele, L. (2013). Notch signaling: targeting cancer stem cells and epithelial-to-mesenchymal transition. *Onco Targets Ther, 6*, 1249-1259. doi: 10.2147/OTT.S36162
- Esposito, D., & Chatterjee, D. K. (2006). Enhancement of soluble protein expression through the use of fusion tags. *Curr Opin Biotechnol, 17*(4), 353-358. doi: 10.1016/j.copbio.2006.06.003

- FairJourneyBiologics. Phage Display. Version 22 September 2015, http://fjb.pt/phage-display/
- Falk, R., Falk, A., Dyson, M. R., Melidoni, A. N., Parthiban, K., Young, J. L., . . . McCafferty, J. (2012). Generation of anti-Notch antibodies and their application in blocking Notch signalling in neural stem cells. *Methods, 58*(1), 69-78. doi: 10.1016/j.ymeth.2012.07.008
- Fryer, C. J., White, J. B., & Jones, K. A. (2004). Mastermind recruits CycC:CDK8 to phosphorylate the Notch ICD and coordinate activation with turnover. *Mol Cell, 16*(4), 509-520. doi: 10.1016/j.molcel.2004.10.014
- Gazdar, A. F., Kurvari, V., Virmani, A., Gollahon, L., Sakaguchi, M., Westerfield, M., Shay, J. W. (1998). Characterization of paired tumor and non-tumor cell lines established from patients with breast cancer. *Int J Cancer, 78*(6), 766-774.
- Gibert, J. M., & Simpson, P. (2003). Evolution of cis-regulation of the proneural genes. *Int J Dev Biol, 47*(7-8), 643-651.
- Giudicelli, V., & Lefranc, M. P. (2012). Imgt-Ontology 2012. *Front Genet, 3*, 79. doi: 10.3389/fgene.2012.00079
- Gridley, T. (1997). Notch signaling in vertebrate development and disease. *Mol Cell Neurosci, 9*(2), 103-108. doi: 10.1006/mcne.1997.0610
- Gridley, T. (2003). Notch signaling and inherited disease syndromes. *Hum Mol Genet, 12 Spec No 1*, R9-13.
- Gustafsson, M. V., Zheng, X., Pereira, T., Gradin, K., Jin, S., Lundkvist, J., . . . Bondesson, M. (2005). Hypoxia requires notch signaling to maintain the undifferentiated cell state. *Dev Cell, 9*(5), 617-628. doi: 10.1016/j.devcel.2005.09.010
- Hambleton, S., Valeyev, N. V., Muranyi, A., Knott, V., Werner, J. M., McMichael, A. J., Downing, A. K. (2004). Structural and functional properties of the human notch-1 ligand binding region. *Structure, 12*(12), 2173-2183. doi: 10.1016/j.str.2004.09.012
- Hamel, S., Fantini, J., & Schweisguth, F. (2010). Notch ligand activity is modulated by glycosphingolipid membrane composition in Drosophila melanogaster. *J Cell Biol, 188*(4), 581-594. doi: 10.1083/jcb.200907116
- Hammers, C. M., & Stanley, J. R. (2014). Antibody phage display: technique and applications. *J Invest Dermatol, 134*(2), e17. doi: 10.1038/jid.2013.521
- Harrison, H., Farnie, G., Howell, S. J., Rock, R. E., Stylianou, S., Brennan, K. R., Clarke, R. B. (2010). Regulation of breast cancer stem cell activity by signaling through the Notch4 receptor. *Cancer Res, 70*(2), 709-718. doi: 10.1158/0008-5472.CAN-09-1681
- Heitzler, P., & Simpson, P. (1991). The choice of cell fate in the epidermis of Drosophila. *Cell, 64*(6), 1083-1092.
- Henderson, S. T., Gao, D., Christensen, S., & Kimble, J. (1997). Functional domains of LAG-2, a putative signaling ligand for LIN-12 and GLP-1 receptors in Caenorhabditis elegans. *Mol Biol Cell, 8*(9), 1751-1762.
- Henderson, S. T., Gao, D., Lambie, E. J., & Kimble, J. (1994). lag-2 may encode a signaling ligand for the GLP-1 and LIN-12 receptors of C. elegans. *Development, 120*(10), 2913-2924.

- Henry, T. J., & Pratt, D. (1969). The proteins of bacteriophage M13. *Proc Natl Acad Sci U S A, 62*(3), 800-807.
- Hoogenboom, H. R. (2005). Selecting and screening recombinant antibody libraries. *Nat Biotechnol, 23*(9), 1105-1116. doi: 10.1038/nbt1126
- Hoogenboom, H. R., de Bruine, A. P., Hufton, S. E., Hoet, R. M., Arends, J. W., & Roovers, R. C. (1998). Antibody phage display technology and its applications. *Immunotechnology, 4*(1), 1-20. doi: S1380293398000074 [pii]
- Iso, T., Hamamori, Y., & Kedes, L. (2003). Notch signaling in vascular development. *Arterioscler Thromb Vasc Biol, 23*(4), 543-553. doi: 10.1161/01.ATV.0000060892.81529.8F
- Itoh, M., Kim, C. H., Palardy, G., Oda, T., Jiang, Y. J., Maust, D., . . . Chitnis, A. B. (2003). Mind bomb is a ubiquitin ligase that is essential for efficient activation of Notch signaling by Delta. *Dev Cell, 4*(1), 67-82.
- Jalalirad, Reza. (2013). *Production of antibody fragment (Fab) throughout Escherichia coli fed-batch fermentation process: Changes in titre, location and form of product*.
- Jana, S., & Deb, J. K. (2005). Strategies for efficient production of heterologous proteins in Escherichia coli. *Appl Microbiol Biotechnol, 67*(3), 289-298. doi: 10.1007/s00253-004-1814-0
- Janson, J.C. (2012). *Protein Purification: Principles, High Resolution Methods, and Applications*: Wiley.
- Kershaw, N. J., Church, N. L., Griffin, M. D., Luo, C. S., Adams, T. E., & Burgess, A. W. (2015). Notch ligand delta-like1: X-ray crystal structure and binding affinity. *Biochem J, 468*(1), 159-166. doi: 10.1042/BJ20150010
- Klueg, K. M., & Muskavitch, M. A. (1999). Ligand-receptor interactions and trans-endocytosis of Delta, Serrate and Notch: members of the Notch signalling pathway in Drosophila. *J Cell Sci, 112 ( Pt 19)*, 3289-3297.
- Koch, U., Lacombe, T. A., Holland, D., Bowman, J. L., Cohen, B. L., Egan, S. E., & Guidos, C. J. (2001). Subversion of the T/B lineage decision in the thymus by lunatic fringe-mediated inhibition of Notch-1. *Immunity, 15*(2), 225-236.
- Koch, U., & Radtke, F. (2007). Notch and cancer: a double-edged sword. *Cell Mol Life Sci, 64*(21), 2746-2762. doi: 10.1007/s00018-007-7164-1
- Koo, B. K., Yoon, K. J., Yoo, K. W., Lim, H. S., Song, R., So, J. H., Kong, Y. Y. (2005). Mind bomb-2 is an E3 ligase for Notch ligand. *J Biol Chem, 280*(23), 22335-22342. doi: 10.1074/jbc.M501631200
- Kopan, R. (2012). Notch signaling. *Cold Spring Harb Perspect Biol, 4*(10). doi: 10.1101/cshperspect.a011213
- Kopan, R., & Ilagan, M. X. (2009). The canonical Notch signaling pathway: unfolding the activation mechanism. *Cell, 137*(2), 216-233. doi: 10.1016/j.cell.2009.03.045
- Lai, E. C., & Rubin, G. M. (2001). Neuralized is essential for a subset of Notch pathway-dependent cell fate decisions during Drosophila eye development. *Proc Natl Acad Sci U S A, 98*(10), 5637-5642. doi: 10.1073/pnas.101135498

- Lee, C. M., Iorno, N., Sierro, F., & Christ, D. (2007). Selection of human antibody fragments by phage display. *Nat Protoc, 2*(11), 3001-3008. doi: 10.1038/nprot.2007.448
- Lee, So-Hee, Kim, Jung-Soo, & Kim, Chan-Wha. (2003). Optimization of buffer conditions for the removal of endotoxins using Q-sepharose. *Process Biochemistry, 38*(7), 1091-1098. doi: 10.1016/S0032-9592(02)00243-1
- Li, D., Masiero, M., Banham, A. H., & Harris, A. L. (2014). The notch ligand JAGGED1 as a target for anti-tumor therapy. *Front Oncol, 4*, 254. doi: 10.3389/fonc.2014.00254
- Li, L., Krantz, I. D., Deng, Y., Genin, A., Banta, A. B., Collins, C. C., . . . Spinner, N. B. (1997). Alagille syndrome is caused by mutations in human Jagged1, which encodes a ligand for Notch1. *Nat Genet, 16*(3), 243-251. doi: 10.1038/ng0797-243
- Lobstein, J., Emrich, C. A., Jeans, C., Faulkner, M., Riggs, P., & Berkmen, M. (2012). SHuffle, a novel Escherichia coli protein expression strain capable of correctly folding disulfide bonded proteins in its cytoplasm. *Microb Cell Fact, 11*, 56. doi: 1475-2859-11-56 [pii]
- 10.1186/1475-2859-11-56
- Logeat, F., Bessia, C., Brou, C., LeBail, O., Jarriault, S., Seidah, N. G., & Israel, A. (1998). The Notch1 receptor is cleaved constitutively by a furin-like convertase. *Proc Natl Acad Sci U S A, 95*(14), 8108-8112.
- Lubman, O. Y., Korolev, S. V., & Kopan, R. (2004). Anchoring notch genetics and biochemistry; structural analysis of the ankyrin domain sheds light on existing data. *Mol Cell, 13*(5), 619-626.
- Luft, J. R., Wolfley, J. R., & Snell, E. H. (2011). What's in a drop? Correlating observations and outcomes to guide macromolecular crystallization experiments. *Cryst Growth Des, 11*(3), 651-663. doi: 10.1021/cg1013945
- Malhotra, A. (2009). Tagging for protein expression. *Methods Enzymol, 463*, 239-258. doi: 10.1016/S0076-6879(09)63016-0
- Marks, J. D., & Bradbury, A. (2004). Selection of human antibodies from phage display libraries. *Methods Mol Biol, 248*, 161-176.
- Mead, D. A., & Kemper, B. (1988). Chimeric single-stranded DNA phage-plasmid cloning vectors. *Biotechnology, 10*, 85-102.
- Mittal, S., Subramanyam, D., Dey, D., Kumar, R. V., & Rangarajan, A. (2009). Cooperation of Notch and Ras/MAPK signaling pathways in human breast carcinogenesis. *Mol Cancer, 8*, 128. doi: 10.1186/1476-4598-8-128
- Mundy, G. R. (2002). Metastasis to bone: causes, consequences and therapeutic opportunities. *Nat Rev Cancer, 2*(8), 584-593. doi: 10.1038/nrc867
- Murphy, K.M. (2011). *Janeway's Immunobiology*: Taylor & Francis Group.
- Nelson, D.L., & Cox, M.M. (2010). *Lehninger Principles of Biochemistry*: W. H. Freeman.
- Nichols, J. T., Miyamoto, A., & Weinmaster, G. (2007). Notch signaling--constantly on the move. *Traffic, 8*(8), 959-969. doi: 10.1111/j.1600-0854.2007.00592.x

- Niesen, Frank H., Berglund, Helena, & Vedadi, Masoud. (2007). The use of differential scanning fluorimetry to detect ligand interactions that promote protein stability. *Nat. Protocols, 2*(9), 2212-2221.
- Noguera-Troise, I., Daly, C., Papadopoulos, N. J., Coetzee, S., Boland, P., Gale, N. W., . . . Thurston, G. (2006). Blockade of Dll4 inhibits tumour growth by promoting non-productive angiogenesis. *Nature, 444*(7122), 1032-1037. doi: 10.1038/nature05355
- Palmer, I., & Wingfield, P. T. (2004). Preparation and extraction of insoluble (inclusion-body) proteins from Escherichia coli. *Curr Protoc Protein Sci, Chapter 6*, Unit 6 3. doi: 10.1002/0471140864.ps0603s38
- Panin, V. M., Shao, L., Lei, L., Moloney, D. J., Irvine, K. D., & Haltiwanger, R. S. (2002). Notch ligands are substrates for protein O-fucosyltransferase-1 and Fringe. *J Biol Chem, 277*(33), 29945-29952. doi: 10.1074/jbc.M204445200
- Pantoliano, M. W., Petrella, E. C., Kwasnoski, J. D., Lobanov, V. S., Myslik, J., Graf, E., Salemme, F. R. (2001). High-density miniaturized thermal shift assays as a general strategy for drug discovery. *J Biomol Screen, 6*(6), 429-440. doi: 10.1089/108705701753364922
- Pavlopoulos, E., Pitsouli, C., Klueg, K. M., Muskavitch, M. A., Moschonas, N. K., & Delidakis, C. (2001). neuralized Encodes a peripheral membrane protein involved in delta signaling and endocytosis. *Dev Cell, 1*(6), 807-816.
- Petcherski, A. G., & Kimble, J. (2000). Mastermind is a putative activator for Notch. *Curr Biol, 10*(13), R471-473.
- Pintar, A., De Biasio, A., Popovic, M., Ivanova, N., & Pongor, S. (2007). The intracellular region of Notch ligands: does the tail make the difference? *Biol Direct, 2*, 19. doi: 1745-6150-2-19 [pii] 10.1186/1745-6150-2-19
- Porath, J., & Flodin, P. (1959). Gel filtration: a method for desalting and group separation. *Nature, 183*(4676), 1657-1659.
- Purow, B. (2012). Notch inhibition as a promising new approach to cancer therapy. *Adv Exp Med Biol, 727*, 305-319. doi: 10.1007/978-1-4614-0899-4_23
- Rader, C., Steinberger, P. and Barbas III, C. F. 2001. Selection from Antibody Libraries. *In* Phage Display – A Laboratory Manual (C. F. Barbas III, D. R. Burton, J. K. Scott and G. J. Silverman eds), 1st ed., pp 10.1-10.20, Cold Spring Harbor Laboratory Press, New York.
- Rader, C. (2012). Selection of human Fab libraries by phage display. *Methods Mol Biol, 901*, 81-99. doi: 10.1007/978-1-61779-931-0_5
- Radtke, F., & Raj, K. (2003). The role of Notch in tumorigenesis: oncogene or tumour suppressor? *Nat Rev Cancer, 3*(10), 756-767. doi: 10.1038/nrc1186
- Raya, A., Kawakami, Y., Rodriguez-Esteban, C., Ibanes, M., Rasskin-Gutman, D., Rodriguez-Leon, J., Izpisua Belmonte, J. C. (2004). Notch activity acts as a sensor for extracellular calcium during vertebrate left-right determination. *Nature, 427*(6970), 121-128. doi: 10.1038/nature02190

- Rebay, I., Fleming, R. J., Fehon, R. G., Cherbas, L., Cherbas, P., & Artavanis-Tsakonas, S. (1991). Specific EGF repeats of Notch mediate interactions with Delta and Serrate: implications for Notch as a multifunctional receptor. *Cell, 67*(4), 687-699.
- Ridgway, J., Zhang, G., Wu, Y., Stawicki, S., Liang, W. C., Chanthery, Y., Yan, M. (2006). Inhibition of Dll4 signalling inhibits tumour growth by deregulating angiogenesis. *Nature, 444*(7122), 1083-1087. doi: 10.1038/nature05313
- Sainson, R. C., & Harris, A. L. (2006). Hypoxia-regulated differentiation: let's step it up a Notch. *Trends Mol Med, 12*(4), 141-143. doi: 10.1016/j.molmed.2006.02.001
- Sblattero, D., & Bradbury, A. (2000). Exploiting recombination in single bacteria to make large phage antibody libraries. *Nat Biotechnol, 18*(1), 75-80. doi: 10.1038/71958
- Schatz, D. G., Oettinger, M. A., & Schlissel, M. S. (1992). V(D)J recombination: molecular biology and regulation. *Annu Rev Immunol, 10*, 359-383. doi: 10.1146/annurev.iy.10.040192.002043
- Schirrmann, T., Meyer, T., Schutte, M., Frenzel, A., & Hust, M. (2011). Phage display for the generation of antibodies for proteome research, diagnostics and therapy. *Molecules, 16*(1), 412-426. doi: 10.3390/molecules16010412
- Sethi, N., Dai, X., Winter, C. G., & Kang, Y. (2011). Tumor-derived JAGGED1 promotes osteolytic bone metastasis of breast cancer by engaging notch signaling in bone cells. *Cancer Cell, 19*(2), 192-205. doi: 10.1016/j.ccr.2010.12.022
- Sharma, M., Magenheimer, L. K., Home, T., Tamano, K. N., Singhal, P. C., Hyink, D. P.,Fields, T. A. (2013). Inhibition of Notch pathway attenuates the progression of human immunodeficiency virus-associated nephropathy. *Am J Physiol Renal Physiol, 304*(8), F1127-1136. doi: 10.1152/ajprenal.00475.2012
- Sharma, P. S., Sharma, R., & Tyagi, T. (2011). VEGF/VEGFR pathway inhibitors as anti-angiogenic agents: present and future. *Curr Cancer Drug Targets, 11*(5), 624-653.
- Shimizu, K., Chiba, S., Kumano, K., Hosoya, N., Takahashi, T., Kanda, Y.,Hirai, H. (1999). Mouse jagged1 physically interacts with notch2 and other notch receptors. Assessment by quantitative methods. *J Biol Chem, 274*(46), 32961-32969.
- Schumann, Wolfgang, & Ferreira, Luis Carlos S. (2004). Production of recombinant proteins in Escherichia coli. *Genetics and Molecular Biology, 27*, 442-453.
- Silva, M.S.S. 2014. Assessement of Notch 1 Ligands production – Key Protein Targets in Breast Cancer. Tese de Mestrado. Faculdade de Ciências e Tecnologia, Universidade Nova de Lisboa.
- Singh, S., & Chellappan, S. (2014). Lung cancer stem cells: Molecular features and therapeutic targets. *Mol Aspects Med, 39*, 50-60. doi: 10.1016/j.mam.2013.08.003
- Smith, G. P. (1985). Filamentous fusion phage: novel expression vectors that display cloned antigens on the virion surface. *Science, 228*(4705), 1315-1317.
- Song, R., Koo, B. K., Yoon, K. J., Yoon, M. J., Yoo, K. W., Kim, H. T., . . . Kong, Y. Y. (2006). Neuralized-2 regulates a Notch ligand in cooperation with Mind bomb-1. *J Biol Chem, 281*(47), 36391-36400. doi: 10.1074/jbc.M606601200

- Sorensen, H. P., & Mortensen, K. K. (2005). Advanced genetic strategies for recombinant protein expression in Escherichia coli. *J Biotechnol, 115*(2), 113-128. doi: 10.1016/j.jbiotec.2004.08.004
- Sprinzak, D., Lakhanpal, A., Lebon, L., Santat, L. A., Fontes, M. E., Anderson, G. A., . . . Elowitz, M. B. (2010). Cis-interactions between Notch and Delta generate mutually exclusive signalling states. *Nature, 465*(7294), 86-90. doi: 10.1038/nature08959
- Takahashi, K., Tanabe, K., Ohnuki, M., Narita, M., Ichisaka, T., Tomoda, K., & Yamanaka, S. (2007). Induction of pluripotent stem cells from adult human fibroblasts by defined factors. *Cell, 131*(5), 861-872. doi: 10.1016/j.cell.2007.11.019
- Tax, F. E., Yeargers, J. J., & Thomas, J. H. (1994). Sequence of C. elegans lag-2 reveals a cell-signalling domain shared with Delta and Serrate of Drosophila. *Nature, 368*(6467), 150-154. doi: 10.1038/368150a0
- Tegel, H., Ottosson, J., & Hober, S. (2011). Enhancing the protein production levels in Escherichia coli with a strong promoter. *FEBS J, 278*(5), 729-739. doi: 10.1111/j.1742-4658.2010.07991.x
- Timmerman, L. A., Grego-Bessa, J., Raya, A., Bertran, E., Perez-Pomares, J. M., Diez, J., de la Pompa, J. L. (2004). Notch promotes epithelial-mesenchymal transition during cardiac development and oncogenic transformation. *Genes Dev, 18*(1), 99-115. doi: 10.1101/gad.276304
- Vallejo, L. F., & Rinas, U. (2004). Strategies for the recovery of active proteins through refolding of bacterial inclusion body proteins. *Microb Cell Fact, 3*(1), 11. doi: 10.1186/1475-2859-3-11 [pii]
- van Es, Johan H., van Gijn, Marielle E., Riccio, Orbicia, van den Born, Maaike, Vooijs, Marc, Begthel, Harry, Clevers, Hans. (2005). Notch/[gamma]-secretase inhibition turns proliferative cells in intestinal crypts and adenomas into goblet cells. *Nature, 435*(7044), 959-963.
- Xie, Y., & Wetlaufer, D. B. (1996). Control of aggregation in protein refolding: the temperature-leap tactic. *Protein Sci, 5*(3), 517-523. doi: 10.1002/pro.5560050314
- Wang, M. M. (2011a). Notch signaling and Notch signaling modifiers. *Int J Biochem Cell Biol, 43*(11), 1550-1562. doi: 10.1016/j.biocel.2011.08.005
- Wang, Y., & Zhou, B. P. (2011b). Epithelial-mesenchymal transition in breast cancer progression and metastasis. *Chin J Cancer, 30*(9), 603-611. doi: 10.5732/cjc.011.10226
- Wang, Q. O., Zhang, L. S., Wu, J. F., Wang, W. D., Song, W. G., & Wang, W. (2010). A Parallel Solid-State NMR and Sensor Property Study on Flower-like Nanostructured SnO2. *Journal of Physical Chemistry C, 114*(51), 22671-22676. doi: Doi 10.1021/Jp1098156
- Watkins, N. A., & Ouwehand, W. H. (2000). Introduction to antibody engineering and phage display. *Vox Sang, 78*(2), 72-79. doi: 31154
- Weng, A. P., & Aster, J. C. (2004). Multiple niches for Notch in cancer: context is everything. *Curr Opin Genet Dev, 14*(1), 48-54. doi: 10.1016/j.gde.2003.11.004

- Weng, A. P., Ferrando, A. A., Lee, W., Morris, J. P. th, Silverman, L. B., Sanchez-Irizarry, C., Aster, J. C. (2004). Activating mutations of NOTCH1 in human T cell acute lymphoblastic leukemia. *Science, 306*(5694), 269-271. doi: 306/5694/269 [pii] 10.1126/science.1102160
- Wright, T. R. (1970). The genetics of embryogenesis in Drosophila. *Adv Genet, 15*, 261-395.
- Wu, L., Aster, J. C., Blacklow, S. C., Lake, R., Artavanis-Tsakonas, S., & Griffin, J. D. (2000). MAML1, a human homologue of Drosophila mastermind, is a transcriptional co-activator for NOTCH receptors. *Nat Genet, 26*(4), 484-489. doi: 10.1038/82644
- Yavropoulou, M. P., Maladaki, A., & Yovos, J. G. (2015). The role of Notch and Hedgehog signaling pathways in pituitary development and pathogenesis of pituitary adenomas. *Hormones (Athens), 14*(1), 5-18.
- Yeh, E., Dermer, M., Commisso, C., Zhou, L., McGlade, C. J., & Boulianne, G. L. (2001). Neuralized functions as an E3 ubiquitin ligase during Drosophila development. *Curr Biol, 11*(21), 1675-1679.
- Zavadil, J., Cermak, L., Soto-Nieves, N., & Bottinger, E. P. (2004). Integration of TGF-beta/Smad and Jagged1/Notch signalling in epithelial-to-mesenchymal transition. *EMBO J, 23*(5), 1155-1165. doi: 10.1038/sj.emboj.7600069 [pii]
- Zhao, M., Wu, M., Guo, L., Jiang, J., Huang, W., Lin, X., Han, W. (2010). Expression, purification, and characterization of a novel soluble form of human Delta-like-1. *Appl Biochem Biotechnol, 160*(5), 1415-1427. doi: 10.1007/s12010-009-8603-2
- Zou, Q., Bennion, B. J., Daggett, V., & Murphy, K. P. (2002). The molecular mechanism of stabilization of proteins by TMAO and its ability to counteract the effects of urea. *J Am Chem Soc, 124*(7), 1192-1202.

# 5 Appendix

## 5.1 Reagent List

**Table 5.1 – List of reagents used.**

| Product | Supplier | Catalogue number |
|---|---|---|
| 24-well plate (VDX plate) | Hampton Research | HR3-142 |
| RPMI medium | Gibco | 12633-012 |
| 2xyT medium | Applichem | A0981 |
| Agar | Nzytech | MB02902 |
| Agarose | SeaKem | 50004 |
| Amicon 10 kDa MWCO | Millipore | UFC901024 |
| Amicon Stirred Cell unit | Millipore | 8050 |
| Ampicillin | Sigma | A9518 |
| Anti-M13-HRP conjugated | GE Healthcare | 27-9421-01 |
| Bio-Rad Protein Assay Dye Reagent Concentrate | Bio-Rad | 500-0006 |
| Bio-Rad silver stain kit | Bio-Rad | 1610443 |
| BME | Carl Roth GmbH | 4227.1 |
| BRIJ® 35 Detergent, 30% Aqueous Solution | Calbiochem | 203724 |
| BugBuster Protein Extraction Reagent | Novagen | 70584 |
| Calcium chloride ($CaCl_2$) | Calbiochem | 3000 |
| Cloranphenicol | Sigma | C0378 |
| Criterion XT Precast Gel | Bio-Rad | 345-0124 /345-0125 |
| CrystalQuick™ 96 Well, Greiner | Hampton Research | HR3-281 |
| Deoxynucleotide (dNTP) mix | Nzytech | MB08604 |
| DMEM | Gibco | 41966 |
| DMSO | Sigma | 472301 |
| Dnase I | Roche | 10104159001 |
| DPBS | Gibco | 14190 |
| DTT | Promega | V3155 |
| *Eag*I | Fermentas | ER0331 |
| EDTA | Carl Roth GmbH | 8040.2 |
| Expedeon - Protein Stain - InstantBlue | Expedeon | ISB1L |
| FastStart DNA SYBR Green I mix | Roche | 04913850001 |
| FBS | Gibco | 16250-078 |
| Gene Pulser/MicroPulser Electroporation Cuvettes | Bio-Rad | 1652086 |
| GeneJET Plasmid Miniprep Kit | Fermentas | K0502 |
| GeneRuler 1 kb DNA Ladder | Fermentas | SM0311 |
| Glucose | Sigma | G8270 |
| Glycerol | Calbiochem | 4760 |
| Goat Anti-Human IgG (Fab specific)-HRP conjugated | Sigma | A0293 |
| Goat anti-human IgG Fab specific | Sigma | I9010 |
| Goat α-mouse IgG-HRP conjugated antibody (Anti-mouse) | Sigma | A3682-1ML |
| GSH | Sigma | G4251 |
| GSSG | Sigma | G4376 |
| Guanidine-HCl | Roth | 0037-1 |
| HiLoad 16/600 Superdex 75 pg column | GE Healthcare Life Sciences | 28-9893-33 |
| *Hind*III | Fermentas | ER0501 |
| HiPrep 26/10 desalting column | GE Healthcare Life Sciences | 17-5087-01 |
| HiPrep Q HP 16/10 column | GE Healthcare Life Sciences | 29-0181-83 |

| Product | Supplier | Catalogue number |
|---|---|---|
| HisTrap FF column | GE Healthcare Life Sciences | 17-5255-01 |
| JCSG-plus™ HT-96 screen | Molecular Dimensions | MD1-37 |
| Imidazole | Merck | 1.04716.1000 |
| Index HT screen | Hampton Research | HR2-134 |
| IPTG | Sigma | I5502 |
| Kanamycin | Sigma | K1876 |
| L-arabinose | Sigma | A3256 |
| L-arginine | Sigma | W381918 |
| Luria-Bertani (LB) medium | NzyTech | MB02804 |
| M9 minimal medium | Sigma | M6030 |
| MaxiSorp™ ELISA Plates, Uncoated | NUNC | 44-2404-21 |
| MES Running Buffer | Bio-Rad | 161-0789 |
| $MgSO_4$ 25mM | Fermentas | R0971 |
| Milk Powder | Molico | n/a |
| MIDAS™ | Molecular Dimensions | MD1-59 |
| Mini-PROTEAN TGX precast Gels | Bio-Rad | 456-1083 / 456-1086 |
| *Nco*I | Fermentas | ER0571 |
| Overnight Express™ Autoinduction System 1 | Millipore | 71300-3 |
| Nitrocellulose membranes | GE Healthcare Life Sciences | RPN203D |
| NuPAGE Transfer Buffer | Life Technologies | NP0006-1 |
| NZYColour Protein Marker II | NzyTech | MB090 |
| PACT premier™ HT-96 screen | Molecular Dimensions | MD1-36 |
| NzyTech GelPure Kit | NzyTech | MB011 |
| PBS Tablets | Calbiochem | 524650 |
| *Pci*I | NEB | R0655L |
| PEG 3350 | Sigma | 202444 |
| PEG 6000 | Sigma | 81260 |
| Penta-His Antibody, BSA-free | Qiagen | 34660 |
| Penicillin streptomycin | Life Technologies | 15140-122 |
| pET47b(+) ($kan^R$) | Novagen | 71461-3 |
| *Pfu* DNA polymerase | Fermentas | EP0501 |
| pGro7 ($Cm^R$) | TaKaRa | 3340 |
| Potassium chloride (KCl) | Calbiochem | 7360 |
| Potassium phosphate dibasic | Prolabo | 26931.263 |
| Rneasy mini kit | Qiagen | 74104 |
| Roche transcriptor first strand cDNA synthesis kit | Roche | 04379012001 |
| Power Broth (PB) | AthenaES | MD12-106-1 |
| Protease inhibitor cocktail | Roche | 11873580001 |
| *Sac*I | Fermentas | ER1131 |
| SeeBlue® Plus2 Pre-Stained Standard | Fermentas | LC5925 |
| *Sfi*I | Roche | |
| SG1 (ShotGun) Screen | Molecular Dimensions | MD1-89 |
| SHuffle® T7 express competent cells | NEB | C3029 |
| Sodium Chloride ($NaCl_2$) | Carl Roth GmbH | 9265.1 |
| Sodium phosphate monobasic | Merck | 1.06346 |
| *Spe*I | Fermentas | ER1251 |
| Structure 1 + 2 HT-96 Screen | Molecular Dimensions | MD1-30 |
| Superdex 75 10/300 GL column | GE Healthcare Life Sciences | 17-5174-01 |
| SYPRO Orange Dye | Molecular Probes | S6650 |
| T4 DNA ligase | Fermentas | EL0011 |
| *Taq* DNA polymerase | Fermentas | EP0402 |
| TCEP-HCl | Amresco | K831 |
| TMAO | Sigma | 92277 |
| TMB | Invitrogen | 00-2023 |
| Triethylamine (TEA) | Invitrogen | 90279 |
| Tris-HCl | Invitrogen | 15567-027 |

| Product | Supplier | Catalogue number |
|---|---|---|
| Triton X-100 | Sigma | 9002931 |
| Trypan-Blue 0.4% solution | Gibco | 25300 |
| Trypsin-EDTA | Gibco | 15250-061 |
| Tween-20 | Sigma | P7949 |
| Urea | Sigma | U1250 |
| Vivaflow 10kDa MWCO | Sartorius | VF20P0 |
| Vivaspin 2 10kDa MWCO | Sartorius | VS0201 |
| Vivaspin 50010kDa MWCO | Sartorius | VS0101 |
| Western Lightning Plus-ECL Enhanced Chemiluminescence Substrate | Perkin-Elmer | NEL104001EA |
| *Xba*I | Fermentas | ER0681 |
| *Xho*I | Fermentas | 15231-012 |
| mTeSR™1 | Stemcell Technologies | 05857 |

## 5.2 Strains genotype

**DH5α**:

$F^-$ endA1 glnV44 thi-1 recA1 relA1 gyrA96 deoR nupG Φ80d*lacZ*ΔM15 Δ(*lacZYA-argF*)U169, hsdR17($r_K^-$ $m_K^+$), λ–

**BL21 (DE3):**

$F^-$ ompT gal dcm lon hsd$S_B$($r_B^-$ $m_B^-$) λ(DE3 [lacI lacUV5-T7 gene 1 ind1 sam7 nin5])

**BL21 Star (DE3) prare2:**

$F^-$*omp*T *hsd*$S_B$ ($r_B^-$, $m_B^-$) *galdcmrne*131. Contains a plasmid encoding argU, argW, argX, glyT, ileX, leuW, metT, proL, thrT, thrU and tyrU – pRARE2 ($Cam^R$)

**SHuffle® T7 express:**

F´ *lac*, *pro*, *lacIQ* / *Δ(ara-leu)7697 araD139 fhuA2 lacZ::T7 gene1 Δ(phoA)PvuII phoR ahpC* galE (or U) galK λatt*::pNEB3-r1-*cDsbC* (SpecR, *lacIq*) *ΔtrxB rpsL150*(StrR) *Δgor Δ(malF)*

**TG1:**

F' [*traD36 proAB*$^+$ *lacI*$^q$ *lacZΔM15*]*supE thi-1 Δ(lac-proAB) Δ(mcrB-hsdSM)5, (*$r_K^- m_K^-$*)*

**TOP10 F':**

F'[lacI$^q$ Tn10(tet$^R$)] mcrA Δ(mrr-hsdRMS-mcrBC) φ80lacZΔM15 ΔlacX74 deoR nupG recA1 araD139 Δ(ara-leu)7697 galU galK rpsL(Str$^R$) endA1 $λ^-$

## 5.3 Buffers and Solutions

SDS-PAGE Loading Buffer 4x: 200mM Tris-HCl pH 6.8, 8% SDS, 0.4% Bromophenol Blue, 40% Glycerol, 400mM BME, 44mM EDTA

SB medium: 10g of MOPS (3(N-Morpholino) propanesulfonic acid) ,30g of tryptone, 20g of yeast extract, distilled water to final volume of 1L, pH 7.0

M9 minimal medium: 1x M9 medium, 2mM $MgSO_4$, 0.4% glucose, 0.1mM $CaCl_2$, 0.005% thiamine, distilled water to a final volume of 150mL

Na/KPi (Sodium / Potassium Phosphate): 1M $NaH_2PO_4$ + 1M $H_2HPO_4$ (adjust the volumes of each reagent to a final pH of 7.0)

### 5.3.1 hDLL1-DE3 purification from *E.coli* (inclusion bodies)

#### 5.3.1.1 Solubilisation with Guanidine-HCl and refolding with L-arginine

Lysis Buffer A- 50mM Tris-HCl, 100mM KCl, 0,5% Triton X-100, 1/2 tablet protease inhibitors, 2% glycerol, pH 8.0

Wash IA- 50mM Tris-HCl, 100mM KCl, 0,5% Triton X-100, pH 8.0

Wash IIA- 50mM Tris-HCl, 100mM KCl, pH 8.0

Solubilisation Buffer A- 50mM Tris-HCl, 100Mm KCl, 6M Guanidine-HCl, 10mM DTT, pH 8.0

Refolding Buffer A- 50 mM Na/KPi, 300mM NaCl, 1mM EDTA, 1mM GSH, 0.1mM GSSG, 1M L-arginine, 1M TMAO, pH 8.0

Desalting- 50mM Na/KPi, 300mM NaCl, pH 8.0

#### 5.3.1.2 Solubilisation with urea and refolding

Lysis Buffer B- 1x PBS, 1mM EDTA, 0,5% Triton X-100, 1 tablet protease inhibitors, 5mM DTT, pH 7.4

Wash IB- 1x PBS, 50mM NaCl, 10mM EDTA, 0,5% Triton X-100, 1 tablet protease inhibitors, pH 7.4

Wash IIB- 1x PBS , 50mM NaCl, 10mM EDTA, 1 tablet protease inhibitors, pH 7.4

Solubilisation Buffer A- 50mM Tris-HCl, 50mM NaCl, 1mM EDTA, 8M Urea, 1 tablet protease inhibitors pH 8.5

Refolding Buffer IB- 50mM $NaH_2PO_4$, 1 tablet protease inhibitors, pH 10.7

Refolding Buffer IIB- 20mM Tris-HCl, 1 tablet protease inhibitors, pH 8.0

AIC-I- 20mM Tris-HCl pH 9.1

AIC-II- 20mM Tris-HCl, 1M NaCl, pH 9.1

Histrap A- 20mM Tris-HCl, 500mM NaCl, 50mM imidazole, pH 9.1

Histrap B- 20mM Tris-HCl, 500mM NaCl, 60mM imidazole, pH 9.1

Histrap C- 20mM Tris-HCl, 500mM NaCl, 500mM imidazole, pH 9.1

Histrap D- 20mM Tris-HCl, 500mM NaCl, 1M imidazole, pH 9.1

### 5.3.2 hDLL1-DE3 purification from HEK293T

#### 5.3.2.1 First srategy

Histrap 1A- 1x PBS, 20mM imidazole, pH 7.5

Histrap 1B- 1x PBS, 20mM imidazole, 500mM NaCl, pH 7.5

Histrap 1C- 1x PBS, 500mM imidazole, pH 7.5

Histrap 1D- 1x PBS, 1M imidazole, pH 7.5

Sec Buffer 1 - 1x PBS

#### 5.3.2.2 Second strategy

Histrap 2A- 1x PBS , 20mM imidazole, 500mM NaCl 0,03% Brij 35, 10% glycerol,0,5 mM TCEP, pH 7.5

Histrap 2B- 1x PBS , 500mM imidazole, 0,03% Brij 35, 10% glycerol,0,5 mM TCEP, pH 7.5

Sec Buffer 2- 1x PBS, 10% glycerol, 0,5 mM TCEP, pH 7.5

### 5.4 Mass spectrometry report (provided by Mass Spectometry Unit (UniMS), ITQB/Ibet, Oeiras, Portugal

**Methodology**

The protein bands, excised from a 1D-PAGE gel, were destained, reduced, alkylated and digested with trypsin (Promega, 6.7ng/µl) overnight at 37 ºC. The tryptic peptides were desalted and concentrated using POROS R2 (Applied Biosystems) and eluted directly onto the MALDI plate using 0.6µl of 5mg/ml CHCA (alpha-cyano-4-hydroxycinnamic acid, Sigma) in 50% (v/v) acetonitrile and 5% (v/v) formic acid.

The data was acquired in positive reflector MS and MS/MS modes using a 4800plus MALDI-TOF/TOF (AB Sciex) mass spectrometer and using 4000 Series Explorer Software v.3.5.3 (Applied Biosystems). External calibration was performed using Pepmix1 (Laser BioLabs).

The fifty most intense precursor ions from the MS spectra were selected for MS/MS analysis.

The raw MS and MS/MS data were analyzed using Protein Pilot Software v. 4.5 (ABSciex) with the Mascot search engine (MOWSE algorithm). The search parameters were as follows: monoisotopic peptide mass values were considered, maximum precursor mass tolerance (MS) of 50 ppm and a maximum fragment mass tolerance (MS/MS) of 0.3 Da. The searches were performed against a protein database UniProt with taxonomic restriction to Human (145672 sequences; 46020319 residues). A maximum of two missed cleavage was allowed. Carboxyamidomethylation of cysteines, oxidation of methionines and N-Pyro Glu of the N-terminal Q were set as variable modifications.

Protein identification was only accepted when significant protein homology scores were obtained ($p<0.05$, protein scores greater than 64) and at least one peptide was fragmented with a significant individual ion score ($p<0.05$)

**Assay report**

MATRIX SCIENCE **MASCOT SEARCH RESULTS**

## PROTEIN VIEW

Match to: **DLL1_HUMAN** Score: **145** Expect: **4.6e-010**
**Delta-like protein 1 OS=Homo sapiens GN=DLL1 PE=2 SV=2**
Nominal mass ($M_r$): **78004;** Calculated pI value: **5.85**
NCBI BLAST search of DLL1_HUMAN against nr
Unformatted sequence string for pasting into other applications
Variable modifications: Carbamidomethyl (C),Deamidated (NQ),Gln->pyro-Glu (N-term Q),Oxidation (M)
Cleavage by Trypsin: cuts C-term side of KR unless next residue is P
Sequence Coverage: **17%**

Matched peptides shown in **Bold Red**

**1** MGSRCALALA VLSALLCQVW SSGVFELKLQ EFVNKK**GLLG NRNCCRGGAG**
**51** **PPPCACRTFF R**VCLKHYQAS VSPEPPCTYG SAVTPVLGVD SFSLPDGGGA
**101** DSAFSNPIRF PFGFTWPGTF SLIIEALHTD SPDDLATENP ERLISRLATQ
**151** RHLTVGEEWS QDLHSSGRTD LKYSYR**FVCD EHYYGEGCSV FCRPRDDAFG**
**201** **HFTCGER**GEK VCNPGWK**GPY CTEPICLPGC DEQHGFCDKP GECK**CRVGWQ
**251** GRYCDECIRY PGCLHGTCQQ PWQCNCQEGW GGLFCNQDLN YCTHHKPCKN
**301** GATCTNTGQG SYTCSCRPGY TGATCELGID ECDPSPCKNG GSCTDLENSY
**351** SCTCPPGFYG KICELSAMTC ADGPCFNGGR CSDSPDGGYS CRCPVGYSGF
**401** NCEKKIDYCS SSPCSNGAK**C VDLGDAYLCR** CQAGFSGRHC DDNVDDCASS
**451** PCANGGTCRD GVNDFSCTCP PGYTGRNCSA PVSRCEHAPC HNGATCHERG
**501** HRYVCECARG YGGPNCQFLL PELPPGPAVV DLTEKLEGQG GPFPWVAVCA
**551** GVILVLMLLL GCAAVVVCVR LRLQKHRPPA DPCRGETETM NNLANCQREK
**601** DISVSIIGAT QIKNTNKKAD FHGDHSADK**N GFKARYPAVD YNLVQDLKGD**
**651** **DTAVRDAHSK R**DTKCQPQGS SGEEKGTPTT LRGGEASERK RPDSGCSTSK
**701** DTKYQSVYVI SEEKDECVIA TEV

## 5.5 Supplementary figures

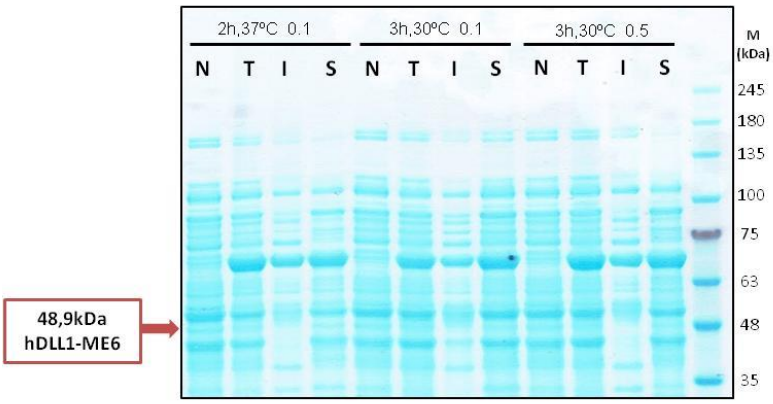


**Figure 5.1 - SDS-PAGE of expression tests in hDLL1-ME6.** Expression tests using PB medium and 2h37ºC with 0.1mM IPTG,3h30ºC with 0.1mM IPTG and 3h30ºC with 0.5mM IPTG.M- Marker; N- Non-induced culture; T- Total induced culture; I- Insoluble fraction; S- soluble fraction. Red arrow pointing the induced band with the molecular mass predicted for this construct

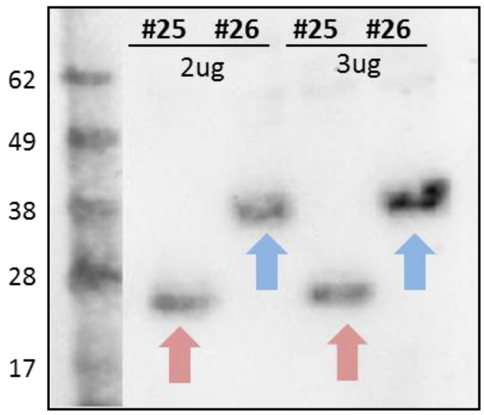


**Figure 5.2 - Anti-His Western Blot of expression tests for hDLL1-DE6 and hDLL1-DE3 in T25cm$^2$.** Two quantities of DNA were tested for each construct – 2 and 3µg. M - Marker. Blue arrows - marks the bands induced in the molecular mass expected for hDLL1_DE6 (32,3kDa). Red arrows - marks the bands induced in the molecular mass expected for hDLL1_DE3 (20,2kDa).

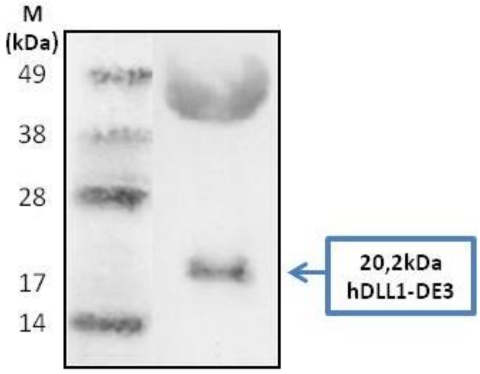


**Figure 5.3 - Anti-His Western Blot of hDLL1-DE3 large scale production in HEK293T.** Blue box marks the molecular mass estimated for this protein.
.

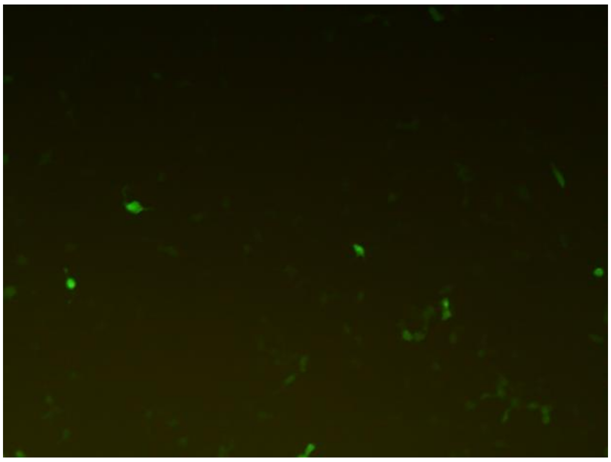

**Figure 5.4 - Transfection efficiency evaluation after 48 hours post-transfection in T225cm$^2$.** Image obtained by fluorescence microscopy using pAAVpuro-GFP.

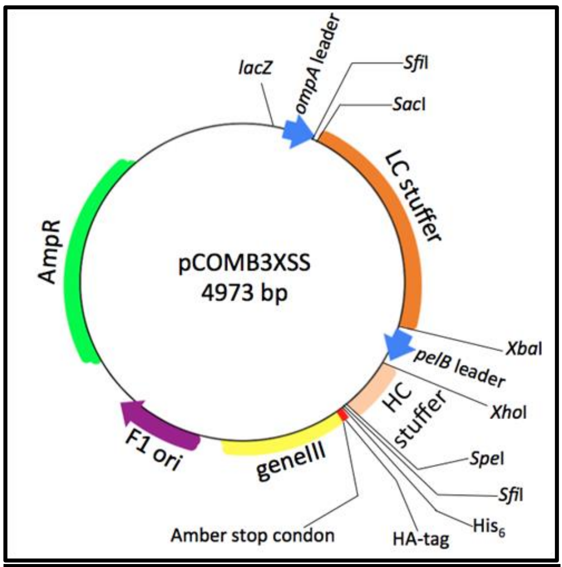


**Figure 5.5 - Illustration of pCOMB3XSS. Adapted from *Cabral, 2014.***